University of Southampton

Faculty of Environmental and Life Sciences

School of Ocean and Earth Science

Sedimentary Filters for Emerging Contaminants in Estuarine and Coastal Systems

by

Jana-Sophie Appelt

ORCID ID 0000-0002-0717-5386

Thesis for the degree of Doctor of Philosophy

January 2026

“The more clearly we can focus our attention on the wonders and realities of the universe about us, the less taste we shall have for destruction.”

— Rachel Carson

University of Southampton

Abstract

Faculty of Environment and Life Sciences

School of Ocean and Earth Science

Thesis for the degree of Doctor of Philosophy

Sedimentary Filters for Emerging Contaminants in Estuarine and Coastal Systems

by

Jana-Sophie Appelt

Estuarine sediments serve as critical sinks and archives for a range of contaminants, including trace metals, polycyclic aromatic hydrocarbons (PAHs), and emerging contaminants like steroidal hormones. While sequestration mechanisms for trace metals and PAHs in estuarine sediments are relatively well-studied, the behaviour and fate of steroidal hormones, especially the role of sedimentary organic matter on hormone retention, are not as well understood. This thesis integrates field investigations from two contrasting estuarine systems, Southampton Water (UK) and the Pearl River Delta (PRD) (China), with laboratory adsorption experiments to evaluate the spatial and temporal distribution of contaminants and examine how sediment properties, particularly the origin of organic matter, affect contaminant retention.

Surface and core sediments were analysed to determine contaminant concentrations and historical deposition trends, and sediment properties were characterised. In Southampton Water, elevated concentrations of trace metals were observed, particularly near Southampton Port and wastewater treatment plants (WWTPs), with concentrations reaching up to 2570 mg/kg for Cu, 5560 mg/kg for Zn, and 810 mg/kg for Pb. Hormones like estrone, estradiol, and progesterone, were detected in sediments at all sites (average concentrations 3.3 - 40 ng/g). Ethinylestradiol, a synthetic hormone, was found only near WWTP discharges (average concentration 7.4 ng/g). Principal component analysis (PCA) suggests that sediment properties such as total organic carbon (TOC) and total organic nitrogen (TON) influence the retention of organic contaminants and mercury (Hg).

In the PRD, spatial gradients in trace metal and PAH concentrations indicate nearshore retention, with total trace metal concentrations ranging between 124 – 435 mg/kg, and 2 – 177 ng/g for PAHs. In contrast, estrone showed no consistent spatial pattern and was present only in surface sediments, with concentrations up to 13.1 ng/g. This suggests diffuse sources or low sedimentary sequestration. Unlike Southampton Water, sediment properties in the PRD varied only slightly throughout the estuary. PCA indicated that TOC and grain size significantly influence trace metal distribution but had minimal control over PAH and hormone distribution.

To better understand interactions between hormones and organic matter source, adsorption experiments were performed using sorbents derived from estuarine plant materials. The sorption behaviour of estrone varied depending on the organic matter source, with TON being a more significant driver of estrone adsorption than TOC. Additionally, salinity had minimal influence on adsorption, suggesting a threshold effect related to estuarine ionic strengths. Together, these findings demonstrate the complexity of sediment-contaminant interactions, emphasising the need to consider environmental and geochemical characteristics when assessing the fate of hormones and other contaminants in estuarine systems. This integrated approach offers new insights into contaminant dynamics in estuarine systems.

Table of Contents

Table of Tables

Table of Figures

Table of Figures

Table of Figures

Table of Figures

Research Thesis: Declaration of Authorship

Print name: Jana-Sophie Appelt

Title of thesis: Sedimentary filters for emerging contaminants in estuarine and coastal systems

I declare that this thesis and the work presented in it are my own and has been generated by me as the result of my own original research.

I confirm that:

1. This work was done wholly or mainly while in candidature for a research degree at this University;
2. Where any part of this thesis has previously been submitted for a degree or any other qualification at this University or any other institution, this has been clearly stated;
3. Where I have consulted the published work of others, this is always clearly attributed;
4. Where I have quoted from the work of others, the source is always given. With the exception of such quotations, this thesis is entirely my own work;
5. I have acknowledged all main sources of help;
6. Where the thesis is based on work done by myself jointly with others, I have made clear exactly what was done by others and what I have contributed myself;
7. None of this work has been published before submission

Signature: ..... Date:.....

Acknowledgements

“Give credit where credit is due”- this thesis was a team effort, and many people deserve to be acknowledged for supporting my journey to this point:

Firstly, I want to thank my fantastic supervisors Andrew Cundy, Jessica Whiteside and Sargent Bray for entrusting me with this project and supporting me along the way. Thank you, Andy, for sharing your knowledge with me, and for always making time and providing guidance and help when I needed it. Throughout this PhD I experienced all the emotions from curiosity and excitement over boredom and frustration and back, but in nearly four years, I don’t think I’ve ever seen you in a bad mood. Thank you for always keeping my spirits up and encouraging me on this journey!

A special thanks goes out to Sarge. Thank you for managing all the smaller and bigger catastrophes in the lab, your endless efforts to keep the GC-MS up and running, your creative, solution-oriented approaches and all the time you spent discussing experimental set-ups and problem-solving with me, meanwhile always being enthusiastic and telling bad jokes! I’m incredibly grateful to have had you on my team and can only wish to work with colleagues as kind and fun as you in the future.

Thank you, Jessica for sacrificing your nights and sleep to join meetings, for always coming up with ideas to solve problems, for your prompt and helpful feedback during editing and proofreading this thesis and for your constant encouragement and kind words of support!

A shoutout also to the entire OG group at NOCS, especially Elise, Emily and Joe! It was a pleasure being part of the team, working alongside you guys in the lab and having chats during extended coffee breaks.

I would also like to express my gratitude for the help and support I received from around the University, especially Pawel and the GAU team, Bastian and Megan, Matt Cooper and Laval, John and Julie at Highfield. I’m also grateful to Martin Hansen and Emil Egede Frøkjær for introducing me to the very cool and very overwhelming world of NTA during my placement!

To the best officemates (and the whole “extended zoo”) I could ever wish for – starting with Lorenza and Jon, Kai and Yuntong, our newbies Ruby and Liesl and especially Amavi and Sunke - I am most grateful to not only call you colleagues, but friends! At times we might not have gotten a lot of work done, but I will always remember the gravity stick and other shenanigans and all the laughter we shared!

Lastly, but most importantly, I am incredibly grateful for the support and friendships that carried me through every up and down: Thank you for your emotional support, Julija, Lary, and Theda. Kai, thank you for all the nerdy chemistry talks, writing sessions and always cheering me on! Jenny, Laura and Jenny thank you for always being by my side no matter the distance between us, your friendship means the world to me. Thank you Zsolt for your unconditional love and unwavering belief in me. And finally, to my sister, Christina and my parents, Andrea and Klaus: I always felt free to choose my own path in life without pressure (other than employment) and even if you were sceptical at times, you always believed in me and supported me on this (very long) journey! I appreciate that more than anything, thank you! This thesis would not have happened without you.

Definitions and Abbreviations

ANT..... Anthracene

ASE..... Accelerated Solvent Extraction

BPA..... Bisphenol A

BSTFA-TMCS..... N,O-bis(trimethylsilyl)tri-fluoroacetamide +1% trimethylchlorosilane

C_{org}/N_{total}..... Total organic carbon to total nitrogen ratio

$CaCO_3$ ..... Calcium carbonate

CECs ..... Contaminants of Emerging Concern

CF:CS ..... Constant Flux : Constant Sedimentation Rate Model

CH_3Hg..... Methylmercury

$\delta^{13}C$ ..... Stable Carbon Isotope ratio (^{13}C:^{12}C), expressed in parts per thousand (‰) relative to a standard.

$\delta^{15}N$ ..... Stable Nitrogen Isotope ratio (^{15}N:^{14}N), expressed in parts per thousand (‰) relative to a standard.

DCM ..... Dichloromethane

DDT ..... Dichlorodiphenyltrichloroethane

DOC ..... Dissolved Organic Carbon

DOM ..... Dissolved Organic Matter

E1 ..... Estrone

E2 ..... Estradiol

EI ..... Electron Ionisation

EDCs ..... Endocrine Disrupting Chemicals

EE2 ..... Ethinylestradiol

EF ..... Enrichment Factor

EtOAc ..... Ethyl Acetate

FLA ..... Fluoranthene

GCxGC-MS ..... Two dimensional GC-MS

GC-MS..... Gas Chromatography Mass Spectrometry

H_2S ..... Hydrogen Sulphide

HPGe ..... High Purity Germanium

I.D. ..... Inner Diameter

I_{geo} ..... Geoaccumulation Index

IRMS ..... Isotope Ratio Mass Spectrometer

IS ..... Internal Standards

K_d ..... Sediment Adsorption/Partition Coefficient

K_{OC} ..... Organic Carbon Normalised Adsorption Coefficient

LOD ..... Limit of Detection

$\log K_{OC}$ ..... Natural Logarithm of K_{OC}

$\log K_{OW}$ ..... N-Octanol Water Partition Coefficient

LOI ..... Loss on Ignition

LOQ ..... Limit of Quantification

MeOH ..... Methanol

NIST ..... National Institute of Standards and Technology

NTA ..... Non-Targeted Analysis

OC ..... Organic Carbon

OM ..... Organic Matter

P4 ..... Progesterone

PACs ..... Polycyclic Aromatic Compounds

PAHs ..... Polycyclic Aromatic Hydrocarbons

PCA ..... Principal Component Analysis

PCBs ..... Polychlorinated Biphenyls

PFAS ..... Per- and Polyfluoroalkyl Substances

PHE ..... Phenanthrene

POC ..... Particulate Organic Carbon

PRD ..... Pearl River Delta

PYR ..... Pyrene

QQQ-ICP-MS ..... Triple-Quadrupole Inductively Coupled Plasma Mass Spectrometer

RMSE ..... Root Mean Square Error

RSD ..... Relative Standard Deviation

SIM ..... Single Ion Monitoring

S/N ..... Signal to Noise Ratio

SPE ..... Solid-Phase Extraction

SPM ..... Suspended Particulate Matter

SWAC ..... Southampton Water Activity Centre

TIC ..... Total Ion Current

TOC ..... Total Organic Carbon

TON ..... Total Organic Nitrogen

UAE ..... Ultrasound-Assisted Extraction

UK ..... United Kingdom

USA ..... United States of America

VPDB ..... Vienna PeeDee Belemnite Reference Material

wt% ..... Weight Percentage

WWTPs ..... Wastewater Treatment Plants

XRF ..... X-ray Fluorescence Analysis

Chapter 1 Introduction

1.1 Estuarine Systems and their Significance

Estuaries are semi-enclosed aquatic environments situated between land and ocean, where rivers feed into the sea. As transitional environments, they are characterised by strong gradients from marine conditions at the mouth to brackish water through freshwater inflow from rivers. They are highly dynamic systems and exhibit unique physicochemical properties due to both marine and fluvial processes, including waves, tides, salinity, and sediment inflow. Defining and classifying estuaries is challenging because of this continuity. The latest definition by Potter et al. (2010) tries to include all main characteristics of estuaries: "*An estuary is a partially enclosed coastal body of water that is either permanently or periodically open to the sea and which receives at least periodic discharge from a river(s), and thus, while its salinity is typically less than that of natural sea water and varies temporally and along its length, it can become hypersaline in regions when evaporative water loss is high and freshwater and tidal inputs are negligible*." Additionally, estuaries can be classified based on their water balance (positive, negative or neutral), salinity (salt wedge or highly stratified, partially mixed, and homogeneous) or tidal range (microtidal, mesotidal, macrotidal and hypertidal) (McLusky and Elliott, 2004; Valle-Levinson, 2010). The most common classification is according to their geomorphology and includes four main types, which can be subdivided further: Drowned river valleys or coastal plain estuaries originating from flooding of pre-existing valleys as a consequence of sea level rise in the Pleistocene; Bar-built estuaries (also embayments), which are drowned river valleys but semi enclosed with sand bars across their mouths; Fjords, usually found in high latitudes and characterised by deep and narrow basins, formed by drowned glacial troughs; And tectonic estuaries, which were formed by tectonic activity and resulting creases and faults within the earth's crust that were flooded (Elliott and McLusky, 2002; McLusky and Elliott, 2004; Valle-Levinson, 2010). A schematic estuary is shown in Figure 1.1.

Sediments, organic matter, and inorganic nutrients from terrestrial sources are carried into estuaries by rivers and lead to high primary production and high biodiversity in these ecosystems (Bianchi, 2006). The salt marshes and mudflats found in estuaries are productive ecosystems and provide rich feeding grounds and habitats for numerous bird, mammal and fish species (Chapman and Wang, 2001; Wilson, 2002; McLusky and Elliott, 2004).

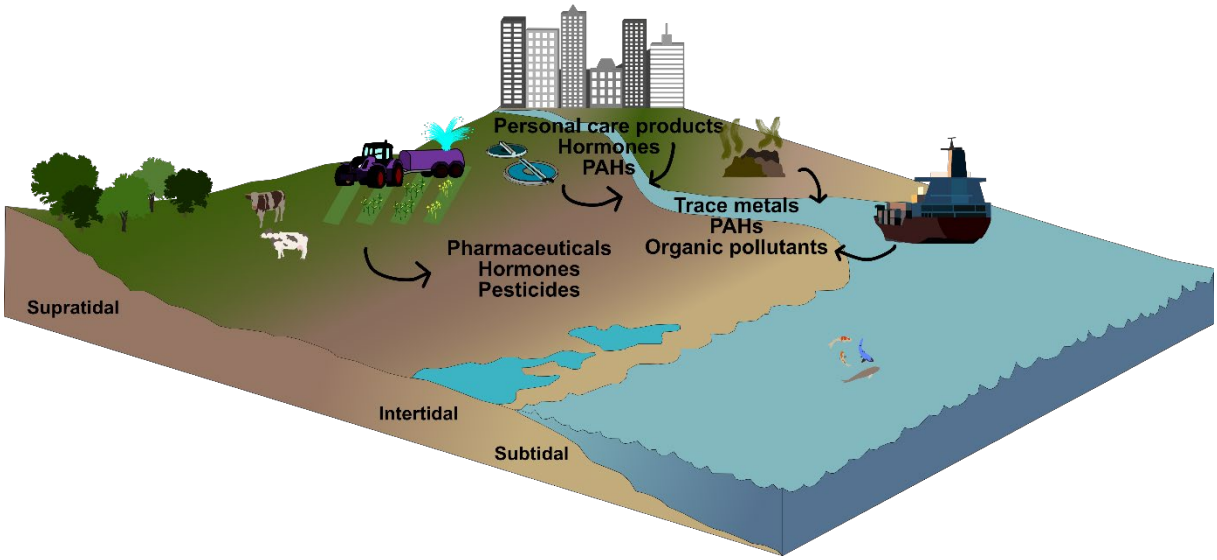

Figure 1.1: Graphic of a drowned river valley estuary with different contaminant groups (e.g. pharmaceuticals, hormones, trace metals,..) and their sources, such as agriculture, landfills, and urban wastewater runoff. Created using Affinity Designer 1.

Moreover, estuaries are central points of human activity and offer essential services, such as freshwater supply, transportation routes, fisheries and recreational opportunities. A study noted that, as of 2018, nearly 30 % of the global population lived within 50 miles of the coastlines, a number that continues to rise (Cosby *et al.*, 2024). Growing world population and increase in anthropogenic activity have significant effects on coastal ecosystems, and in particular estuaries (Freeman *et al.*, 2019). Through industrial, agricultural and urban wastewater run-off, an increasing range of pollutants, including trace metals, pesticides and contaminants of emerging concern (CECs) enter estuarine environments, as illustrated in Figure 1.1. Rivers play an important role in the transport of nutrients and contaminants from point and regional terrestrial sources and cause the pollutants to travel long distances until they reach the sea. In addition to river inflow, atmospheric deposition and groundwater inflow are contributing sources to estuarine pollution (Iglesias et al., 2020). The variety of chemical compounds and their degradation products entering estuaries reduces water and sediment quality and poses risks for both ecosystems and human health.

Estuarine systems have been shown to filter the input of different contaminants before they enter the ocean due to their physicochemical gradients and biogeochemical processes (de Souza Machado *et al.*, 2016; Cundy and Croudace, 2017; Celis-Hernandez *et al.*, 2021). In particular fine-grained estuarine sediments, due to their large reactive surface area and frequently high organic matter content, can act as sinks for more particle-reactive contaminants affecting contaminant transport, deposition and accumulation. As such, estuarine sediments play a crucial role in contaminant sequestration and mediating the contaminant transfer from land to ocean. Understanding these sediment-contaminant interactions is therefore essential

for evaluating contaminant behaviour and ecosystem risk in estuarine, and ultimately in coastal and offshore marine systems (Cundy and Croudace, 2017).

1.2 Contaminants of (Emerging) Concern

Pollution is one of the drivers of the "triple planetary crisis", alongside climate change and biodiversity loss, threatening the health of our planet's ecosystems (Baste and Watson, 2022). While plastic pollution in rivers and on coastlines represents a more obvious problem, a substantial portion of environmental contamination remains largely invisible. Globally, over 350,000 chemicals and mixtures for production and use have been registered in 19 countries, with many of these compounds' identities unknown (Wang *et al.*, 2020). This vast and largely uncharacterised chemical inventory stems from all sectors of anthropogenic activity, highlighting the complexity of potential environmental contamination.

These substances differ in their physical and chemical properties, impacting their environmental behaviour, with many known to persist in the environment and pose risks to human and ecological health. Some contaminants have been known to occur in the environment since the 1970s or earlier and are relatively well researched, for example trace metals and polycyclic aromatic hydrocarbon (PAHs)(Laxen and Harrison, 1977; Lake *et al.*, 1979; Nriagu, 1996). The environmental and health risks associated with some of these substances became apparent early on, leading to their regulation or ban, such as dichlorodiphenyltrichloroethane (DDT) which was restricted by the Stockholm Convention on Persistent Organic Pollutants (United Nations Environment Programme (UNEP), 2019b). Other contaminants have gained attention more recently due to advances in analytical methods or their novelty (Fawell and Ong, 2012). These contaminants are often referred to as contaminants of emerging concern (CECs) and include different substance groups, such as pesticides, pharmaceuticals and personal care products, of which many are either toxic, persistent, endocrine disrupting, bioaccumulative in organisms, or all of these (Kümmerer, 2011; Chaturvedi *et al.*, 2021). What they have in common is the lack of regulation or monitoring due to their relatively recent emergence as contaminants of significant health and environmental impact.

1.2.1 Trace Elements

1.2.1.1 Sources and Pathways

Major and trace metals are naturally occurring compounds with regionally varying environmental concentrations. The chemical form and speciation of metals influence their

environmental fate, behaviour, and toxicity to humans. Some metals, including trace elements such as Zn, are essential to living organisms and help to maintain biological functions and health. However, even essential metals cause harm and show toxic effects on organisms exposed to excessive quantities. When trace element concentrations exceed natural background levels, they are classified as contaminants (Hanfi, Mostafa and Zhukovsky, 2020). Major sources of metal contamination include anthropogenic activities, such as smelting, mining, traffic emissions, fossil fuel combustion, industrial manufacturing processes, and agricultural and domestic applications (Hanfi, Mostafa and Zhukovsky, 2020).

International and national treaties try to control the release of these contaminants, such as the Aarhus Protocol from 1998 for controlling emissions of heavy metals in Europe, the Minamata Convention from 2013 for Hg globally, or the global phaseout of tetraethyllead as an antiknock agent in gasoline over the past 20 - 40 years (United Nations, 1998; United Nations Environment Programme (UNEP), 2021, 2024). Nriagu (1996) noted, that trace metal emissions have declined since the 1970s, with average reductions of 46% for Cd, Hg and Pb emissions between 2005 and 2022 in Europe (Figure 1.2), due to stricter legislative controls on the emissions of these metals (European Environment Agency, 2024).

Figure 1.2: European emission trends for trace elements Cd, Hg and Pb, constantly declining from 2005 to 2022 (European Environment Agency, 2024).

Despite global restrictions, emissions of trace metals remain high. In 2015, an estimated 2220 tons of Hg were emitted worldwide, and production of mined metals continues to rise (United Nations Environment Programme (UNEP), 2019a). As of 2023, global copper production has increased to 22.4 million tons, while Zn and Pb production have remained stable at approximately 12.9 million tons and 13.7 million tons, respectively, between 2020 and 2024 (International Copper Study Group, 2024; International Lead and Zinc Study Group (ILZSG), 2025). Unlike organic substrates, metals cannot be broken down in the environment; instead; they change from one chemical form to another. Therefore, every toxic trace metal released into the environment stays there unless it is actively removed.

1.2.1.2 Environmental and Health Risks

Trace elements such as Hg, Pb, Zn and Cu can be highly toxic at elevated concentrations and possible health consequences for long-term exposure to those metals include neurological, physical and muscular degeneration (Järup, 2003). Common pathways for human exposure to metals include food and air. Fish and seafood are prominent examples for metal exposure, as they accumulate toxic compounds in their tissues by feeding on microorganisms and other small fish that have absorbed metals from the surrounding environment (Stemberger and Chen, 1998; Hillyer *et al.*, 2022). Consequently, the ingested chemicals become enriched within the trophic food chain and ultimately lead to human exposure through the consumption of contaminated fish, often at toxicologically relevant concentrations of trace metals. One notable example of trace metal poisoning from seafood consumption is Minamata disease, which arose from excess methylmercury (CH_3Hg). In the 1950s, several outbreaks of a severe neurological illness in fishing villages around Minamata City, Japan, were traced back to years of discharging mercury into the sea by industrial manufacturing (Förstner and Wittmann, 1981).

The presence of trace metals in estuarine sediments can harm benthic species in various ways. For instance, Sunda, Tester and Huntsman (1990) reported that elevated Cu and Zn concentrations in the Elisabeth River Estuary (USA) reduced the survival rate of copepod larvae (*Acartia tonsa*). King, Gale and Stauber (2006) demonstrated that the ingestion of sediment is an important source of Zn and Cu for the estuarine amphipod species *Melita plumulosa*, leading to toxic effects. Exposure to Pb, Zn and Hg resulted in cellular damage and oxidative stress responses in three benthic invertebrate species (Hillyer *et al.*, 2022). In another study, the estuarine fish species *Pomatoschistus microps* was exposed to Cu and Hg and results indicated a decline in fitness and subsequently, survival in the wild (Vieira *et al.*, 2009). Furthermore, Ye et al. (2021) found that while the estuarine species *Cyprinodon variegatus* can be tolerant to CH_3Hg, it simultaneously serves as a source of this toxic compound for higher trophic level predators.

The bioavailability and toxicity of trace metals to estuarine organisms varies based on the chemical form of the metals, which in turn, depends on specific estuarine conditions.

1.2.1.3 Occurrence and Fate in Estuarine Systems

The fate and behaviour of trace metals in estuarine environments have been investigated previously. Trace metals, including Cu, Zn, Pb, Ni, Cd and Cr have been found to be enriched in estuaries across the United Kingdom (UK), Iran, Brazil and Vietnam, with several concentrations at levels that pose environmental risks (Koukina and Lobus, 2020; Jahromi *et al.*, 2021; Celis-Hernandez *et al.*, 2022; Passos *et al.*, 2022). The interactions between trace metals and

estuarine sediments have been the focus of extensive study. Iftikhar et al. (2022) identified correlations between the distribution of trace metals and organic carbon content, a finding that Miranda et al. (2021) partly confirmed by noting that particulate organic matter is the predominant nutrient factor in riverine sediments, whereas particulate phosphorus has a greater influence under estuarine conditions. They also concluded that the mineralogical composition of sediments influencing the cation exchange capacity and surface area is the most important factor in trace metal – sediment interactions overall (Miranda *et al.*, 2021). Other factors affecting the fate and behaviour of trace metals in estuarine sediments include precipitation and salinity, as shown in the Cai-Nha Trang estuary in Vietnam, located in the South China Sea (Koukina and Lobus, 2020).

Due to their ability to sequester trace metals, sediment cores have been used to assess the history of coastal contamination (Goldberg *et al.*, 1977; Valette-Silver, 1993). The recognition that sediments could be used as records for anthropogenic contamination has driven further research into the mechanisms of trace metal binding to sediments. Salomons & Mook (1977) studied trace metal concentrations in sediments from two German river estuaries, and hypothesised, that trace metals bind to fine-grained particles within the organic matter fraction. Sholkovitz & Copland (1981) examined the physical and chemical properties of trace elements and humic acids in estuarine sediments from Scotland, UK and discovered that field observations do not always align with predictions from models or lab experiments (Sholkovitz and Copland, 1981). The adsorption behaviour of Cd and Pb to Fe/Mn oxides and organic coatings of estuarine particulate matter was researched by Lion et al. (1982) in the San Francisco Bay estuary sediments. In the same estuary forty years later, the effectiveness of sediment cores in capturing non-native metal species such as Hg as indicators of anthropogenic activities was successfully demonstrated (Himson *et al.*, 2023). Globally, sediments have been used to characterise trace metal concentrations; for example, studies conducted in Chinese estuaries by Zhou et al. (2014). They examined the vertical distribution of trace metals in sediment cores and found several trace elements, such as Cu, Cr and Hg, enriched in fine particles and clays. Cundy et al. (1997) validated the reliability of salt marsh sediment cores as “geochemical recorders” of trace metal pollution in estuaries in southern England. The fact that anthropogenic metals, such as Cu, Pb, Zn and Co have been preserved in the cores over years without significant migration agrees with previous findings about the potential of estuaries as sediment traps for contaminants.

Although many studies exist about trace metal behaviour in sediments, varying environmental conditions might result in unexpected metal behaviour. Furthermore, the influence of sedimentary properties on contaminant mobility remains unclear, necessitating additional

research to identify the drivers behind trace metal sequestration in light of increasing anthropogenic activity.

1.2.2 Polycyclic Aromatic Hydrocarbons (PAHs)

1.2.2.1 Sources and Hazards

Polycyclic aromatic hydrocarbons (PAHs) are a group of well-known organic contaminants that include hundreds of components based around the "building block" of a benzene ring structure. A key physicochemical property of PAHs is their hydrophobicity, which is commonly quantified using the n-octanol-water partition coefficient ($\log K_{OW}$). Compounds with values <1 are considered hydrophilic. The higher the value (> 1), the more soluble the substance is in n-octanol or other lipophilic compounds. Values for PAH $\log K_{ow}$ lie between 3 and 7 and increase with the number of aromatic rings, hence hydrophobicity for PAHs increases with molecular weight (Sahu and Pandit, 2003).

PAHs are primarily generated through incomplete combustion of organic materials. While natural processes such as forest fires and volcanic activity do contribute to PAH emissions, predominant sources are anthropogenic, and include residential heating via combustion, motor vehicle exhausts, and industrial processes such as asphalt, coke, and aluminium production. The emitted PAHs ultimately return to terrestrial and aquatic environments through atmospheric deposition (Mallah *et al.*, 2022). Oil spills are another pathway for PAHs to enter marine and estuarine environments. Due to their chemical stability and hydrophobicity, PAHs are persistent and ubiquitous in the environment. Their lipophilic nature facilitates bioaccumulation in organisms, leading to considerable ecological and human health risks. PAHs have been shown to have several ecotoxicological impacts on marine organisms, including cardiotoxicity and hepatocarcinogenesis (Incardona and Scholz, 2016; Souza *et al.*, 2016). Studies have shown that PAHs can have similar toxic effects as dioxin-like substances, causing haemorrhaging, morphological abnormalities and early-life stage mortality in fish embryos (Barron, Heintz and Rice, 2004; Magnuson *et al.*, 2018).

The main exposure pathways for humans to PAHs are inhalation and ingestion (Menzie and Santodonato, 1992). PAH compounds have been detected in human breast milk and placentas, demonstrating their widespread presence (Yu *et al.*, 2011; Torres-Moreno *et al.*, 2022). Some of these compounds are highly carcinogenic; they are also related to cardiovascular diseases and sleeping disorders (Boffetta, Jourenkova and Gustavsson, 1997; Armstrong *et al.*, 2004; Holme *et al.*, 2019; Yang *et al.*, 2025).

Due to serious environmental and health consequences to the exposure of PAHs, environmental restrictions have been implemented for some PAH compounds, e.g., in the European Parliament and Council framework directives for environmental quality standards and the framework directive on industrial emissions (European Parliament and Council, 2008, 2010).

1.2.2.2 Occurrence and Fate in Estuarine Systems

Due to their hydrophobic nature, PAHs tend to accumulate in sediments, driven primarily by hydrophobic and π-π interactions with sediment surfaces (Yang, Wang and Niu, 2011). PAHs have been found in all compartments of the environment and relatively extensive work has been done on PAH fate and behaviour in estuarine sediments and their sorption behaviour. In Narragansett Bay, United States of America (USA), PAHs in sediments were detected already in 1979 with clear indication of anthropogenic activity as cause for the PAH distribution (Lake *et al.*, 1979). PAHs were also found in surface and core sediments in correlation with organic matter of the Portuguese shelf (Mil-Homens *et al.*, 2025). In the Yangtze River estuary, China, PAHs were found at a mean concentration of 140 ng/g, indicating low to medium ecological risks, whereas the Thames estuary, UK, was used to reconstruct historical PAH trends from sediment cores (Liu *et al.*, 2020; Downham *et al.*, 2024). In the Pearl River estuary, China, PAHs were predominantly associated with the particulate, rather than the dissolved phase and water temperature was found to be a dominant factor controlling the transport and distribution of PAHs (Niu *et al.*, 2018). Chen et al. (2020) demonstrated in the Salt River estuary, Taiwan, that lower molecular weight PAHs show a different partition behaviour in estuarine sediment-water systems than higher molecular weight PAHs. Seasonal variations in salinity and suspended sediment concentration were identified as key factors controlling the PAH association with suspended particulate matter (SPM) in the Cross River estuary, Nigeria (Oyo-Ita *et al.*, 2022). Additionally, mass-transfer models have been employed to analyse sorption behaviour in marine environments, using phenanthrene as a representative compound and revealing correlations with water temperature and organic carbon content (Yu *et al.*, 2024). Recent studies have suggested that the presence of trace metals can change the adsorption behaviour of PAHs, promoting non-linear adsorption (Duan *et al.*, 2022).

PAHs as more established contaminants have been investigated relatively extensively in the scientific literature. However, their fate and behaviour in changing and highly dynamic environments is difficult to assess, particularly if combination with other contaminants changes their behaviour. Due to their hydrophobicity, PAHs easily adsorb to sediments. Given their ecological and human health impacts, it is essential to understand the processes that control their distribution and persistence in estuarine sediments.

1.2.3 Hormones

1.2.3.1 Chemical Properties

Hormones are biomolecules that play vital roles in various processes within both vertebrates and invertebrates. Through complex signalling pathways and hormone receptors, they regulate critical tissue and organ functions, such as reproduction and metabolism throughout the lifespan of an organism (United Nations Environment Programme (UNEP) and World Health Organisation (WHO), 2013). Slight fluctuations in hormonal balance can disrupt organ and tissue functions, potentially causing serious diseases, obesity or infertility (United Nations Environment Programme (UNEP) and World Health Organisation (WHO), 2013).

Steroidal hormones are characterised by a carbon skeleton of three cyclohexane rings and one cyclopentane ring, alongside various functional groups. The carbon framework contributes to their hydrophobic character. Steroidal hormones have $\log K_{OW}$ values between 2.1 and 4.1 and are moderately hydrophobic (Dai *et al.*, 2022).

The more hydrophobic a hormone, the more readily it partitions into sediments through hydrophobic interactions. Consequently, $\log K_{OW}$ values are useful indicators for estimating the sediment-water distribution of hormones. Other parameters for describing a compound's behaviour in soil or sediments include the soil/sediment adsorption coefficient K_d and the organic carbon normalised adsorption coefficient K_{OC} (or $\log K_{OC}$) of a substance. Higher $\log K_{OC}$ values indicate stronger adsorption onto organic matter (Lee *et al.*, 2003). Several studies found that $\log K_{OW}$ values significantly correlate with $\log K_{OC}$, indicating that hydrophobic partition interaction between the hormone and sediment is an important factor driving sorption processes of hormones in sediments (Yang *et al.*, 2019; Dai *et al.*, 2022).

In addition to their hydrophobic carbon core, steroidal hormones also contain polar functional groups, such as hydroxy or ketone groups, which can form hydrogen bonds with compatible functional groups in the soil/sediment (Yang, Lin, Zhang, *et al.*, 2020). Moreover, due to the aromatic rings in the hormone structure, π-π bonds can form between those aromatic rings and aromatic groups of the organic matter, such as aromatic amines (Zhu *et al.*, 2004; Lima, Schneider and Esteves, 2012). Thus, in addition to hydrophobic partition interactions and hydrogen bonding, π-π bonds play an important role in the sorption mechanisms of hormones (Figure 1.3). Positive correlations between the aromatic units in organic matter and K_{OC} values of hormones have been reported by both Lima, Schneider and Esteves (2012) and Yamamoto et al. (2003). The potential interactions between hormones and sediments discussed above are illustrated in Figure 1.3.

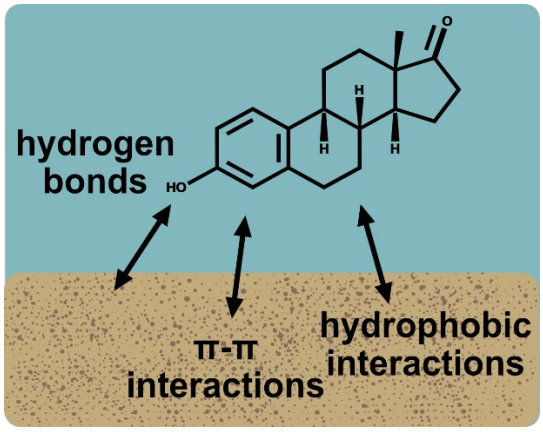

Figure 1.3: Hormone-sediment adsorption interactions: hydrogen bonds between a hydrogen atom and a hydrogen bond acceptor, π-π interactions between aromatic groups and hydrophobic interactions between nonpolar regions. Created using Affinity Designer 1.

Naturally occurring hormones have been repurposed for various applications in modern activities, including supplemental growth hormones for livestock and human contraceptives (Adeel *et al.*, 2017). It is estimated that farm animals in the EU and USA excrete approximately 990 tons of hormones per year, which substantially exceeds the natural and synthetic hormone excretion by the human population, estimated at around 750 kg annually (Lange *et al.*, 2002; Combalbert and Hernandez-Raquet, 2010). When present in excess, or metabolised by unintended organisms, these hormones act as endocrine disruptors, blocking or interfering with natural hormonal functions, leading to various illnesses or infertility issues. Awareness of the risks associated with widespread occurrences of hormones in the environment has arisen more recently than that of PAHs and trace metals. Hormones are considered contaminants of emerging concern, and as such, are neither regulated nor regularly monitored in the environment.

1.2.3.2 Environmental and Health Risks

Hormones play vital roles in numerous bodily processes. However, unintended or excessive hormone exposure can interfere with the endogen system of organisms (United Nations Environment Programme (UNEP) and World Health Organisation (WHO), 2013). Numerous studies have explored the impacts of hormones on different organisms.

For instance, Purdom et al. (1994) were the first to investigate vitellogenin concentrations in fish near sewage treatment works in England. Under natural (estrogen-poor) conditions, male fish do not express the vitellogenin gene, making plasma vitellogenin levels reliable biomarkers for estrogen exposure (Harries *et al.*, 1997). Exposed trout showed significant increases in plasma vitellogenin concentration at 15 different sites, which Purdom et al. (1994) ascribed to the

artificial hormone ethinylestradiol (EE2), or other endocrine-disrupting substances. Subsequent laboratory experiments assessed the risks of hormones on aquatic organisms. For example, in vivo laboratory experiments showed that increased progestin concentrations led to masculinisation of female fish and adversely affected reproduction and egg production even at low levels (Runnalls *et al.*, 2013). Conversely, estrogen hormones such as estrone (E1), estradiol (E2), EE2 and estriol (E3) caused pathologic effects, including intersex conditions and mortality in male Japanese rice fish ("medaka") (Nimrod and Benson, 1998; Metcalfe *et al.*, 2001). Long-term studies by Kidd et al. (2007, 2014) in the Experimental Lake Area of Canada found that chronic exposure to low hormone concentrations did not harm invertebrate communities, likely because these organisms lack hormone receptors (Kidd *et al.*, 2014). However, chronic low exposure caused feminisation in male fish of smaller species, leading to near extinction of the species, which consequently allowed zooplankton and insect populations to thrive, highlighting that even minimal hormone elevation can disrupt entire ecosystems (Kidd *et al.*, 2007, 2014). A risk assessment conducted in 2022 found that three steroid hormones (estriol, estrone and cyproterone) ranked among the top ten endocrine-disrupting chemicals (EDCs) posing significant environmental risks (Grobin, Roškar and Trontelj, 2022).

1.2.3.3 Occurrence and Fate in Estuarine Systems

Hormones primarily enter aquatic environments through effluents from municipal and industrial wastewater treatment plants (WWTPs), leachates from landfills, and agricultural runoff. As a result, they have been detected in soils, rivers, and marine environments all over the world (Chaturvedi *et al.*, 2021).

The Pearl River Delta (PRD) in China is among the most studied regions for the occurrence of hormones and other endocrine disrupting chemicals (EDCs). Yuan et al. (2015) reported total EDC concentrations of approximately 40 ng/g in sediment samples of the Pearl River. Further studies in this region identified natural hormones such as estrone (E1) and estradiol (E2), as well as the synthetic hormone ethinylestradiol (EE2), in surface waters of the northern shelf of the South China Sea (Deich *et al.*, 2021). Untreated sewage discharges have been shown to significantly contribute to the river pollution by EDCs (Xu *et al.*, 2014). Residues of E1, E2 and other EDCs were also detected in tissues of wild fish collected in the area (Lv *et al.*, 2019).

Similar results were found in other regions globally, e.g. in coastal and estuarine ecosystems In Brazil and Portugal, or in surface water from Cape Town, South Africa (Olatunji *et al.*, 2017; de Sousa *et al.*, 2018; Morais *et al.*, 2023; Santos *et al.*, 2024). In rivers within Greater London and Southern England, mean concentrations for EE2 were 0.23 ng/L, with sediment cores revealing varying concentrations of E1, E2, and EE2 (Labadie *et al.*, 2007; Wilkinson *et al.*, 2017). For

example, E1 levels ranged from 3.3 ng/g to 28.8 ng/g in different sediment depths, indicating that hormones migrate through sediments (Labadie *et al.*, 2007).

In the Scheldt estuary, Belgium, hormone concentrations were assessed across dissolved, particulate, and sediment phases and results showed higher concentrations in the dissolved phase. Compared to previous studies, the authors concluded that estrogenic activity in sediments decreased during the last 40 years (Jia *et al.*, 2024). Yarahmadi et al. (2018) detected E1 and E3 only in the dissolved phase, while EE2 was primarily found in the particulate phase, with hormone concentrations exhibiting seasonal variations.

Several studies have examined the relationship between sediment properties and the environmental behaviour of steroidal hormones. Bioavailability experiments simulating turbulent conditions (e.g., flood events) demonstrated that hormones E1, E2, and EE2 can be remobilized from sediments and become bioavailable at ecotoxicologically relevant concentrations (Müller *et al.*, 2019). One study found that natural mineral colloids, like illite, and the presence of humic acid enhanced EE2 transport through saturated porous media, while loamy clay hindered it (Song *et al.*, 2024). Research by Sangster et al. (2015, 2016) showed that organic carbon content in sediments significantly influences estrogen behaviour, more so than particle size. Additionally, the ecotoxicological impact of progesterone on fathead minnows was found to be lower in silty loam compared to sand (Sangster *et al.*, 2016). Neale et al. (2009) showed that sorption of estrogens to organic matter was pH-dependent, with stronger sorption occurring at lower pH levels when bulk organic matter remains in a neutral, non-dissociated form.

Due to the harmful effects on ecosystems, it is important to better understand the environmental fate and behaviour of hormones. Knowledge gaps include, for example, the formation and risk of intermediates, as well as the effects of hormones with co-occurring contaminants such as trace metals or organic pollutants. Important, yet hardly addressed questions also involve the different degradation mechanisms of hormones in different environments. In particular, the extent and pathways of hormone degradation in sediments are largely unknown, and the influence of environmental factors such as redox conditions, organic matter content, and microbial activity on these processes is not yet well established. Furthermore, sediments may act as long-term sinks for hormones, potentially preserving the contaminants without any significant degradation processes.

1.3 Role of Sediments as Contaminant Sinks

The three groups of contaminants discussed here (trace metals, PAHs, and steroidal hormones) are found worldwide in estuarine sediments. Numerous studies have explored their behaviour and fate in these dynamic environments, consistently revealing that sediment properties play a crucial role in determining contaminant retention and mobility. Different sedimentary and environmental factors and their influence on contaminant adsorption, in specific, hormone adsorption are represented in Figure 1.4.

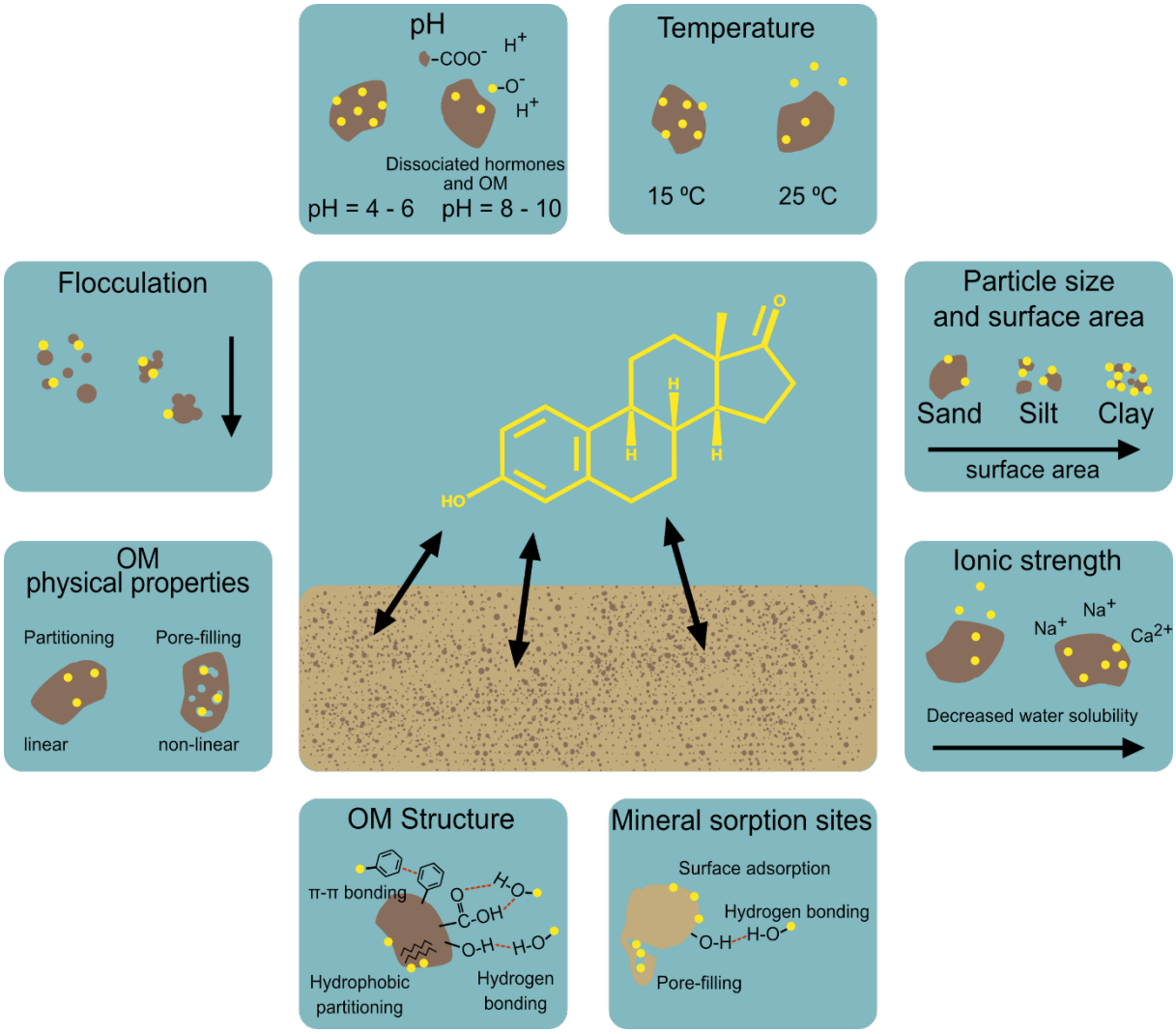

Figure 1.4: Different organic matter properties and environmental factors that influence hormone adsorption to sediments: Yellow dots indicate hormone molecules, brown blotches symbolise organic matter particles (after Dai et al. (2022)), created using Affinity Designer V1).

An important mechanism to remove contaminants from the aqueous phase and into sediments is the flocculation of suspended particulate matter (SPM), as illustrated in Figure 1.4. Fine-grained suspended sediments, including mineral fragments, organic matter and colloids, can

aggregate into larger flocs due to environmental factors such as salinity, temperature, pH, fluid shear, and sediment concentration (Kranck, 1973; Burban, Lick and Lick, 1989). It has been shown that particles flocculate faster in seawater than in freshwater, emphasising the significant role of salinity (Burban, Lick and Lick, 1989). This process is particularly relevant in estuarine sediments, where salinity changes caused by the mixing of freshwater and seawater promote the aggregation of fine particles. Once flocs form, heavier aggregates settle into the sediment bed, taking along any contaminants associated with them, and effectively removing them from the water phase. This process has been documented for trace metals and is widely used in wastewater treatment facilities to remove organic contaminants (Sholkovitz and Copland, 1981; Rodríguez-Hernández *et al.*, 2022; Virtasalo, Österholm and Asmala, 2023). Therefore, flocculation not only influences sediment transport but also significantly affects contaminant partitioning and retention in estuarine systems.

The organic carbon content in sediments has a major impact on the sequestration of organic contaminants through adsorption and partitioning processes. Sediments consist of both inorganic and organic fractions, each contributing to contaminant sorption (Figure 1.4). The hydrophobic partitioning of organic contaminants is influenced by the organic carbon content of the sediment organic matter (OM) and the presence of hydrophobic siloxane groups on mineral surfaces (Dai *et al.*, 2022). Generally, a higher organic carbon content leads to increased sorption of hydrophobic compounds. In addition, the presence of aromatic units or polar groups in both OM and the inorganic materials can favour π-π interactions and hydrogen bonds, respectively (Lima, Schneider and Esteves, 2012). Other controlling factors include particle size, mineral composition and the redox potential of sediments, all of which significantly impact sediment-contaminant interactions and therefore, persistence, bioavailability, and potential ecological risks associated with these contaminants in estuarine systems.

In addition to sedimentary properties, environmental conditions, such as pH, temperature and salinity, play a major role in the sorption processes of contaminants. These factors are particularly important in a dynamic environment such as estuaries (Figure 1.4). Moreover, changing climatic conditions have a major influence on these environmental parameters. As Müller et al. (2019) demonstrated, hormones become readily bioavailable from sediments during flood events. Hence, sediments may release a range of previously sequestered contaminants under changing environmental conditions, acting as source, rather than sink. Consequently, it is of particular importance to understand the sorption behaviour of contaminants in sediments under changing environmental conditions.

1.4 Knowledge Gaps

Sediments are increasingly recognised as both sinks and potential sources of organic contaminants, including hormones. However, our understanding of the processes that govern contaminant trapping and mobility in sediments remains limited and inconsistent. Despite considerable research on the fate and behaviour of trace metals and PAHs, studies focusing on the fate of CECs and hormones in particular are still relatively scarce.

A broader review of pharmaceuticals and personal care products in the environment showed that hormones were addressed in only 18% of the reviewed studies, with estuarine and marine environments being the least represented ecosystems, appearing in just 1% of the studies each (Meyer, Powers and Hampton, 2019). This significant under-representation highlights a critical gap in understanding the fate of endocrine-disrupting compounds in estuarine environments, that differ widely from freshwater systems in terms of salinity, mineralogy, and organic matter composition.

Previous studies have reported conflicting results regarding the mobility and long-term fate of hormones and other contaminants in sediment cores. For instance, Labadie et al. (2007) examined two sediment cores for estrogens, one from a freshwater site and one from a clay-rich estuary in the UK. In the clay-rich core, E1 concentrations declined downcore, whereas E1 remained detectable in deeper, undisturbed layers of the freshwater core, showing the potential of migration for hormones in sediments (Labadie *et al.*, 2007). Similarly, pharmaceuticals, perfluorinated compounds and plasticisers were found to be mobile in salt marsh cores (Celis-Hernandez *et al.*, 2021). However, contrasting results also exist: some pharmaceuticals and antimicrobial agents were shown to be stable and immobile over long periods, remaining trapped in the sediment (Tamtam *et al.*, 2011; Thiebault *et al.*, 2017). These variations clearly demonstrate the need for further research into sediments as traps for contaminants.

Many existing sorption studies are limited by the lack of environmentally relevant contaminant concentrations or laboratory conditions that do not accurately reflect field environments. Such shortcomings may fail to capture the complexities of natural systems, leading to discrepancies between laboratory and field results. Furthermore, critical environmental variables, including salinity, pH, redox conditions, and temperature, significantly influence sorption. However, it is challenging to account for every variable in adsorption experiments due to the intricate experiment set-up required. Typically, only a limited range of variables is studied, leading to variable and sometimes contradictory outcomes. For instance, while some studies have reported preferential sorption of steroidal hormones on finer particle sizes, other studies added that particle size is a subordinate influence compared to organic carbon content (Qi, Zhang and

Ren, 2014; Sangster *et al.*, 2015). Similarly, findings on the influence of pH are inconsistent: some studies observed increased sorption with lower pH, while others found no impact from pH (Yamamoto and Liljestrand, 2003; Neale, Escher and Schäfer, 2009; J. Zhang *et al.*, 2013).

Organic carbon content has been frequently identified as a key factor influencing the sorption of hormones to sediments (Lai *et al.*, 2000; Sun *et al.*, 2012; Sangster *et al.*, 2015; Dai *et al.*, 2022). However, "organic carbon" is an umbrella term representing a broad range of compounds with varying structures, sources, and physicochemical properties. While many studies have reported correlations between organic carbon content and sorption capacity, relatively few have explored how specific types or sources of organic matter (e.g., algal-derived vs. terrestrial) affect sorption behaviour (Chen *et al.*, 2012; Sun *et al.*, 2012). Given that contaminant binding is likely controlled by organic matter quality (or composition) as well as quantity, this remains a crucial area for further research.

Even within the same class of compounds, significant differences in environmental behaviour have been observed. For example, natural estrogens tend to remain predominantly in the aqueous phase, while synthetic estrogens, due to their higher partition coefficients (K_{OW}), are more likely to associate with particulates (Lai *et al.*, 2000; Yarahmadi *et al.*, 2018) These differences underscore the need for compound-specific studies rather than broad generalisations across contaminant classes.

In conclusion, existing literature reveals uncertainties regarding the fate and behaviour of hormones in sediments. The interaction among contaminant properties, sediment characteristics, and environmental conditions is complex and often site-specific. Retention mechanisms that apply to one compound in one environment may not apply in another. Given the toxicity and widespread occurrence of these compounds, it is essential to improve our understanding of the processes that control their retention and mobility in sediments. Future research should focus on organic matter composition, realistic experimental setups, and under-researched environments such as estuaries.

1.5 Aims and Objectives

Knowledge gaps remain concerning the adsorption behaviour of contaminants in estuarine systems, largely due to the complex interplay of environmental variables such as sediment geochemistry, organic matter composition, salinity, and redox conditions. Given the potential ecological and human health risks many of these contaminants pose, understanding their behaviour in estuarine environments is essential for effective mitigation and management.

This thesis explores the fate and behaviour of three distinct contaminant groups (trace metals, PAHs and steroidal hormones) in two contrasting estuarine systems, with a focus on steroidal hormones as CECs and the role of sedimentary organic carbon source on the sequestration of these contaminants. The PAHs and steroidal hormones analysed within the scope of this thesis are shown in Figure 1.5.

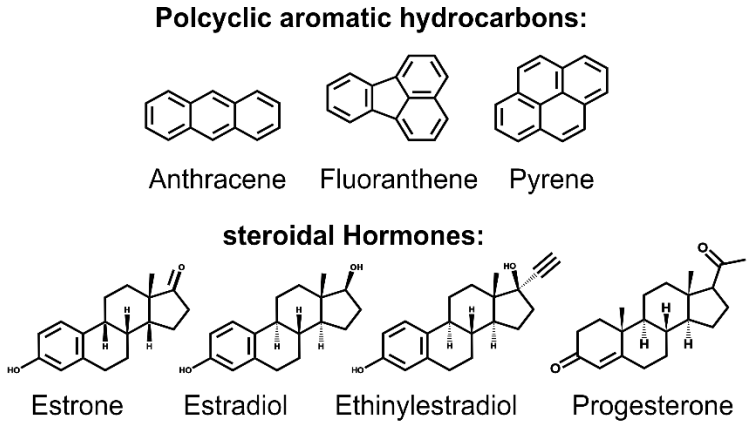

Figure 1.5: Molecular structure of three polycyclic aromatic hydrocarbons (PAHs) and four steroidal hormones, that are analysed in the scope of this thesis.

The primary aim is to understand how the type and source of sedimentary organic carbon affect the adsorption behaviour of different contaminant groups under contrasting environmental conditions. This research aim connects three studies, each described in a separate chapter of this thesis:

- Chapter 3: Spatial and Temporal Trends in Trace Element, PAH and Steroidal Hormone Contamination in a Major Urban and Industrial Estuary: Southampton Water, UK

This study examines three chemically and behaviourally distinct contaminant groups to provide an extensive overview of these contaminants in Southampton Water, an urbanised and industrialised estuary in the southern UK. It assesses spatial and temporal trends for total organic carbon (TOC), stable carbon isotopes ($\delta^{13}C$), major and trace elements, PAHs, and steroid hormones to understand the correlations between contaminant distribution, sources and sediment properties.

- Chapter 4: Controls on the Distribution and Sequestration of Steroidal Hormones, PAHs and Trace Metals in the Pearl River Delta, Southeast China

This chapter assesses the spatial distribution of various contaminant groups at a single point in time and their contamination trends over more than 100 years in the Pearl River Delta, China. Alongside trace metals, PAHs, and hormones, it analyses overall sediment characteristics (TOC, $\delta^{13}C$ and major elements). Furthermore, controls of sediment properties (including

organic matter characteristics) on contaminant distribution and behaviour, both at surface and deeper (buried) sediment levels are determined, contributing to a deeper understanding of the adsorption behaviour of chemically distinct contaminant groups in one of the most urbanised estuaries globally.

Southampton Water and the Pearl River Delta represent two estuaries that vary widely in size, levels of urbanisation, climate conditions and sediment properties. By comparing the occurrence and the fate of trace metals, PAHs and hormones in these contrasting estuarine systems, we can identify the key factors that influence contaminant fate in estuarine sediments. This includes the role of organic matter source and anthropogenic pressures. Additionally, this approach highlights how regional environmental and geochemical context affect contaminant sequestration and behaviour.

- Chapter 5: Influence of Organic Matter Type and Source on the Adsorption of Steroidal Hormones in Estuarine Systems

In this chapter, adsorption experiments are conducted using estuarine plant material derived from different organic carbon sources as sorbents. The study investigates the adsorption behaviour of the steroidal hormone estrone in the presence of varying types of organic carbon. Moreover, adsorption studies are conducted with seawater and estuarine brackish water to replicate different environmental conditions found in a dynamic estuary. Results are analysed using linear and nonlinear adsorption isotherms to determine distribution coefficients (K_d) and carbon-normalised partition coefficients (K_{OC}). This study aims to evaluate the influence of organic carbon source and salinity on the sorption behaviour of the steroidal hormone estrone in estuarine systems, thereby providing insights into the key factors controlling hormone mobility and retention in estuarine sediments.

Chapters 3, 4, and 5 are presented as manuscripts that contain individual abstracts, introductions, methods, results and conclusions, all intended for publication. In each of these co-authored manuscripts, the thesis author has led on experimental design, data collection and interpretation, and manuscript writing, while other authors contributed through experimental or sampling design, discussions on method development, data interpretation, and manuscript editing. Details of individual author contributions for each chapter can be found in the Contributor Roles Taxonomy (CRediT) (Table 1.1).

Table 1.1: Contributor Roles Taxonomy (CRediT) table for each chapter of this thesis.

Author	**CRediT**	**Chapter**
Jana-Sophie Appelt	Conceptualisation, data curation, formal analysis, investigation, methodology, validation, visualisation, writing - original draft	1 - 6
Andrew Cundy	Conceptualisation, data curation, funding acquisition, methodology, project administration, resources, supervision, writing – review & editing	1 - 6
Sargent Bray	Conceptualisation, methodology, resources, supervision, writing – review & editing	1 - 6
Jessica Whiteside	Conceptualisation, methodology, supervision, writing – review & editing	1 - 6
Wenxiong Wang	Conceptualisation, data curation	4

Chapter 2 Methods and Method Development

2.1 Sampling and Sampling Sites

In this thesis, sediment samples from two geographically distinct localities were analysed. The first site is Southampton Water in the United Kingdom, and the second is the Pearl River Delta in the South China Sea. These locations vary widely in terms of urbanisation, contamination levels, climate, and sediment properties. The diversity allows examination of contaminant trapping in two systems with differing sources and pathways, as well as variations in sediment composition and the origin of organic matter.

2.1.1 Southampton Water, UK

Southampton Water is one of the largest estuaries in southern England and is an extension of the Solent (Figure 2.1).

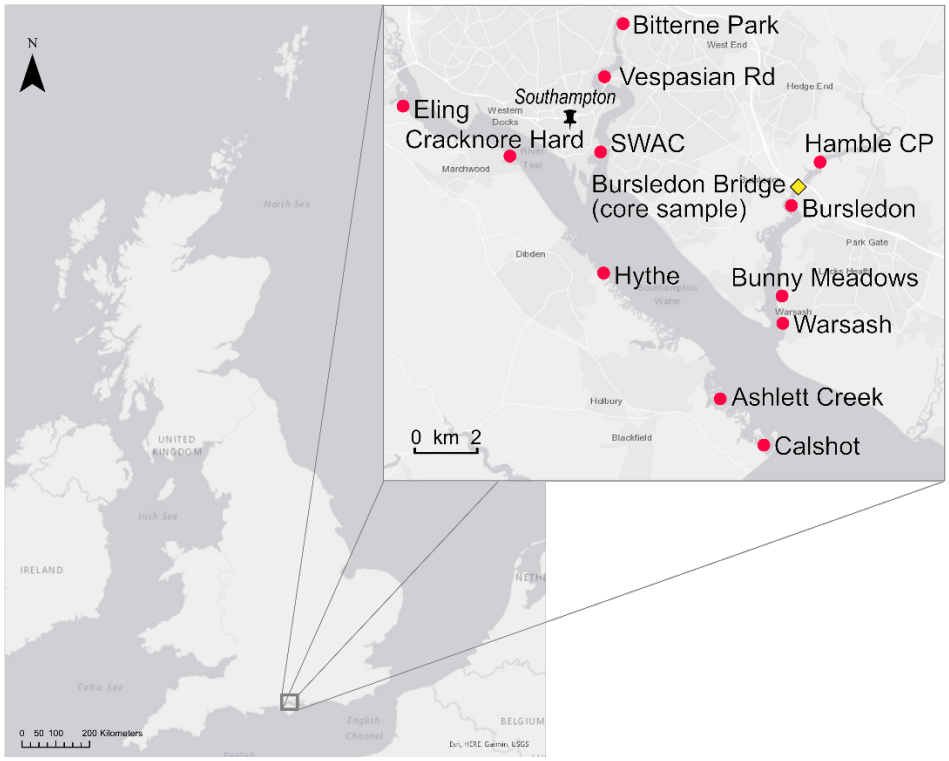

Figure 2.1: Map of the UK and Southampton Water with surface sediment sampling sites (red circles) and sediment core sampling site (yellow diamond). Created with ArcGIS Pro 3.3 using map data from Table 2.1 and Affinity Designer 1.

Southampton Water is a drowned river valley extending approximately 17 km from the estuary mouth to the tidal limit in the north and features extensive mudflat and saltmarsh areas that are influenced by tides (Figure 2.1). The rivers Test, Itchen and Hamble feed freshwater to the

estuarine system, with a combined discharge of approximately $1.54*10^6$ m^3 per day and $2*10^4$ tons of suspended sediment annually (Tubbs *et al.*, 1980). The annual suspended-sediment discharge is based on measurements from the 1980s and may have changed substantially due to land-use or hydrological changes since then. To my knowledge, no recent estimates are available for direct comparison. The estuary is partially mixed, with tidal currents facilitating the mixing of the water column. The residence time of water in the estuary ranges from 5 to 10 days (Tubbs *et al.*, 1980; Sharples, 2000). As a result, salinity levels do not vary drastically; they are nearly marine at the mouth and more estuarine near the town quay of Southampton. Due to the influence of the English Channel, Southampton Water has a unique tidal curve with a double high-water stand, and the tidal range varies between 1.5 and 3.5 m, making it a meso-tidal estuary (McLusky and Elliott, 2004; Levasseur, 2008). The concentration of suspended particulate matter (SPM) in the estuary is relatively low, ranging from 2 – 50 mg/L (Tubbs *et al.*, 1980). The saltmarsh vegetation is primarily comprised of *Halimione portulacoides* bushes, *Spartina sp.* grass and *Aster tripolium*. Southampton Water is an urbanised area with the city of Southampton to the North (population of approximately 265,000 as of 2023) and includes one of the UK's largest container ports, the Fawley oil refinery, and chemical plants on the western shore, along with several marinas (Celis-Hernandez *et al.*, 2021; Southampton City Council; and Southampton Data Observatory, 2024).

In August 2021, twelve surface scrape samples (measuring 15 cm x 15 cm x 3 cm), along with duplicates, were collected during low tide from intertidal mudflat areas around Southampton Water. The duplicates were archived in a freezer, while the working samples were freeze-dried. After drying, the samples were gently sieved using pre-cleaned 2 mm mesh sieves to remove larger shell fragments, stones and roots, and then ground to homogeneity using a pestle and mortar. Specific sampling sites are reported in Table 2.1 and are indicated in the map in Figure 2.1.

Additionally, two 30 cm long sediment cores were collected from the undisturbed Hamble saltmarsh using a Russian-style coring device in August and November 2021. The cores were placed in PVC pipes and wrapped in clingfilm to keep them hydrated. The core collected in November was frozen for archiving.

Table 2.1: Sample names, sampling dates and what3words coordinates of sampling locations for Southampton Water samples.

Sample name	Sampling Date	What3words Coordinate
Ashlett Creek	03/08/2021	draining.backyards.trainers
Bitterne Park	04/08/2021	ahead.poem.boat
Bunny Meadows	04/08/2021	creatures.tumblers.funds
Bursledon	04/08/2021	haven.dime.couple
Calshot	03/08/2021	important.riper.motored
Cracknore Hard	03/08/2021	either.bumpy.lung
Eling	03/08/2021	plants.topic.began
Hamble CP	04/08/2021	round.applies.tastings
Hythe	03/08/2021	price.sailor.zone
SWAC	04/08/2021	assure.rises.bets
Vespasian Road	04/08/2021	guitar.unless.pumps
Warsash	04/08/2021	archive.suitably.parkland
Bursledon (Hamble) Core	06/08/2021	trap.share.finds

2.1.2 Pearl River Delta, China

The Pearl River Delta (PRD) is a coastal plain estuary and covers an area of approximately $4.4*10^5$ km^2 in southern China, making it one of the largest estuarine systems globally (Figure 2.2) (Zhang, Gan and Yang, 2024).

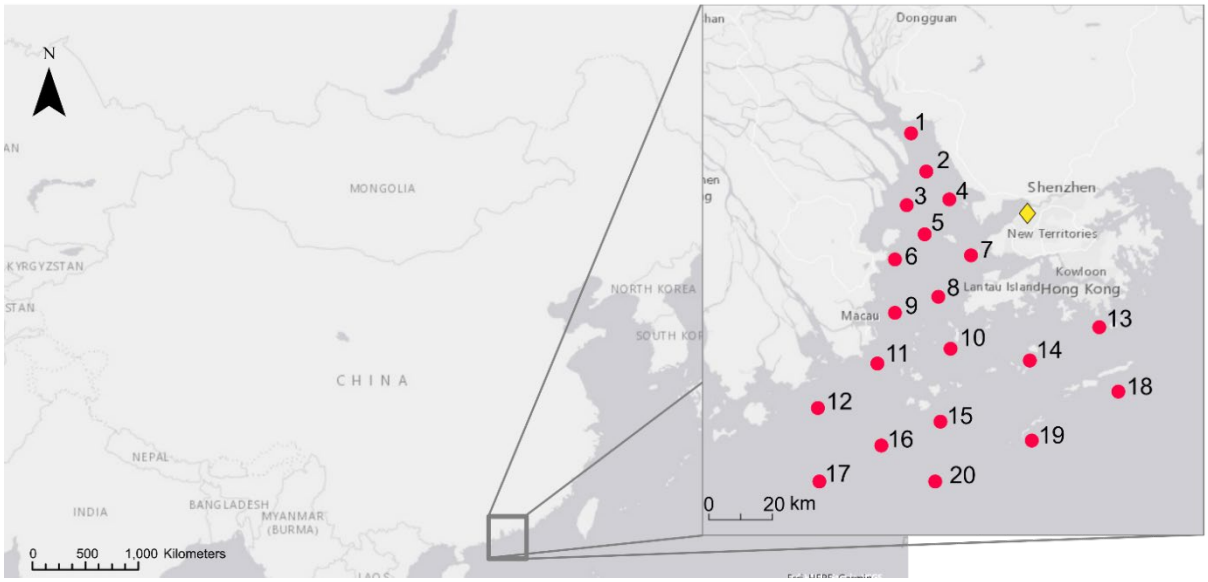

Figure 2.2: Location of the PRD surface sediment (red circles) and core (yellow diamond) sampling sites in China. Created with ArcGIS Pro 3.3 using map data from Table 2.2 and the software Affinity Designer 1.

It spans both tropical and subtropical climate zones and is annually influenced by monsoon rains. The rivers Xijiang, Beijiang and Dongjiang deliver roughly $3.5*10^{11}$ m^3 of fresh water and $8.5*10^7$ tons of sediment each year into the South China Sea (He *et al.*, 2016; Li *et al.*, 2023). The mean suspended sediment concentration is 172 mg/L, which varies both spatially and seasonally (Wai *et al.*, 2004). The mean tidal range in the delta varies between 1 and 1.7 m (Li *et al.*, 2023).

Over the past thirty years, the PDR has experienced rapid growth and is now one of the most densely populated and urbanised regions in the world, with an estimated population of over 86 million people, including major cities such as Hong Kong, Macau and Guangdong. The region is also the economically wealthiest in Southern China and serves as a manufacturing hub for the pharmaceutical, electronic and textile industries. However, excessive anthropogenic activity and monsoon-related increased discharge rates from rivers contribute to massive contamination in the PRD (Mai *et al.*, 2005).

In January 2021, twenty surface sediment samples were collected via surface grab sampling from a research vessel operated by the Chinese Academy of Sciences. Additionally, a 90 cm

long sediment core was obtained from the Mai Po wetland of Shenzhen Bay in May 2022. This core was subsampled into 1.5 cm sections. Both the surface and core subsamples were freeze-dried and shipped to the UK for further analysis.

Table 2.2: Sampling dates and what3words coordinates for the 20 PRD surface sediment and core samples.

Sample name	Sampling Date	What3words Coordinate
1	07/01/2021	fibs.unforgettable.springs
2	07/01/2021	seedlings.twists.charters
3	07/01/2021	misuses.amply.squirmy
4	09/01/2021	inflect.strewn.mighty
5	09/01/2021	commonness.bravery.ungreased
6	10/01/2021	homeward.pirouetted.occasionally
7	09/01/2021	stalemated.oversight.handbasket
8	10/01/2021	tangled.reflected.remedial
9	10/01/2021	deftly.flood.scowls
10	10/01/2021	crumbling.concussion.controls
11	11/01/2021	twitch.crank.unregistered
12	11/01/2021	thanks.misdirection.forgives
13	14/01/2021	exists.motive.stems
14	14/01/2021	dissect.pentagon.sunglasses
15	11/01/2021	cleanses.outweigh.defeatist
16	12/01/2021	gangling.festivity.diversified
17	12/01/2021	advertises.allot.decompression

18	13/01/2021	gastronomy.lobs.safety
19	13/01/2021	playpens.brotherly.nerds
20	12/01/2021	ambidextrous.longs.awfulness
PRD Core	22/05/2022	(approx.) crest.liners.valid

2.2 Inorganic Analysis

The sediment core collected from Southampton Water in August 2021 was analysed at the British Ocean Sediment Core Research Facility (BOSCORF, Southampton, UK) using a COX Analytical Systems ITRAX X-ray Fluorescence (XRF) Scanner. The scanner operated with a step size of 200 µm and 30-second scan time for the target elements including copper (Cu), lead (Pb), zinc (Zn), barium (Ba), iron (Fe), manganese (Mn), and sulphur (S). To ensure instrument reproducibility, 10% of the core length was scanned in triplicate, resulting in percentage deviations for the target analytes as follows: S: 20%, Mn: 10%, Fe: 11%, Cu: 6%, Zn: 10%, Pb: 11%. Following XRF analysis, the core was sectioned in 150 mm segments, which were then freeze-dried, sieved (at 2 mm) and ground to homogeneity for further analysis.

To date the sediment cores, measurements of the radionuclides ^{210}Pb and ^{137}Cs were made using γ-ray spectrometry with High Purity Germanium (HPGe) well-type detectors (Mirion Technologies, Hampshire, UK). Sedimentation rates were determined using the "simple" constant flux, constant sedimentation rate (CF:CS) model for ^{210}Pb and by correlating subsurface activity maxima with periods of known fallout from events such as above-ground nuclear weapons testing for ^{137}Cs (Abril-Hernández, 2023). Counting errors for both ^{210}Pb and ^{137}Cs were around 2σ, with a limit of detection (LOD) of 0.5 Bq/kg.

Mercury (Hg) concentrations in the sediment surface and core samples were measured using a Milestone Direct Mercury Analyzer, with each sample measured twice. The LOD for Hg was 0.007 mg/kg and the method uncertainty was 8%.

For the freeze-dried surface samples from Southampton Water, major and trace elements were analysed externally with a Rigaku ZSX Primus II wavelength dispersive X-ray fluorescence (WDXRF) spectrometer equipped with a Rh tube at the School of Earth and Environment, University of Leeds. Trace element analyses involved mixing powdered samples with CEROX binder in a 4:1 ratio. Major elements were determined from fused glass beads prepared with a

sample to flux ratio 1:10 (66% Lithium (Li) tetraborate: 34% Li metaborate flux). The loss on ignition (LOI) was calculated by measuring the mass difference of sample aliquots before and after heating to 1025 °C. Reproducibility for certified reference material BCR was ± <3% for TiO_2, Fe_2O_3, MgO, CaO, Na_2O and K_2O; ± 3 – 5% for SiO_2 and P_2O_5, and ± 8.5 and 8.2 for Al_2O_3 and MnO, respectively. A second reference material (stream sediment, STSD4) was analysed alongside the samples, yielding a relative standard deviation (RSD) of ± <3% for MnO, MgO, CaO, Na_2O, K_2O, and P_2O_5; 3.5% for SiO_2 and 6 to 8% for TiO_2 and Al_2O_3.

To minimize the effects of grain size on heavy metals and assess possible enrichment, trace metal concentrations (excluding Hg) in the surface samples were normalised to the conservative Al_2O_3 contents before conducting statistical analysis. Aluminium-corrected values were used for all statistical calculations, except for the geoaccumulation index.

For the PRD surface and core samples, major elements were determined using a PANalytical Axios mAX wavelength dispersive XRF spectrometer. LOI was measured by weighing samples before and after heating to 950 °C, followed by the preparation of glass fusion beads with a di-lithium tetraborate (flux) to sample ratio of 10:1 using a Vulcan Automatic Fusion Machine. The RSD for reference materials BHVO2 and PM-S for Al_2O_3, CaO, Fe_2O_3, K_2O, MgO, MnO, Na_2O, P_2O_5, SiO_2, TiO_2 and Cr_2O_3 ranged from 0.6-1.7%, and 0.6-6.1%.

For the PRD samples, trace elements were prepared by digesting 0.2 g of freeze-dried sample with acid (aqua regia) using a CEM Mars6 Microwave Digestion System, followed by analysis with an Agilent 8900 triple-quadrupole inductively coupled plasma mass spectrometer (QQQ-ICP-MS) in He mode. Analytes were measured alongside four procedural blanks and eight external standards (with concentrations ranging from 0.2 to 240 µg/kg) used for quantification. The RSD from five repeated measurements for the elements Cr, Ni, Cu, Zn, Ba and Pb varied between 0.3 and 5.2%. LODs were calculated based on 3*σ of the blank concentrations, yielding the following: Cr: 0.2 µg/kg, Co: 0.04 µg/kg, Ni: 0.8 µg/kg, Cu: 0.1 µg/kg, Zn: 18.2 µg/kg, Ba: 0.02 µg/kg, Pb: 0.02 µg/kg.

Total inorganic carbon (TIC) for the core and surface sediment samples from both the PRD and Southampton Water was determined using an AutoMate with CM5015 coulometer (LOD 1.6 wt%). A 100% $CaCO_3$ standard was used for quality control, with a percentage deviation of 0.3%. The $\delta^{13}C$ isotope analysis and elemental concentration of %C and %N from bulk organic matter were measured using an Elementar Vario Isotope Select Elemental Analyser interfaced with an Isoprime GeoVisION continuous flow isotope ratio mass spectrometer (IRMS) (Isoprime 100). The isotopic ratios were referenced against Vienna PeeDee Belemnite (VPDB) standard for

$\delta^{13}C$ and atmospheric N_2 served as the reference for $\delta^{15}N$. Analytical precision was 0.02 ‰ for $\delta^{13}C$ and 0.1 ‰ for $\delta^{15}N$, respectively.

2.3 Data Analysis

Principal component analysis (PCA) was performed using the open software RStudio. Prior to PCA, the datasets were standardised to compare variables with varying units and scales, using R's built-in scaling function (scale = TRUE). For triplicate samples, the average, the standard deviation and relative standard deviation were calculated to ensure reproducibility. Datasets were tested for statistical outliers: values falling outside the 1.5 times interquartile range were defined as statistical outliers. Graphics were created using the software Affinity Designer. Language AI models (Grammarly, ChatGPT-4) were used for text editing in the final version of this thesis.

2.4 Method Development for the Simultaneous Analysis of PAHs and Hormones in Sediment

2.4.1 Materials

Methanol (MeOH), dichloromethane (DCM) and hexane were purchased from Rathburn Chemicals, UK, N,O-bis(trimethylsilyl)tri-fluoroacetamide with 1% trimethylchlorosilane (BSTFA-TMCS) for derivatisation was obtained from Sigma Aldrich. The analytical standards for estrone, estradiol, ethinylestradiol, progesterone, estrone-3-methylether, fluoranthene and pyrene were purchased from Merck, while anthracene and bromo-phenanthrene came from Sigma Aldrich. Standard stock solutions (100 ng/µL) were prepared by dissolving pure analyte in DCM and stored at -18 °C. Working solutions were prepared monthly by diluting these standard stock solutions in DCM and kept at -18 °C.

Table 2.3: All organic analytes used with class, Cas No., molecular formula, molecular weight and structure.

Class	Chemical	Cas No.	Mol. Formular	Mol. Weight (g/mol)	Structure
PAHs	Anthracene	120-12-7	$C_{14}H_{10}$	178.23	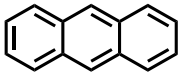
	9-Bromo-Phenanthrene	573-17-1	$C_{14}H_9Br$	257.13	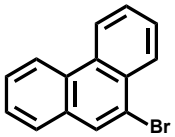
	Fluoranthene	206-44-0	$C_{16}H_{10}$	202.26	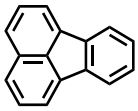
	Pyrene	129-00-0	$C_{16}H_{10}$	202.26	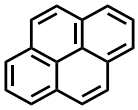
Hormones	Estradiol	50-28-2	$C_{18}H_{24}O_2$	272.38	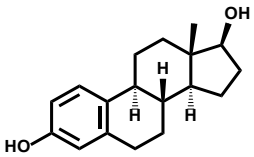
	Estrone	53-16-7	$C_{18}H_{22}O_2$	270.37	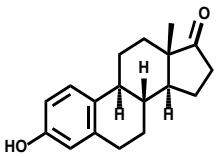
	Estrone-3-methylether	1624-62-0	$C_{19}H_{24}O_2$	284.40	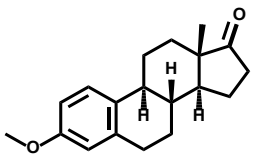
	Ethinylestradiol	57-63-6	$C_{20}H_{24}O_2$	296.41	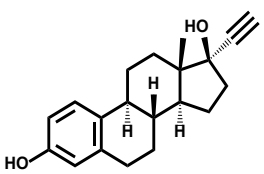
	Progesterone	57-83-0	$C_{21}H_{30}O_2$	314.47	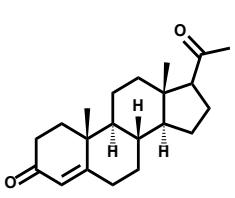

2.4.2 Organic Analysis

2.4.2.1 Sample Preparation

In a series of preliminary experiments, the most effective sample preparation method for the simultaneous extraction of PAHs and hormones from estuarine sediments was evaluated by comparing two sediment extraction techniques. The extraction efficiencies of accelerated solvent extraction (ASE) and ultrasound-assisted extraction (UAE) with silica-gel column clean-ups were tested against an analyte-spiked sand/clay (3:2) mix that was pre-ignited at 400 °C. After spiking, the sand/clay mix was extracted as soon as the solvent of the spike had evaporated. For the ASE method, 3 g of the sand/clay mix was extracted using a Thermo 350 Accelerated Solvent Extractor with the following parameters: preheat for 5 minutes; heat and static for 5 minutes, at a pressure of 1500 psi, followed by a 70% flush and 300-second purge for three cycles, using a solvent mixture of DCM and MeOH (9:1). For the UAE method, 10 mL of DCM:MeOH (9:1) was added to 3 g of blank sediment, sonicated for 15 minutes, and then centrifuged for ten minutes. The supernatant was collected in an ASE vial, and this process was repeated twice to combine the supernatants from three extractions per sample.

The extracts from both ASE and UAE were dried with a GeneVac EZ-2 vacuum centrifuge and subjected to further purification via silica-gel column chromatography to separate the apolar, aromatic and polar fractions. The dried extracts were first transferred onto the column and eluted with hexane for the apolar fraction, followed by transfer and elution with hexane:DCM (4:1) for the aromatic fraction containing PAHs, and finally, with DCM:MeOH (1:1) for the polar fraction containing steroidal hormones. Each fraction was dried under a gentle nitrogen stream. Polar fractions were derivatised with BSTFA-TMCS:DCM (1:1) for 45 min at 50 °C, while aromatic fractions were reconstituted in DCM.

2.4.2.2 Gas Chromatography–Mass Spectrometry (GC–MS) Analysis

The following instrument method was developed in-house: All organic fractions were analysed using a Thermo Scientific TRACE 1310 gas chromatograph coupled to a Thermo Scientific TSQ 8000 Triple Quadrupole mass spectrometer (GC-MS) using a RESTEK Rtx-1 polysiloxane column (60 m, 0.25 mm I.D., 0.1 µm film thickness). The oven temperature program started at 40 °C for 2 min, increased to 200 °C at 20 °C/min, then to 260 °C at 5 °C/min and finally to 310 °C in 2 °C/min where it was held for 2 min. A 1 µL sample was injected in split mode (split ratio of 6.7) into a programmable temperature vaporizer (PTV) set at 50 °C and heated to 320 °C at 10 °C/s with helium as the carrier gas at a constant flow rate of 2 mL/min. The transfer line was kept at 310 °C. Mass spectrometric analysis employed electron ionization (EI) (70 eV) in single ion monitoring (SIM) mode, analysing target compounds based on retention times and

characteristic m/z ions for each compound (Table 2.4), with quantitative analysis determined from the peak areas of the compounds. Example chromatograms for both hormones and PAHs can be found in Figure 2.3.

Table 2.4: GC-MS SIM parameters (m/z, retention time) for the organic target analytes. Retention times may vary over time, depending on the GC column length and sample matrix.

Analyte	**Retention time (approx.) (min)**	**m/z**
Estrone-3-methylether	14.58	284
Estrone (E1), TMS derivative	15.19	342
Estradiol (E2), 2 TMS derivative	16.06	416
Ethinylestradiol (EE2), 2 TMS derivative	16.23	368, 285
Progesterone (P4)	17.38	314, 229
Anthracene (ANT)	9.88	178
Fluoranthene (FLA)	11.07	202
9-Bromo-Phenanthrene	11.16	256
Pyrene (PYR)	11.28	202

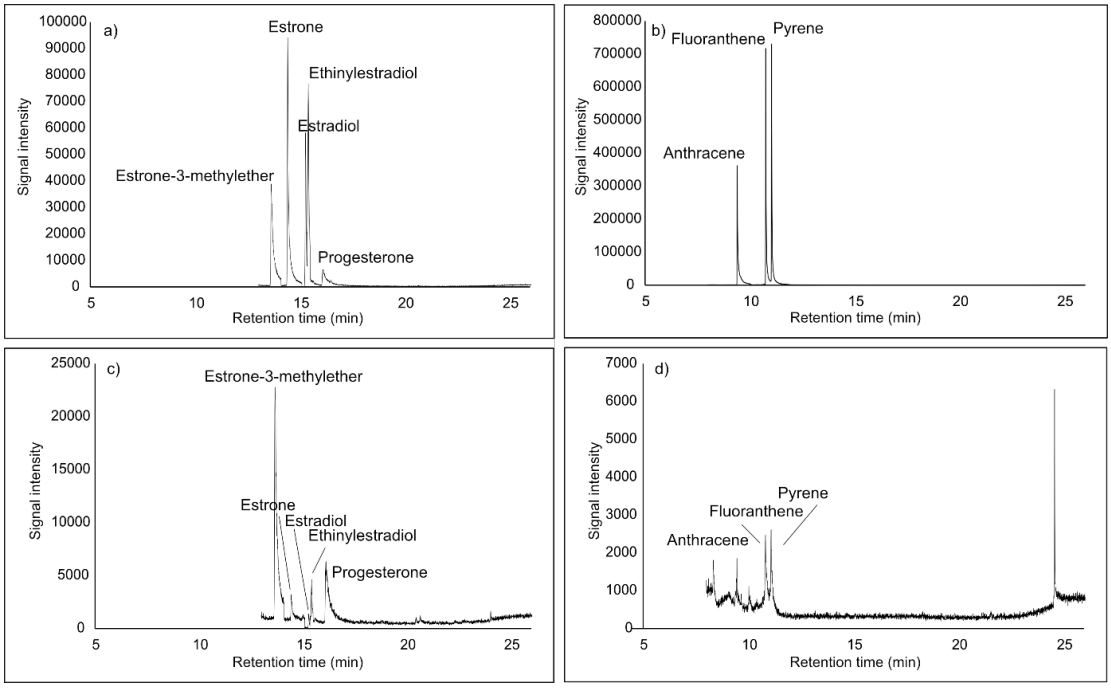

Figure 2.3: SIM chromatograms from a) 1 ng hormone standard mix in solvent b) 1 ng PAHs standard mix in solvent c) 1 ng hormone mix in blank sediment matrix and d) 1 ng PAHs standard mix in blank sediment.

Figure 2.3 shows the chromatograms obtained by measuring standard analytes in solvent and sediment matrix using the hormone and PAHs SIM methods with GC-MS. All peaks are resolved and identifiable by m/z and retention time.

2.4.3 Preliminary Extraction Experiments

A synthetic sediment mixture comprising sand and clay in a 2:1 ratio was created to evaluate two extraction methods. A hormone standard mix containing 100 ng each of estrone, estradiol, ethinylestradiol and progesterone in DCM was prepared and analysed by GC-MS to establish a maximum signal for assessing extraction efficiency. Additionally, triplicates of synthetic sediment were spiked with 100 ng of the standard mix and extracted using ASE and UAE, respectively, after the solvent of the spike had evaporated. For each analyte, the recoveries from the triplicates of one extraction method were averaged, and the relative standard deviation (RSD) was calculated. Recovery percentages of hormone standard spikes extracted from the sediments using ASE and UAE are presented in Figure 2.4. The RSD of the recoveries was used to represent the error bars.

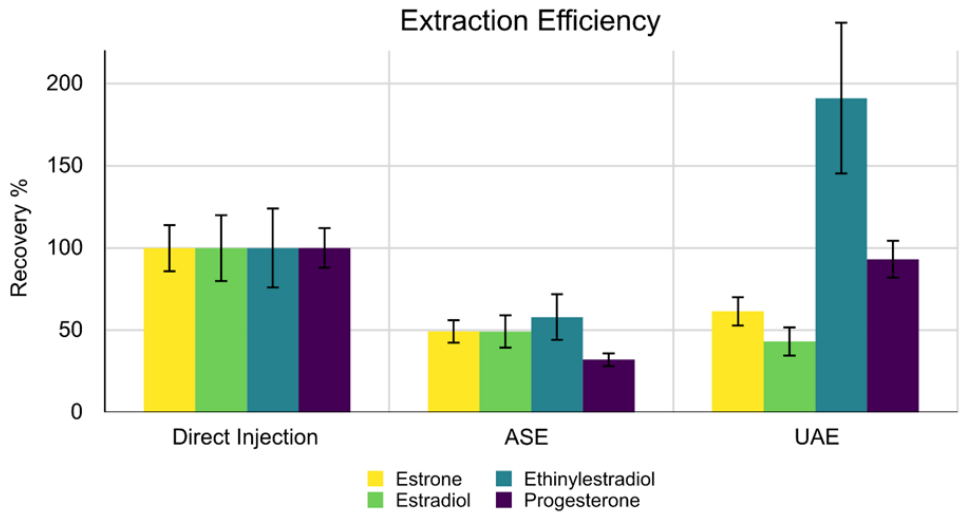

Figure 2.4: Extraction recovery (%) of ASE vs. UAE in comparison to direct injection (100% recovery). Error bars are the relative standard deviation of the recoveries from the triplicate samples for estrone, estradiol, ethinylestradiol and progesterone, respectively.

ASE achieved 45% recovery on average for hormone extraction, while UAE yielded on average 77%. The elevated recovery observed for UAE is largely driven by the apparent overestimation of ethinylestradiol (150%), which may result from matrix-induced signal enhancement or from human error during the preparation of the spiking solution.

Furthermore, the recovery of one, two and three rounds ASE and UAE, respectively, were assessed (Figure 2.5).

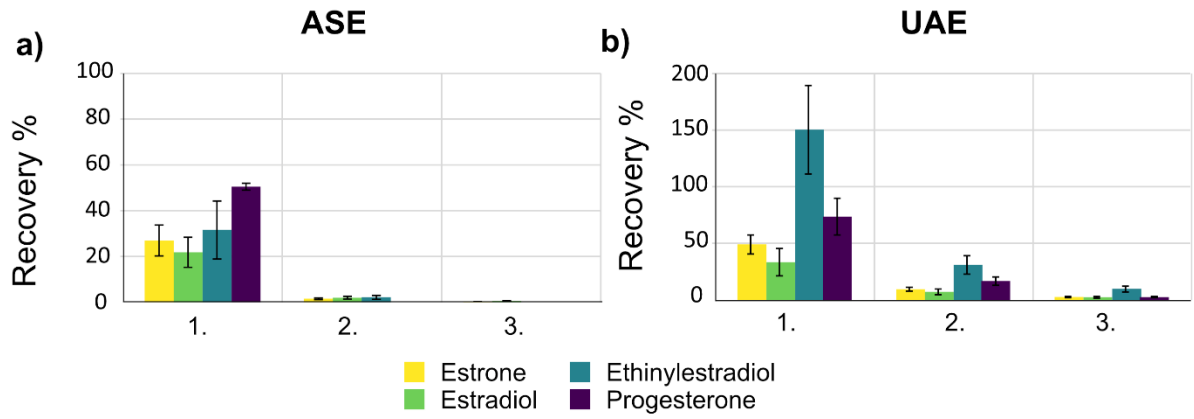

Figure 2.5: Recoveries (%) for four steroidal hormones after three rounds of a) ASE extraction and b) UAE extraction. Error bars are the percent standard deviation of triplicates for each analyte.

The first round of ASE yielded the highest recovery, with the second extraction round adding only about 2% more recovery for estrone, estradiol and ethinylestradiol, as illustrated in Figure 2.5. By the third extraction, ethinylestradiol and progesterone were no longer detected. Although

additional extraction ASE rounds did not significantly enhance recovery, the second and third UAE extraction cycle contributed, on average, 21% to the total recovery. Overall, UAE achieved a higher percentage of analyte recovery in the first extraction round (average 77%, median 61%) with improved results after three rounds: 61% estrone, 43% estradiol, 190% ethinylestradiol, 93% progesterone. Moreover, UAE demonstrated better reproducibility than ASE, with relative standard deviations of 12–26% across triplicate extractions.

After UAE extraction, the hormone standard was assessed by GC-MS before and after column clean-up revealing a loss of 10-36%. The results as well as a flowchart for better overview of the conducted efficiency experiments are shown in Figure 2.6 and Table 2.5.

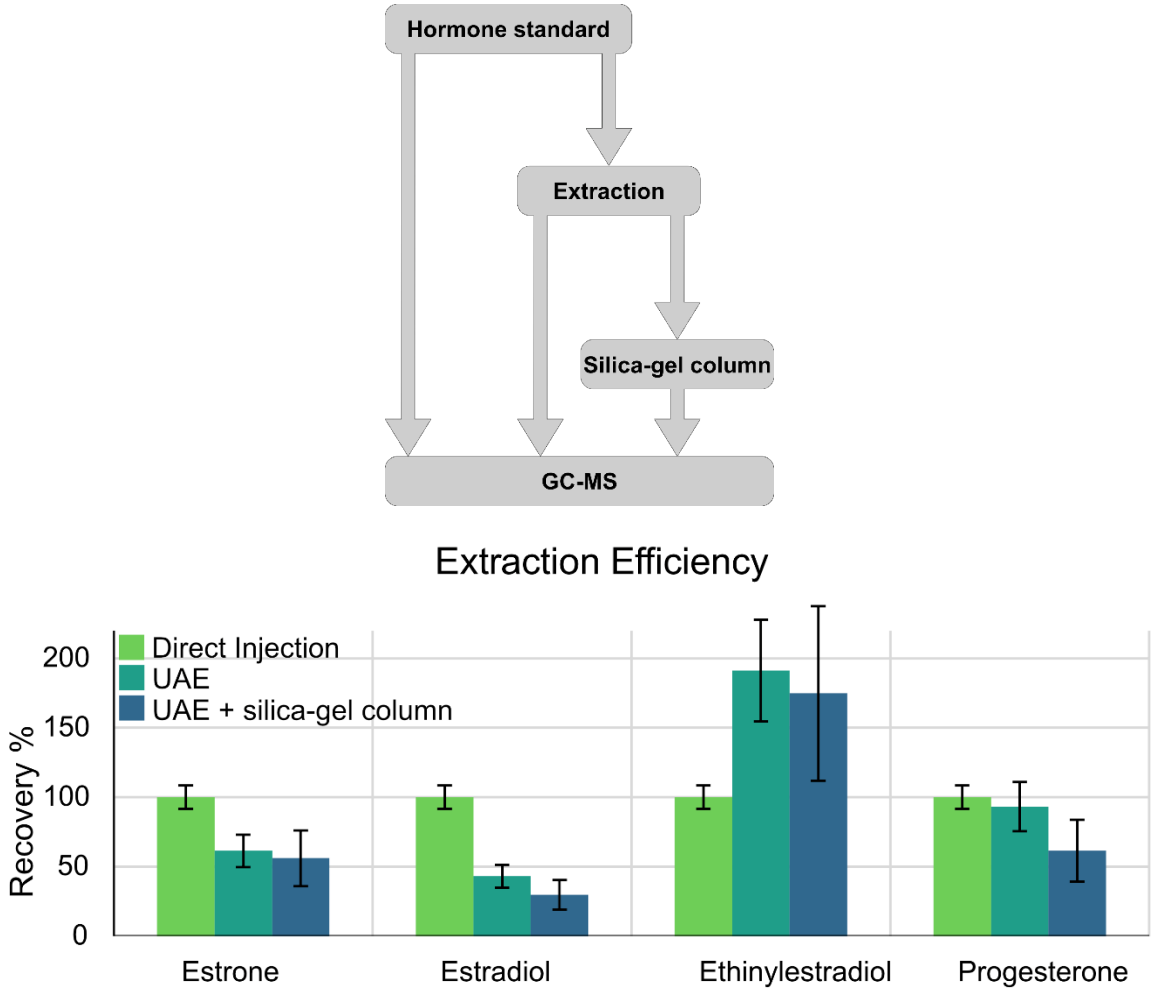

Figure 2.6: Flowchart of efficiency experiments on the top panel and extraction efficiency comparison between direct injection, UAE and UAE in combination with silica-gel column fractionation in the bottom. Error bars are the average RSD% of triplicates for each analyte.

Table 2.5: Average recovery for the four target analytes for UAE and UAE in combination with silica-gel column clean-up and fractionation.

Analyte	Recovery UAE %	Recovery UAE + silica-gel column %
Estrone	61.4	56.0
Estradiol	43.2	29.6
Ethinylestradiol	191.2	174.8
Progesterone	93.3	61.5

As Table 2.5 shows, the recoveries for the four steroidal hormones ranged between 43 – 191 % and additional use of silica-gel columns reduced the recovery on average by 17%. Again, ethinylestradiol exceeded 100% by far, which is likely due to human error in the preparation of the analytical spikes, or potential signal enhancement from matrix effects.

2.4.4 Validation of the Sample Preparation Method using UAE

Accuracy, precision, linearity and detection/quantification limits were determined to understand the effects of UAE, silica-gel column fractionation and measurement via GC-MS for each analyte.

Dilution series for each analyte were prepared in solvent and analysed by GC-MS, with concentrations ranging from 0.02 ng/µL to 15 ng/µL for steroidal hormones and from 0.5 ng/µL to 80 ng/µL for PAHs. Peak areas were plotted against concentration, assuming linearity for $R^2 > 0.98$ after fitting a linear regression model (Figure A.1 and A.3). Quantification of an analyte in samples was only performed if $R^2 > 0.98$ for that analyte.

Blank sediment samples (2:1 sand to clay) were spiked in triplicate with four steroidal hormones at three concentrations (0.1 ng/µL, 1 ng/µL, 10 ng/µL) and three PAHs at 0.1 ng/µL, 1 ng/µL, 50 ng/µL. The corresponding spiked masses were 20 ng, 200 ng and 2000 ng for hormone concentrations and 20 ng, 200 ng and 10000 ng for PAH concentrations from working solutions. Additionally, 1 ng/µL estrone-3-methylether and 1 ng/µL of bromo-phenanthrene (200 ng, each) were added to each sample as internal standards to control sample preparation and instrument performance. Sample preparation was continued after complete evaporation of the spike solvent.

Method accuracy was assessed by calculating the recovery (%) for each analyte in the spiked sediment samples:

$$Recovery\ (\%) = \frac{a_{spiked\ sample}}{a_{spike\ only}} \cdot 100 \qquad \text{(eq. 1)}$$

With $a_{spiked\ sample}$ being the peak area from the blank sediment with known spike concentration, and $a_{spike\ only}$ the peak area from the same amount of analyte in solvent.

Method precision was determined by calculating the relative standard deviation (RSD) (%) for each target analyte from peak areas of the triplicate samples. The limit of detection (LOD) for each analyte was determined using the signal-to-noise ratio (S/N):

$$\frac{S}{N} = \frac{Signal\ (peak\ area)}{Noise\ (baseline)} \qquad \text{(eq. 2)}$$

The LOD was set at S/N ≥ 3, while the limit of quantification (LOQ) was defined for S/N ≥ 10. Parameters for accuracy, precision, LOD and LOQ derived from the nine validation samples (three concentrations in triplicates) are summarised in Table 2.6.

Table 2.6: Recovery and relative standard deviation (%), limit of detection (LOD) and limit of quantification (LOQ) for each target analyte determined by UAE of spiked sediment.

Analyte	**Recovery (%)**	**RSD (%)**	**LOD (ng/µL)**	**LOQ (ng/µL)**
Estrone	44	15	0.02	0.04
Estradiol	48	24	0.02	0.04
Ethinylestradiol	41	21	0.02	0.04
Progesterone	43	35	0.04	0.06
Anthracene	24	22	< 0.01	0.02
Fluoranthene	64	30	< 0.01	0.02
Pyrene	48	26	< 0.01	0.02

The average recoveries for steroidal hormones across three concentrations ranged from 41 – 48%, with relative standard deviations for E1, E2 and EE2, RSD below 30%. For PAHs, recoveries varied from 24 – 64%, with average RSDs between 22 – 30%.

To evaluate the impact of sediment on recovery rates, an additional calibration curve was created by spiking empty vials and extracting them once the spike solvent was dried using UAE without any matrix. The results highlighted that sediments, acting as sorbents, greatly affect the recovery efficiency of analytes during extraction. For instance, when analytes were extracted

from vials using UAE without sediment, average recoveries were 83% at 0.5 ng/µL, 88% at 1 ng/µL and 87% at 10 ng/µL for steroidal hormones (Figure 2.7). In the absence of sediment, fluoranthene and pyrene showed recoveries of 93% and 76%, respectively, at 1 ng/µL and an average recovery of 107% for all three PAHs at 10 ng/µL. However, when sediment was included in the extraction process, recovery rates were lower (Table 2.6), indicating that sediment retains analytes, thus decreasing extraction efficiency.

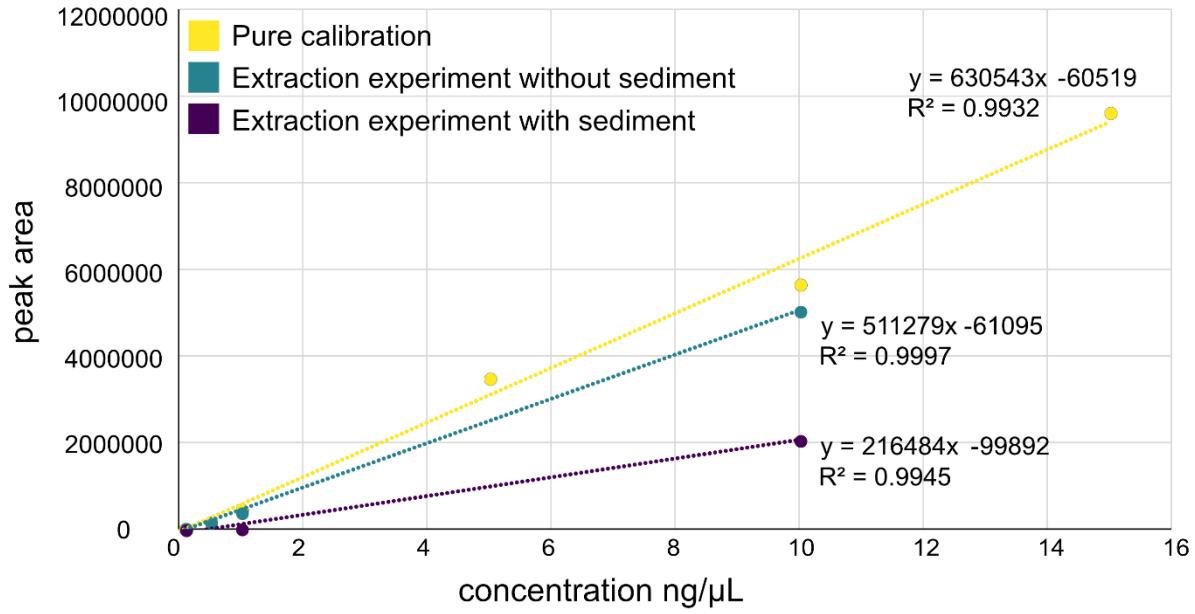

Figure 2.7: Calibration curves with linear regression lines and calibration equations for estrone in four concentrations in pure solvent (yellow), estrone extracted from blank samples without sediment (green), and estrone extracted from blank sediments (purple).

After evaluating the method, environmental samples were processed using the following steps: extraction by UAE, three column fractionations, and analysis by GC-MS in SIM mode. To each freeze-dried sediment sample, the internal standards 9-bromophenanthrene and estone-3-methylether were added before extraction to monitor extraction efficiency, matrix effects and instrument performance. The RSD of 9-bromo-phenanthrene and estrone-3-methylether across all samples of the same batch were used as error bars to visualise the relative variability of internal standard responses and reflect instrumental and procedural consistency rather than sample-specific analytical uncertainty. The whole method (internal standards, UAE, column fractionation and GC-MS analysis) was applied to both surface sediment samples and sediment core samples from Southampton Water and the Pearl River Delta to assess the presence and concentration of steroidal hormones and PAHs. The results are presented in Chapter 3 and 4.

Chapter 3 Spatial and Temporal Trends in Trace Element, PAH and Steroidal Hormone Contamination in a Major Urban and Industrial Estuary: Southampton Water, UK

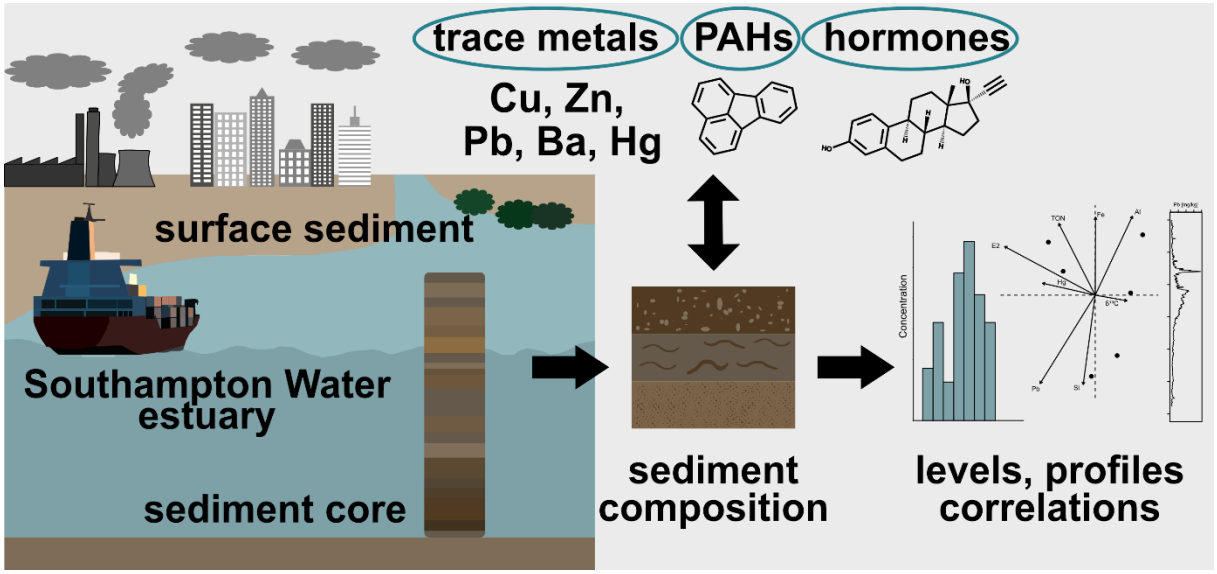

Figure 3.1: Graphic abstract for Chapter 3: Spatial and Temporal Trends in Trace Element, PAH and Steroidal Hormone Contamination in a Major Urban and Industrial Estuary: Southampton Water, UK. Abstract created using Affinity Designer 1.

This chapter is based on a manuscript intended for submission for peer review ("Spatial and temporal trends in trace element, PAH and steroidal hormone contamination in a major urban and industrial estuary: Southampton Water, UK", Appelt, J.-S., Bray, S., Whiteside, J.H., Cundy, A., *Environmental Science and Technology*) and has been reformatted to conform to University of Southampton guidelines for thesis submission.

Author contributions: JSA: Conceptualisation, data curation, formal analysis, investigation, methodology, validation, visualisation, writing - original draft; SB: Conceptualisation, methodology, resources, supervision, writing – review & editing; JHW: Conceptualisation, methodology, supervision, writing – review & editing; AC: Conceptualisation, data curation, funding acquisition, methodology, project administration, resources, supervision, writing – review & editing

3.1 Abstract

Sediments play a crucial role in sequestering certain contaminants, thereby mitigating their impact on the environment. This sequestration is especially significant in estuaries, which act as transitional zones between terrestrial and marine systems and are often heavily urbanised and hotspots for anthropogenic contamination. While the trapping capabilities for polycyclic aromatic hydrocarbons (PAHs) and many trace metals are relatively well-understood, the extent to which emerging contaminants, such as steroidal hormones, are retained based on sediment organic matter composition and source, remains unclear.

In this study, we examine surface sediments and sediment core data to determine the spatial and temporal distribution of trace elements, PAHs, and steroidal hormones in Southampton Water, a major urban and industrial estuary located along the southern UK coast. This area features diverse and complex contaminant sources and inputs, and we analyse how sediment composition relates to contaminant levels. Our findings provide a comprehensive overview of contamination hotspots and establish a geochronology of contamination within the estuary. The data indicate that several sampling sites experienced peak contamination concentrations, particularly those closest to the port. These sites displayed elevated levels of trace metals, such as Cu (15 – 2570 mg/kg), Zn (47 – 5560 mg/kg) and Pb (41 – 810 mg/kg) alongside high PAH concentrations ($\sum \mathrm{PAHs}$ 0.2 - 240 mg/kg). Steroidal hormones were detected at all sampling locations, with average concentrations of 4.2 ng/g for estrone, 3.3 ng/g for estradiol, 7.4 ng/g for ethinylestradiol, and 40 ng/g for progesterone. Notably, the synthetic hormone ethinylestradiol was found exclusively near wastewater treatment plants and sewage discharge pipes. Overall, contaminant concentrations in Southampton Water are high. The activities associated with the port and wastewater treatment facilities significantly contribute to this pollution. Principal component analysis (PCA) suggests that the properties of the sediment, including the composition of sedimentary organic carbon, play a role in the retention and accumulation, particularly of organic contaminants and Hg.

3.2 Introduction

Estuaries are dynamic transitional environments shaped by both marine and terrestrial influences, including tides, salinity, and sediment influx. These factors give estuaries their unique physicochemical properties (Bianchi, 2006). With increasing anthropogenic activity, more and more pollutants enter estuaries through rivers and industrial, agricultural and urban wastewater run-off.

The complex dynamics and sedimentary structures of estuarine systems make them hotspots for biogeochemical activity and potential sinks for a wide range of contaminants. Due to their unique properties, estuarine sediments have shown to act as filters, sequestering some contaminants and thereby mitigating their effects on marine ecosystems (Celis-Hernandez *et al.*, 2021). This makes estuaries critical environments for studying contaminant accumulation and the interactions between sediments and contaminants.

The potential to sequester trace metals and persistent organic pollutants such as polycyclic aromatic hydrocarbons (PAHs) in estuarine sediments is well-established. These contaminants typically enter estuaries through riverine transport, wastewater discharges, urban runoff and atmospheric deposition. Trace metals and PAHs are of concern due to their toxicity and persistence and are thus widely monitored and regulated. Research on trace metals in estuarine sediments has been conducted in locations such as the Brisbane River Estuary in Australia and various estuaries in the South China Sea (Koukina and Lobus, 2020; Miranda *et al.*, 2021; Shi *et al.*, 2022). Similarly, trace metal retention in sediments has also been previously studied in Southampton Water (Cundy and Croudace, 2017; Celis-Hernandez *et al.*, 2022). PAH sequestration has been of interest as well and was assessed e.g., in the Salt River Estuary, Taiwan, the Yangtze River Estuary, China and the Thames estuary, UK (Chen *et al.*, 2020; Liu *et al.*, 2020; Vane *et al.*, 2022).

In contrast, the behaviour and fate of contaminants of emerging concern (CECs), such as steroidal hormones and pharmaceuticals, remain comparatively poorly understood.

The presence of CECs in estuarine sediments has been investigated before, for example, pharmaceuticals, hormones and phenols in a Brazilian estuary; antibiotics in the Pearl River Delta, and CECs alongside PAHs in the Thames estuary (Deng, Li and Ying, 2018; de Oliveira Santos *et al.*, 2022; Vane *et al.*, 2022). However, findings regarding their behaviour in sediments is often contradictory and not all studies show that sediments effectively trap contaminants of interest and sequester them. For instance, Labadie et al. (2007) found that the steroidal hormone estrone was mobile in clay-rich sediments, while Celis-Hernandez et al. (2021) reported the presence of several CECs in sediment depths of an estuarine core that predate

their known introduction into the environment. Similar results were found for nonylphenol in cores from the Pearl River Delta (Peng *et al.*, 2007). These examples show that the effectiveness of sediments as a contaminant trap can vary widely, depending on the environmental context and the specific contaminant, and highlight the difficulty in anticipating the behaviour of contaminants in environmental matrices. Given the diversity of environmental conditions and the variety of chemical groups involved, reliable predictions of contaminant fate are challenging. Therefore, further insights into the fate and behaviour of certain contaminant groups, particularly CECs, and the potential of estuarine sediments as effective contaminant traps are essential (Petrie, Barden and Kasprzyk-Hordern, 2015).

An additional but underexplored aspect of sedimentary trapping of contaminants is the role of organic matter composition and type. Previous research has examined the relationship between trace metals and organic matter or dissolved organic carbon, with similar studies addressing PAHs and some CECs (Yang *et al.*, 2011; Chien, Chen and Li, 2018; Luan *et al.*, 2022; Lin *et al.*, 2024). Although organic matter is frequently associated with contaminant binding, the specific type and source of organic carbon are often neglected in such investigations, even though they can significantly influence retention mechanisms. Moreover, changes in organic matter composition and redox conditions with sediment depth may impact contaminant behaviour, but these processes remain insufficiently understood for both legacy pollutants and CECs.

In this study, we focus on Southampton Water, a heavily industrialised and urbanised estuary in southern England, to examine the spatial and temporal distribution of three major contaminants: trace metals, PAHs and hormones. We explore their correlation with sediment properties to enhance our understanding of how sediment characteristics influence the trapping of various contaminants.

Typically, studies tend to concentrate on one or two contaminant groups due to the time-consuming and costly nature of comprehensive analysis. This study aimed to I) investigate trace metals, PAHs, and hormones, three chemically and behaviourally distinct groups, to provide a comprehensive overview of these contaminants and II) identify correlations between the contaminant distribution, sources and sediment properties, thereby improving our understanding of how sedimentary properties affect trapping of different contaminants. Furthermore, two-dimensional gas chromatography mass spectrometry (GCxGC-MS) was conducted to identify additional contaminants and potential degradation products of steroidal hormones. Insights derived from these correlations and molecular-level analyses will inform monitoring and mitigation strategies aimed at protecting ecosystems and biodiversity.

3.3 Materials and Methods

The locations of 12 surface sediment samples and one sediment core collected from Southampton Water in August 2021 are shown in Figure 3.2.

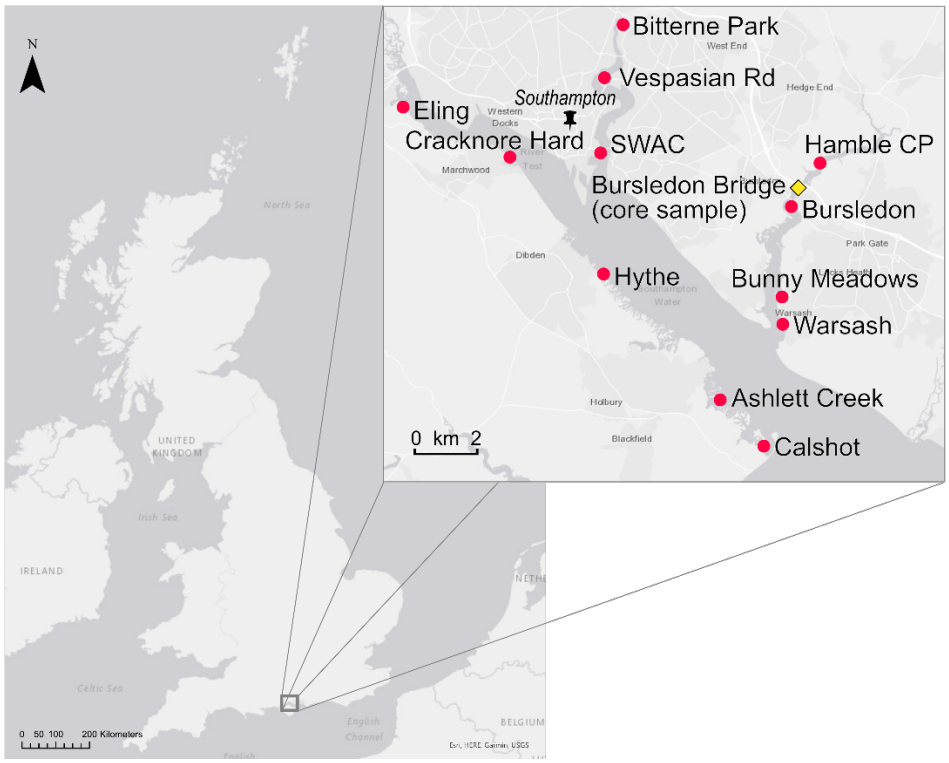

Figure 3.2: Map of Southampton Water within the UK; Surface sediment sampling sites marked with red circles and the sediment core sampling site with a yellow diamond. Map was created in ArcGIS Pro 3.3 using data from Table 2.1 and Affinity Designer 1.

Surface scrape samples (15 cm x 15 cm x 3 cm) and duplicates were gathered during low tide in intertidal mudflat areas. The duplicates were frozen for later analysis, while the samples were immediately freeze-dried. Following this, the dried samples were sieved with pre-cleaned sieves with a 2 mm mesh size to eliminate larger shell fragments, stones and roots that could distort results. The resulting material was then ground to a homogeneous consistency using a mortar and pestle.

A 30 cm long sediment core was collected using a Russian-style coring device at the sampling site Bursledon Bridge. This site is an undisturbed salt marsh (30 m by 40 m) bounded by vegetation of primarily *Halimione portulacoides*, *Spartina sp.* and *Aster tripolium*. The core was transferred to a PVC pipe and wrapped in clingfilm to maintain moisture until X-ray fluorescence analysis could be conducted at the British Ocean Sediment Core Research Facility (BOSCORF, Southampton, UK). This analysis used a COX Analytical Systems ITRAX X-ray Fluorescence (XRF) Scanner (step size of 200 µm and scan time of 30 s for the target elements copper (Cu), lead (Pb), zinc (Zn), barium (Ba), iron (Fe), manganese (Mn), and sulphur (S)). Subsequent to XRF

analysis, the core was sectioned into 150 mm segments; these sections were freeze-dried, sieved (at 2 mm) and ground to homogeneity for further analysis.

3.3.1 Inorganic Analysis

The sediment core was dated by measurement of the radionuclides ^{210}Pb and ^{137}Cs via γ-ray spectrometry using HPGe well-type detectors (Mirion Technologies, Hampshire, UK) to determine sedimentation rates (Cundy and Croudace, 2017; Abril-Hernández, 2023). Mercury (Hg) values in mg/kg for the sediment surface and core samples were obtained using a Milestone Direct Mercury Analyzer. Major and trace elements (S, Si, Al, Fe, Ba, Zn, Cu, Pb) in the freeze-dried surface samples were analysed with a Rigaku ZSX Primus II wavelength dispersive X-ray fluorescence (WDXRF) spectrometer equipped with a Rh tube and are presented in mg/kg. For major and trace elements in the core samples, a COX Analytical Systems ITRAX X-ray Fluorescence (XRF) Scanner was used and the resulting signals (Al, S, Fe, Cu, Zn, Ba, and Pb) are represented in counts per second (cps), as the data show relative comparison and down-core trend analysis, rather than absolute concentrations. Total inorganic carbon (TIC) for both core and surface sediment samples was determined using an AutoMate with CM5015 coulometer. The stable carbon isotope ratio ($\delta^{13}C$) and elemental concentration of %C and %N of bulk organic matter were measured using an Elementar Vario Isotope Select Elemental Analyser interfaced with an Isoprime GeoVisION continuous flow isotope ratio mass spectrometer (IRMS) (Isoprime 100). $\delta^{13}C$ values are reported relative to the Vienna Pee Dee Belemnite (VPDB) standard. All instruments and their respective analytical methods were available in-house, except for the Rigaku ZSX Primus II WDXRF spectrometer. Detailed descriptions of all methods and their associated uncertainties can be found in Chapter 2.2 Inorganic Analysis.

To minimize grain size effects on heavy metals and to identify potential enrichment, the trace metal concentrations in the surface samples (Ba, Zn, Cu and Pb) were normalised to the conservative Al_2O_3 contents before statistical analysis. In contrast, the core samples were analysed using a semi-quantitative ITRAX XRF Scanner, for which trace elements are reported as counts per second (cps) rather than as absolute concentrations (mg/kg) and are therefore not normalised.

3.3.2 Organic Analysis

Methanol (MeOH), dichloromethane (DCM) and hexane were obtained from Rathburn Chemicals, UK, N,O-bis(trimethylsilyl)tri-fluoroacetamide with 1% trimethylchlorosilane (BSTFA-TMCS) for derivatisation was purchased from Sigma Aldrich. The analytical standards

for estrone, estradiol, ethinylestradiol, progesterone, fluoranthene and pyrene, as well as the internal standard estrone-3-methylether were purchased from Merck. Anthracene and 9-bromo-phenanthrene were obtained from Sigma Aldrich. Standard stock solutions (100 ng/µL) were prepared in DCM and stored at -18°C. Working solutions were prepared by diluting the standard stock solutions in DCM. The three PAHs analysed within this chapter were chosen as representatives for the whole group and due to their environmental significance as ubiquitous PAHs. The hormones analysed here cover natural steroidal hormones, as well as hormones used in medication and are commonly found in environmental samples.

3.3.2.1 Sample Preparation

The method used for the extraction of organic compounds was adapted from Chen et al. (2011). More details, including consumables and error analysis are outlined in Chapter 2.3. Freeze-dried sediment samples (3 g) were spiked with 1 ng of estrone-3-methyl ether and bromo-phenanthrene as internal standards. After drying at room temperature, the samples were extracted using a DCM:MeOH (9:1) solvent mix three times for 15 min in an ultrasonic bath. The three extracts from each sample were combined and evaporated using a GeneVac EZ-2 vacuum centrifuge. These extracts were then fractionated using silica-gel columns with the following solvent sequence: hexane, followed by hexane:DCM (4:1), and then DCM:MeOH (1:1). The resultant fractions were dried under a gentle nitrogen stream. The aromatic fraction was reconstituted in 200 µL of DCM, and the polar fraction in 200 µL DCM:BSTFA-TMCS (1:1) before derivatisation at 50 °C for 45 min.

3.3.2.2 Gas Chromatography–Mass Spectrometry (GC–MS) Analysis

All organic fractions were analysed with a Thermo Scientific TRACE 1310 gas-chromatograph coupled to a Thermo Scientific TSQ 8000 Triple Quadrupole mass spectrometer on a RESTEK Rtx-1 polysiloxane column (60 m, 0.25 mm inner diameter (I.D.), 0.1 µm film thickness). The oven temperature program started at 40 °C for 2 min, to 200 °C at 20 °C/min, then to 260 °C at 5 °C/min and finally to 310 °C in 20 °C/min where it was held for 2 min. 1 µL of sample was injected in split mode with a split ratio of 6.7 into the 50 °C programmable temperature vaporizer (PTV) and heated to 320 °C at 10 °C/s. The carrier gas was helium at a constant flow rate of 2 mL/min. The transfer line had a constant temperature of 310 °C. Mass spectrometric analysis (electron ionization (EI), 70 eV) was carried out using single ion monitoring (SIM) mode. Target compounds were analysed in the samples based on retention time and characteristic m/z ions for each compound; quantitative analysis was based on the peak areas of the quantitative compounds. The identification features for each analyte can be found in Table 2.4.

3.3.2.3 Quality Assurance and Control

Internal standards (IS) (9-bromo-phenanthrene and estrone-3-methylether) were used to monitor extraction efficiency, matrix effects and instrument performance. The RSD of 9-bromo-phenanthrene and estrone-3-methylether across all surface samples, respectively was used for error bars. These error bars represent the relative variability of internal standard responses and reflect instrumental and procedural consistency rather than sample-specific analytical uncertainty. Quantification of the analytes was based on at least five-point matrix matched calibration curves with concentrations ranging from 0.05 – 15 ng/µL for the steroidal hormones and 0.5 – 100 ng/µL for the PAHs. Quantification of the analytes was only performed if the calibration curve demonstrated strong linearity ($R^2 > 0.99$). Limits of quantification (LOQ) were set at the lowest calibration point within the linear range. Alongside every batch of samples, procedural blanks consisting of 3 g blank sediment (2/3 sand, 1/3 clay, cleaned in furnace at 400°C) were extracted and analysed. With every GC-MS run, matrix-matched calibration samples, procedural blanks and solvent blanks were included. No target analytes were detected in solvent or procedural blanks.

3.3.2.4 Two-dimensional GC-MS

Two-dimensional gas chromatography – time of flight mass spectrometry (GCxGC-MS) was performed on six surface and six core samples using a LECA Pegasus BT 4D GCxGC-TOFMS equipped with an OPTIC multimode inlet system and PAL3 autosampler. Samples were injected in split mode (2:1) at 60 °C. Separation was achieved using a Rxi-5SilMS column (30 m, 0.25 mm I.D., 0.25 µm film thickness) in the first dimension and a Rxi-17SilMS column (1.3 m, 0.25 mm I.D., 0.25 µm film thickness) in the second. He was used as the carrier gas at 1 mL/min (constant flow). The oven program ramped from 60 °C to 310 °C at 12.5 °C/min over 30 min. Mass spectra (EI,70 eV) were acquired over m/z 33–550 at 200 spectra/s. Peaks with S/N > 100 were selected, and peak areas were derived from the total ion current (TIC). Analyte identification was based on NIST library matches and a multianalyte standard. Data were processed using LECO ChromaTOF BT software.

3.4 Results and Discussion

3.4.1 Surface Sediment Characterisation: Organic Matter Content and Sources

Sources of organic matter (OM) in coastal sediments exhibit distinctly different $\delta^{13}C$ and total organic carbon to total nitrogen ratios (C_{org}/N_{total}). To characterise the surface sediments of Southampton Water and determine the sources of organic matter, $\delta^{13}C$ values were plotted

against C_{org}/N_{total} for each sample, according to Lamb, Wilson and Leng, 2006 (Figure 3.3a)).

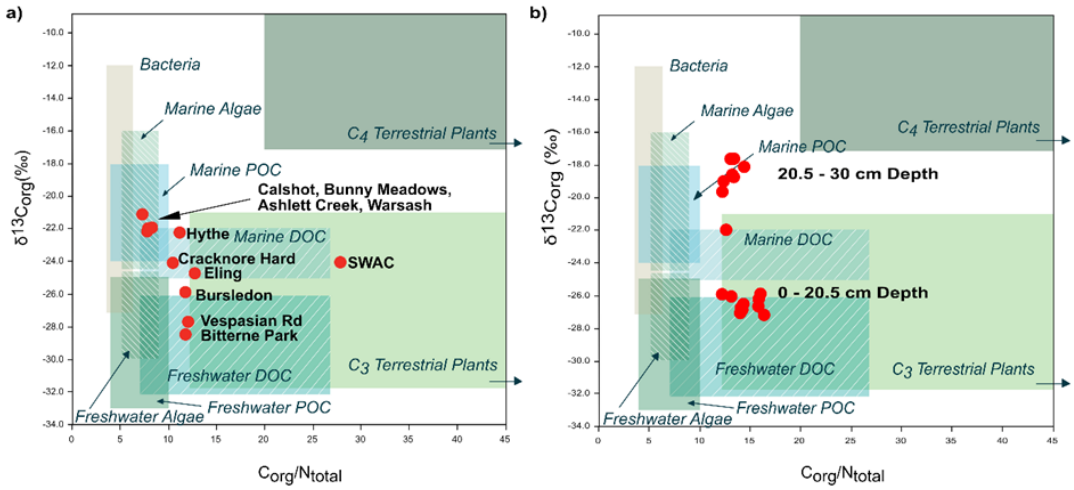

Figure 3.3: $\delta^{13}C$ values vs C_{org}/N_{total} ratio for a) eleven Southampton Water surface samples and b) 20 Southampton core samples after Lamb, Wilson and Leng (2006).

Apart from the SWAC site, the majority of the samples exhibit similar C_{org}/N_{total} ratios, while $\delta^{13}C$ values range between -29‰ and -21‰. The OM from sampling sites closer to the mouth of Southampton Water (Calshot, Bunny Meadows, Ashlett Creek, Warsash) primarily derives from marine particulate organic carbon (POC) and marine algae. In contrast, the $\delta^{13}C$ values decrease towards the river inflows from the Test and Itchen, indicating that sites nearer to the city are more influenced by freshwater dissolved organic carbon (DOC) and C_3 terrestrial plant material. This analysis shows a distinction between the OM sources of the sampling sites closer to marine conditions, and the sampling sites closer to the City and freshwater sources as would have been expected.

3.4.2 Contaminant Analysis in Surface Samples

Data for trace element concentrations can be found in the supplementary information (Table B. 3). To determine whether the source of the observed trace metal concentrations is natural or anthropogenic and to evaluate the level of contamination, the enrichment factor (EF) and the geo-accumulation index were calculated using equations B1 and B2 in the appendix, and the results are shown in TableTable 3.1 and Table 3.2.

Table 3.1: Enrichment factor (EF) for the trace metals Cu, Zn, Ba, Pb and Hg from twelve surface samples in Southampton Water. Values: 1-3: minor enrichment, 3-5: moderate enrichment, 5-10: moderately severe enrichment, >10: severe enrichment (darkest grey shade).

Enrichment Factor					
	Cu	Zn	Ba	Pb	Hg
Ashlett Creek	97.8	69.6	3.8	16.5	0.2
Bitterne Park	144.2	107.9	3.7	26.3	0.5
Bunny Meadows	202.3	136.5	7.6	36.4	0.5
Bursledon	404.4	172.5	4.6	56.3	11.1
Calshot	224.0	92.0	2.5	31.7	0.2
Cracknore Hard	783.0	324.2	7.2	121.6	7.0
Eling	1099.6	458.8	11.8	210.6	2.1
Hamble CP	585.6	236.9	4.0	104.0	0.3
Hythe	7.0	3.9	0.0	10.8	0.9
SWAC	81.8	21.4	5.8	120.8	5.1
Vespasian Road	45.4	21.7	4.3	47.6	4.4
Warsash	6.5	5.1	3.5	16.2	0.2

1 to 3	Minor enrichment
3 to 5	moderate enrichment
5 to 10	moderately severe enrichment
> 10	severe enrichment

Cu, Zn and Pb are severely enriched at most sampling sites with calculated enrichment factors significantly higher than 10. The elevated concentrations of these metals around Southampton Water are most likely from anthropogenic sources, as noted in previous studies (Croudace and Cundy, 1995; Cundy and Croudace, 2017; Celis-Hernandez *et al.*, 2022). Only the sampling sites at Hythe and Warsash, which are closer to the marine mouth of Southampton Water, display moderately severe enrichment, suggesting a greater distance from the contaminant sources. Ba and Hg enrichment is less severe; Ba is severely enriched only at Eling, a sampling site located near the port and the A35 road crossing the River Test. Hg is severely enriched in Cracknore Hard, the site nearest port and at Bursledon, which is adjacent to the M27 motorway bridge that crosses the river Hamble. Notably, the River Hamble consistently fails to meet the Environment Agency's chemical safety assessments due to high levels of Hg and its compounds (Department for Environment Food & Rural Affairs, 2023). Hg concentrations are partly attributed to antifouling agents, which were commonly used for boats.

Table 3.2: Geo-accumulation index (I_{geo}) for the trace elements Cu, Zn, Ba, Pb and Hg in twelve surface sediment samples from Southampton Water. Values 0-1: no to moderate pollution, 1-2: moderate pollution, 2-3: moderate to severe pollution, 3-4: severe pollution, >4: excessive pollution (darkest grey shade).

	I_{geo}				
	Cu	**Zn**	**Ba**	**Pb**	**Hg**
Ashlett Creek	6.0	5.5	1.3	3.5	-2.6
Bitterne Park	6.0	5.6	0.7	3.6	-2.3
Bunny Meadows	6.1	5.5	1.4	3.6	-2.6
Bursledon	7.2	6.0	0.7	4.4	2.0
Calshot	7.2	6.0	0.8	4.4	-2.9
Cracknore Hard	7.2	6.0	0.5	4.5	0.4
Eling	7.4	6.1	0.8	5.0	-1.6
Hamble CP	7.4	6.1	0.2	4.9	-3.7
Hythe	1.0	0.2		1.6	-1.9
SWAC	4.6	2.6	0.8	5.1	0.6
Vespasian Road	3.6	2.6	0.2	3.7	0.3
Warsash	0.6	0.3	-0.3	2.0	-4.3

0 to 1	no to moderate pollution
1 to 2	moderate pollution
2 to 3	moderate to severe pollution
3 to 4	severe pollution
4 to 5	excessive pollution

The Geo-accumulation index (I_{geo}) shows results for Cu, Zn, and Pb that are consistent with those indicated by the EF. Most sampling sites display excessive pollution levels for these metals, with I_{geo} values over 5. Hythe and Warsash again demonstrate the lowest contamination levels, showing either zero or moderate pollution. The Hythe site is particularly relevant, as it is located near a major oil refinery and chemical plant. Although high concentrations of Cu, up to 1022 mg/kg, were previously recorded and linked to the Fawley oil refinery, the trace metal concentrations at the site appear to be declining (Croudace and Cundy, 1995; Cundy and Croudace, 2017; Celis-Hernandez *et al.*, 2022). One explanation for this reduction may be recent sediment erosion or deposition and, therefore, changes in sediment dynamics. At most sites, Hg seems to be depleted, with I_{geo} values below zero and only moderate levels of Hg determined at the Bursledon site.

Overall, the findings from both the EF and I_{geo} analyses reveal similar trends, indicating that Zn, Ba and Pb are enriched and are pollutants at most sampling sites, while Hg contamination is predominantly observed at the Bursledon site. Background concentrations for Cu, Zn, Pb and Al were determined previously from pre-Holocene sediments in the same area, while general upper crust concentrations from sedimentary rocks (e.g., organic rich mudstones, “shales”) were used to represent the background values for Ba and Hg (Turekian and Wedepohl, 1961;

Croudace and Cundy, 1995). The use of different sources for background concentrations in these geochemical indices may explain the differences observed between Cu, Zn, Pb and Ba and Hg. Geochemical indices such as I_{geo} and EF are based on many assumptions and when employing general background values instead of the site-specific background levels, these indices may not be fully reliable and should be interpreted with caution.

Concentrations of three PAHs (anthracene, fluoranthene and pyrene) in all Southampton Water surface samples are visualised in Figure 3.4 a) and b).

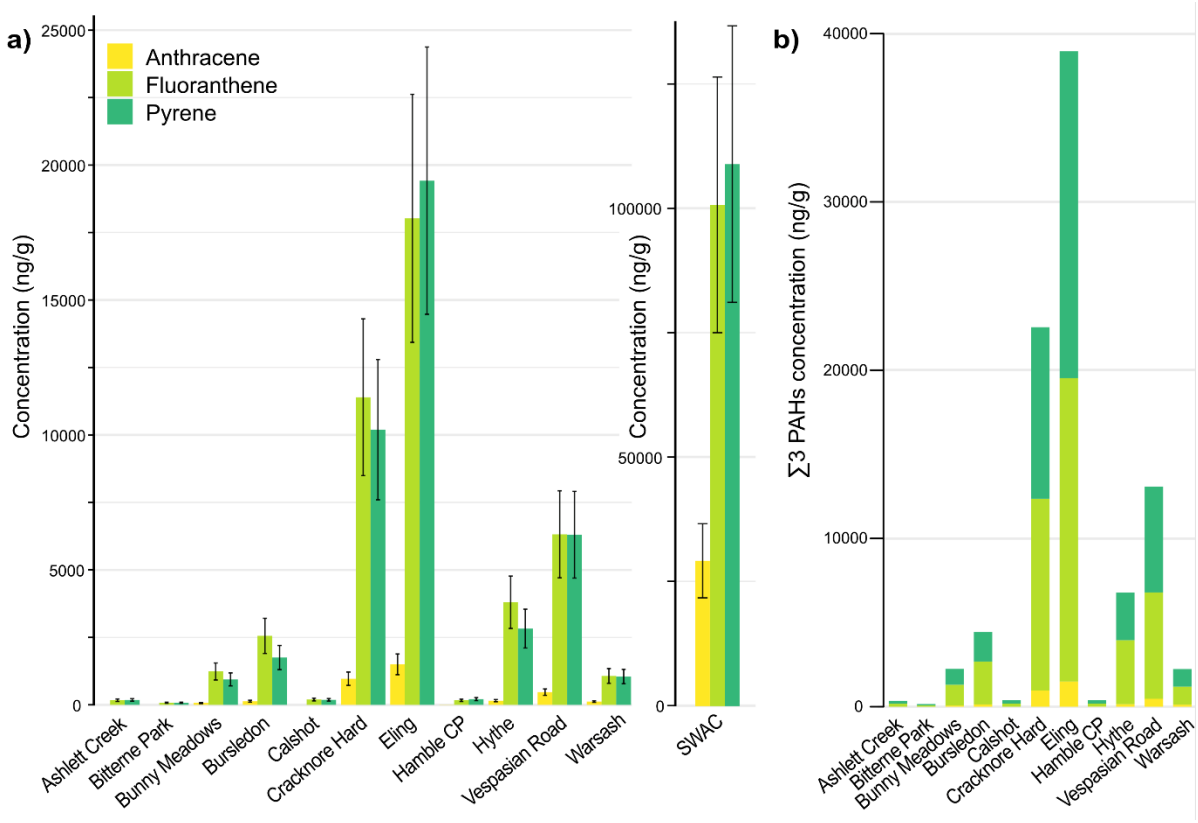

Figure 3.4: a) Concentration of anthracene, fluoranthene and pyrene in ng/g dry weight sediment in twelve Southampton Water surface sediment samples. b) Sum of the three PAHs at each of the twelve sampling sites. The error bars are the RSD of the internal standard 9-bromo-phenathrene across all surface samples and represent instrumental and procedural consistency.

Surface concentrations of three representative PAHs were variably enriched across the estuary (Figure 3.4 a)). Fluoranthene and pyrene were detected at every sampling site (with concentrations ranging 78 – 100,783 ng/g and 79 – 108,962 ng/g, respectively) while anthracene was detected at nine sites (7 – 29,196 ng/g). The total PAH concentrations varied greatly, ranging from 158 – 238,940 ng/g (average 27,540 ng/g; median 3344 ng/g) with fluoranthene and pyrene consistently dominating. The highest concentrations were detected at SWAC. The significantly elevated PAH levels at SWAC, in comparison to other sampling locations along the River Itchen,

suggest that the sources of these pollutants are likely situated between the SWAC site and the areas upstream towards Vespasian Road. The SWAC site is located near the Itchen Bridge, a heavily trafficked route connecting Southampton City Centre with Woolston. The Itchen riverside sees intense industrial activity, numerous marinas, and the Woolston wastewater treatment plant situated directly across from the sampling site—all of which are likely contributors to the high levels of PAH pollution observed here.

Beyond SWAC, the highest PAH concentrations were found in Eling and Cracknore Hard, with total PAH concentrations of 38,947 ng/g and 22,557 ng/g, respectively (Figure 3.4 b)). Both sites are the closest to the port of Southampton, indicating that port-related activities are significant sources of PAH contamination in Southampton Water. The lowest total PAH concentrations were observed at Bitterne Park (158 ng/g), Ashlett Creek (353 ng/g) and Calshot (380 ng/g). All three sampling sites are situated farthest away from the port and the city centre.

Typically, PAH concentrations are described as the total sum of PAHs measured, and in most cases the measured PAHs include the 16 priority PAHs determined by the US EPA (Zelinkova and Wenzl, 2015). Here, only three PAHs were determined but the concentration ranges are comparatively high to PAH concentrations found elsewhere (Chen *et al.*, 2020; Hellawell *et al.*, 2022; Nayak *et al.*, 2023).

Figure 3.5 shows the results for the hormones analysis.

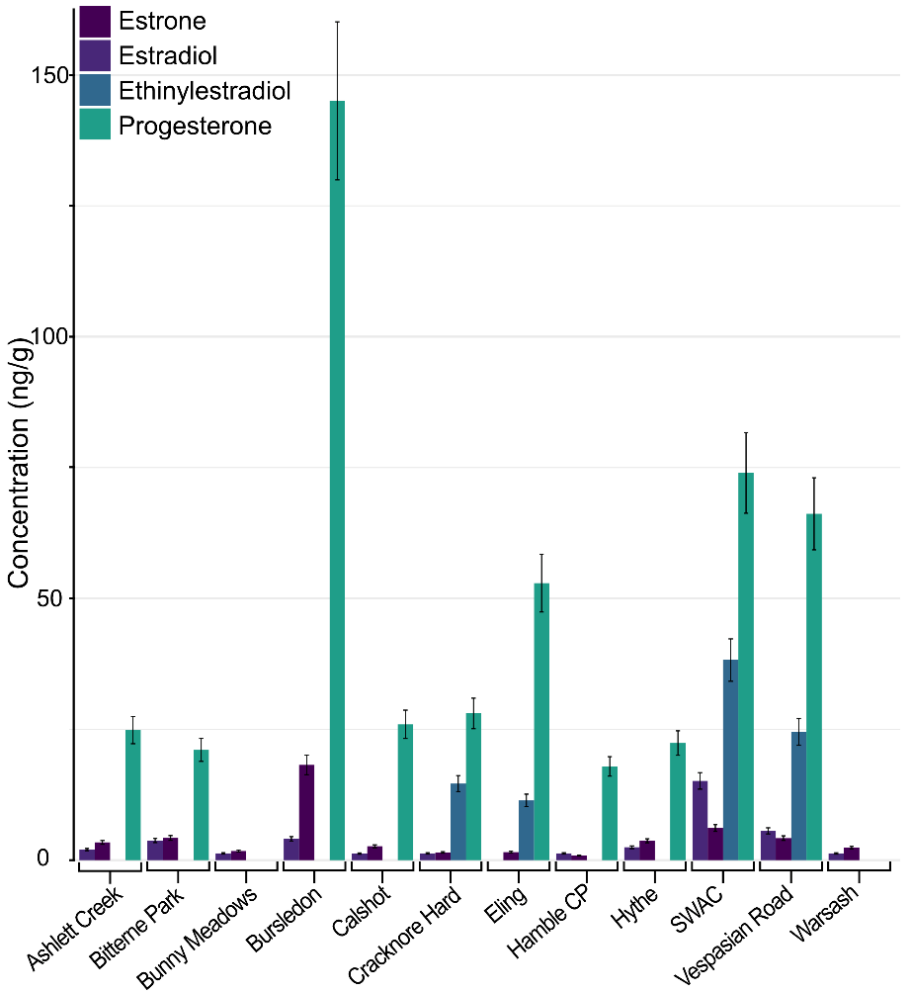

Figure 3.5: Concentrations in ng/g dry weight (y-axis) for the hormones estrone, estradiol, ethinylestradiol and progesterone in the surface samples of Southampton Water (x-axis). The error bars are the RSD of the internal standard estrone-3-methylether across all surface samples and represent instrumental and procedural consistency.

The RSD of the internal standard estrone-3-methylether over all twelve surface samples was 10.4% and indicates good instrument stability. Of the hormones analysed, estrone was found in every sample, with concentrations between 1 and 18 ng/g dry sediment. The highest concentration for estrone was found at the Bursledon site. Estradiol was found in all but one sample and progesterone in ten samples, of which the value at Bursledon was determined to be an outlier as it exceeded the 1.5 times interquartile range and consequently, was excluded. Estrone concentrations were on average higher than estradiol concentrations, probably due to processes in wastewater treatment plants that transform estradiol to estrone (Lee and Liu, 2002). Hence, estrone is often found in higher concentrations in the environment. Progesterone concentrations were highest among all targeted hormones and between 18-66 ng/g, with an average of 37 ng/g and the highest concentration at Vespasian Road.

Ethinylestradiol is of particular interest, since it is the only artificial hormone discussed here. While estrone, estradiol and progesterone can originate from excretion of all mammals, including livestock, ethinylestradiol is only used as human medication in contraceptives. Ethinylestradiol was found in concentrations from 11 to 38 ng/g and only at the four sampling sites Cracknore Hard, Eling, Vespasian Road and SWAC, with SWAC showing the highest ethinylestradiol concentration. The sites with the highest hormone concentration in total are Bursledon with 167 ng/g, followed by SWAC (133 ng/g) and Vespasian Road (100 ng/g). As mentioned above, SWAC is near the Woolston wastewater treatment plant, while Vespasian Road is only 1.5 km downstream of the Portswood wastewater treatment facility. That ethinylestradiol was found at Cracknore Hard and Eling is surprising, since both sampling sites are industrial areas rather than residential or agricultural. However, both locations are close to several sewage entry points, so the organic contaminants might originate from residential sites elsewhere that are being introduced to the estuary here (Southern Water, 2025). Finding ethinylestradiol exclusively in sediments close to wastewater treatment systems indicates insufficient hormone removal. Estrogenic compounds have been found in effluents of wastewater treatment plants that discharge into British rivers as early as 1998, with concentrations for estrone and estradiol ranging from 1 – 80 ng/L (Desbrow *et al.*, 1998). Furthermore, several studies have shown that estrogens sorb to sediments from British rivers, reinforcing that these sediments act as sinks for these compounds (Holthaus *et al.*, 2002; Peck *et al.*, 2004).

Few studies have examined hormone distribution in estuarine sediments. The concentrations identified in this study are generally comparable to those reported in other research. However, progesterone levels stand out as an exception. Wilkinson et al. (2017, 2018) investigated ethinylestradiol (among other contaminants of emerging concern) in sediments, suspended particulate matter (SPM) and water from rivers in southern England. They detected ethinylestradiol in water samples at a mean concentration of 0.23 ng/L, while no ethinylestradiol was detected in SPM or sediments. In a national monitoring program across the French territory, estrone was only detected once (6.4 ng/g) in sediments (Vulliet *et al.*, 2014). Hormones including estrone, estradiol and ethinylestradiol were found in estuarine sediments in Brazil at concentrations up to 5.7 ng/g, 18.1 ng/g and 22.9 ng/g, respectively (de Oliveira Santos *et al.*, 2022). In sediment samples from rivers in the northeast of China, estrone was found in 90% of the samples, at concentrations ranging from 0.1 – 3 ng/g (Zhang *et al.*, 2014). In a study conducted in Spain, sediments from two different rivers were analysed for hormones (López de Alda *et al.*, 2002). Estrone was found in concentrations ranging from 1 – 12 ng/g and ethinylestradiol was found at a concentration of 23 ng/g in one sample. This study was also one

of the few that looked at progestogens and found progesterone in more than 50% of the samples at concentrations between 0.1 and 6.8 ng/g (López de Alda *et al.*, 2002).

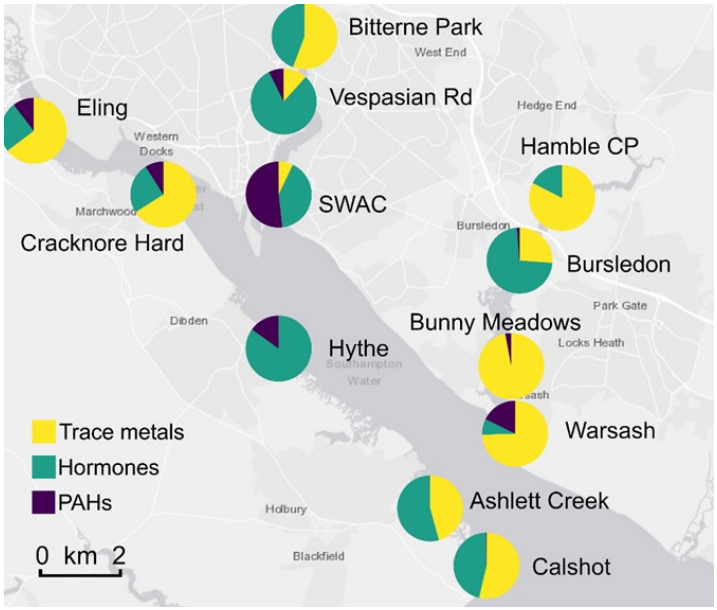

Figure 3.6: Ratio of trace metals, Hormones and PAHs distributed in Southampton Water surface sediments.

To compare the relative contributions of each contaminant group and their distribution across Southampton Water, the total concentrations of hormones, PAHs, and trace metals at each site were normalised using min-max scaling (Figure 3.6). Min-max normalisation is used to compare data with different scales by assigning values between 0 and 1 for each variable (Fang *et al.*, 2023) (eq. B3). For most sampling sites, the trace metals represent the biggest portion of contaminants. Hythe, SWAC, Vespasian Rd, Ashlett Creek and Bursledon have a higher share of hormones. Among these five sampling sites, SWAC, Vespasian Rd and Bursledon are in mainly residential areas. PAHs share a higher proportion in the sampling sites in the north of Southampton Water, close to the city and the port. The sampling sites further away from potential sources such as Bitterne Park, Hamble CP, Ashlett Creek and Calshot have overall the lowest contaminant concentrations and no significant contributions from PAHs.

To investigate the relationship among sediment composition, sampling sites and contaminant concentration, all parameters were analysed using principal component analysis (PCA) (Figure 3.7).

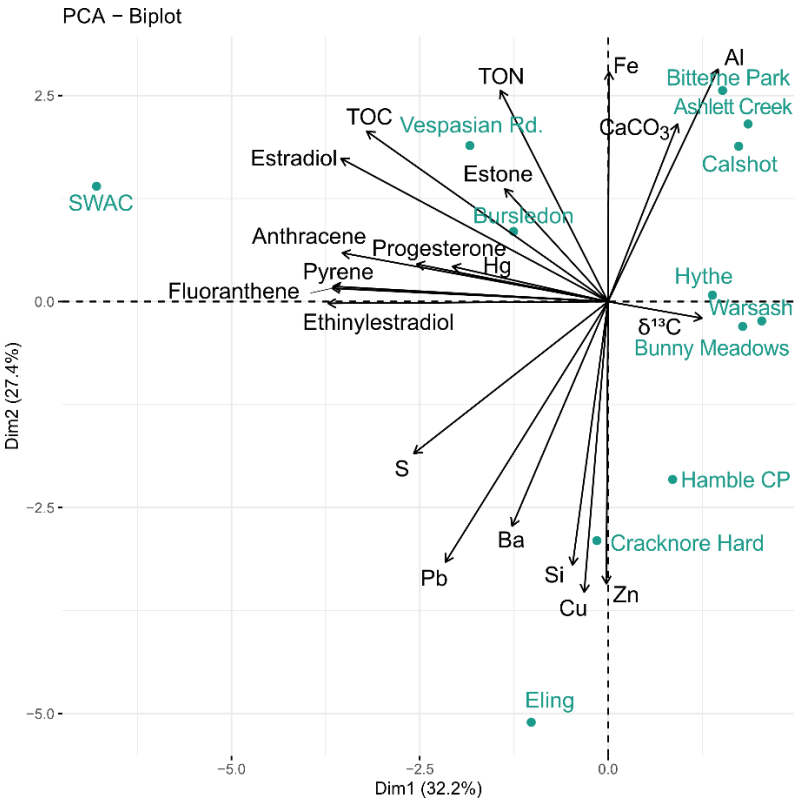

Figure 3.7: Biplot of the PCA for the Southampton Water surface samples: Surface sampling sites are shown in blue-green, the loadings of the measured variables, including sediment properties and contaminant concentrations, are represented by arrows.

Figure 3.7 shows that the sampling sites with the lowest contaminant concentrations (Calshot, Ashlett Creek, and Bitterne Park) are grouped together in the first (upper right) quadrant, despite their significant geographic distances from each other. These sites also show a strong correlation with Al and $CaCO_3$ factors in the PCA analysis. Warsash, Bunny Meadows and Hythe are geographically close and may have similar OC sources. Cracknore Hard and Eling, the sampling sites closest to the port, plot within the third (bottom left) quadrant and are associated with higher concentrations of trace metals (Cu, Zn, Ba and Pb), as well as silicate and sulphur. The inorganic trace metals likely stem from port activities and may manifest as sulphides or silicates. All organic contaminants, as well as TOC, TON and Hg are clustered in the fourth (upper left) quadrant with the sampling sites Vespasian Road, SWAC and Bursledon. The organic contaminants and Hg appear to be closely associated with TOC values, exhibiting similar behaviour to previous observations (Lindberg and Harriss, 1974; Langston, 1982). Moreover, $\delta^{13}C$ lies in the second quadrant, indicating a negative correlation with TOC, TON, organic contaminants and the OM sources. This suggests that higher TOC and contaminant values are linked to terrestrial OM sources. Furthermore, SWAC, Bursledon and Vespasian Road are located in residential areas, implying that their contaminant sources are likely urban wastewater runoff and effluents. At sampling sites with the highest inorganic contaminant

concentrations, such as Cracknore Hard, Eling, and SWAC, the proximity to contamination sources (e.g., near wastewater treatment and ports) seems to play a more substantial role in contamination levels than the sediment properties themselves. Moreover, port activities such as dredging, along with urban influences like wastewater runoff and sewage discharge, can alter sediment properties including grain size and organic carbon content, ultimately affecting the sediment's capacity to retain contaminants.

3.4.3 Sediment Characterisation of the Southampton Water Core

In the following section, the results for the Southampton core are discussed, starting with the characterisation of the sediment. The $\delta^{13}C$ values for each core subsample were plotted against the C_{org}/N_{total} ratio to determine the OM sources (Figure 3.3). The origin of the OM in the core divides clearly between OM originating from more freshwater DOC and C_3 terrestrial plants for the upper 20.5 cm of the core and transitions to marine DOC and POC sources in the deepest 8 cm of the core. A possible explanation for the change in OM supply from more terrestrial to more enriched $\delta^{13}C$ values in these areas could be the accumulation of marsh sediment and subsequent build-up in elevation within the intertidal zone. As a result, the sediment becomes flooded less often and the vegetation becomes increasingly dominated by more terrestrial rather than saltmarsh species. The shift in $\delta^{13}C$ is also seen in Figure 3.8.

The radionuclide ^{210}Pb shows a consistent and near-exponential decline, which is a sign for undisturbed sedimentation and enables the dating of the core (Figure 3.8). The activity of $^{210}Pb_{excess}$ decays at a known rate and can therefore be used to estimate a sedimentation rate with a “simple” constant flux:constant sedimentation rate model (CF:CS). The sedimentation rate in this core is approximately 4.1 mm/year, which is consistent with sedimentation rates found in other cores from this area (Celis-Hernandez *et al.*, 2021). The radionuclide ^{137}Cs occurs solely due to anthropogenic activity and the two peaks in the deeper parts of the ^{137}Cs profile around 250 and 220 mm correspond to the maximum activity of nuclear warfare testing in 1958 and 1963. Using the sedimentation rate estimation from the ^{210}Pb decay places the ^{137}Cs maximum at 250 mm depths in 1959, which is in good agreement of what would be expected. The deepest part of the core corresponds approximately to 1950.

The TOC profile of the sediment core exhibits a constant decay from surface to greater depths, likely resulting from organic matter degradation (Emerson *et al.*, 1987; Middelburg, 1989). The $\delta^{13}C$ profile (Figure 3.8), shows a marked change around 175 mm depth, as discussed above.

Al is a common proxy for sediment grain size, as aluminosilicates are typically associated with finer-grained particles (Loring, 1991). The observed increase in Al concentration with depth in the core indicates that finer-grain-size particles are more prevalent in the deeper sections.

The S and Fe profiles in cores can provide insights into redox processes occurring within the core. At the surface where oxygen is still available, aerobic respiration by benthic microorganisms prevails. However, as depth increases, oxygen levels gradually diminish. At greater depth, sulphate-reducing bacteria are dominant and generate H_2S, a fraction of which may precipitate as solid-phase sulphide minerals. In this core, the Fe profile exhibits strong fluctuations in the upper 70 mm, while a steady increase is noted in the lowest 50 mm. Similarly, an increase of S is observed at greater depths, suggesting oxygen depletion at the core's bottom and potential precipitation of insoluble Fe sulphides.

3.4.4 Geochronology of Contaminants in Southampton Water

In the following sections, the depth profiles of the trace metals Cu, Zn, Ba, Pb and Hg, as well as the organic contaminants anthracene, fluoranthene, pyrene, estrone and estradiol are discussed (Figure 3.8; raw data in Table B. 4).

The trace metals Cu, Zn, Ba and Pb display low background concentrations in the deepest 100 mm of the core. Assuming a constant sedimentation rate, concentrations of these four trace metals increase at a depth of around 150 mm, corresponding to the year 1984. Cu, Zn and Ba show distinct peaks from 1984 onwards, indicating single spill events in the area. Furthermore, at a depth of 80 mm, a marked peak for Cu, Zn and Pb corresponds to the year 2001, likely stemming from a simultaneous release of these pollutants into the environment. These trace metals are commonly linked to sources such as vehicle emissions, mining, smelting and industrial production (Hanfi, Mostafa and Zhukovsky, 2020). The core was collected in close proximity to a bridge that spans the M27 motorway over the River Hamble, with unfiltered road runoff from the motorway contributing directly to the catchment. This section of the M27 opened in 1976 and contaminant peaks in this core appear only after the bridge became operational. The Pb profile shows a concentration increase starting in 1982 (at 160 mm) peaking in 1994 (at 110 mm), followed by a subsequent decline. The peaks observed in Cu, Zn, Ba, and Pb may suggest that spill events related to road or construction activities occurred during that timeframe. Furthermore, the Pb profile likely reflects the historical use of lead as an anti-knock agent in gasoline, alongside its eventual ban in the UK in 2000.

The prominent peaks of Cu, Zn, Ba and Pb indicate that these contaminants have been effectively trapped and preserved in the sediments for decades, remaining intact without degradation, consumption or mobility. In this regard, the estuarine sediments are effective filters for these trace metals, retaining them and mediating their impact on the marine environment.

Hg shows a different profile compared to the other trace metals, as its concentration is highest in the deepest parts of the core. At the surface, Hg levels begin at a low concentration of 0.14 mg/kg and increase steadily to 1.2 mg/kg at 220 mm depth, corresponding to the year 1967. Once released into the environment, Hg quickly binds to sediments, potentially creating "hotspots" (Bryan, Langston and Langston, 1992). Hg is often associated with insoluble sulphides and organic matter, which may explain its elevated concentration in the deeper layers of the sediment core (Bryan, Langston and Langston, 1992). As discussed previously, the River Hamble, from which the core was extracted, has historically recorded high Hg levels, likely due to its background as a major shipbuilding area.

The core profiles for the PAHs anthracene, fluoranthene and pyrene display similar relative distributions throughout the core. Anthracene concentrations vary from 0 to 69 ng/g while the concentrations of fluoranthene and pyrene range from 250 to 1300 ng/g. All three PAHs show relatively low concentrations in the upper 80 mm of the core with higher concentrations at depth. All three show a maximum at 200 mm, which corresponds the year 1972. Vane et al. (2022) analysed PAHs in sediment cores from the Thames estuary and observed comparable PAH profiles, with concentrations for $\sum 16\ \mathrm{PAHs}$ ranging from 6900 – 108,000 ng/g, peaking in the 1950s and declining steadily towards the surface. Moreover, pyrene and fluoranthene are the primary contributors to PAH concentrations in the Thames estuary cores; a trend also observed in this study. Downham et al. (2024) also analysed polycyclic aromatic compounds (PACs), including PAHs in the Thames estuary, demonstrating a correlation between the US EPA 16 PAHs concentration in the cores and the total inland coal consumption in the UK in the respective years. Domestic coal consumption was widespread in the UK in the 1950s and declined in the following years. The high PAH concentrations in the deepest layers of the Southampton core correspond approximately to 1950 and decrease nearer the surface, reinforcing the decadal scale correlation of declining PAH accumulation in sediments with reduced coal usage.

Distinctive molecular PAH patterns are created by different formation pathways. While combustion processes typically generate higher proportions of higher molecular weight PAHs due to the higher temperatures, petrogenic processes produce more low molecular weight PAHs (Ravindra, Sokhi and Van Grieken, 2008; Karp *et al.*, 2020). Moreover, many isomer pairs (e.g. fluoranthene and pyrene, anthracene and phenanthrene) form under different thermal conditions, so their relative abundances reflect the temperature conditions of origin. Because isomers often degrade at comparable rates, their ratios tend to remain relatively stable over a long time (Ravindra, Sokhi and Van Grieken, 2008; Tobiszewski and Namieśnik, 2012). Hence, molecular indices are often used to attribute sources to environmental PAHs (Valizadeh *et al.*, 2014; Potapowicz *et al.*, 2022). To verify that the elevated PAH concentrations in the deeper core

layers are attributable to increased domestic coal consumption during that period, or to identify alternative PAH sources, two molecular indices are used here (Figure B. 2). Due to varying combustion conditions, environmental degradation processes and the mixing of different PAH emitters, the source apportionment of PAHs in sediments needs to be treated with caution (Galarneau, 2008; Katsoyiannis, Sweetman and Jones, 2011).

Here, the molecular diagnostic ratios of ANT (anthracene)/ (ANT + PHE (phenanthrene)) and FLA (fluoranthene)/ (FLA + PYR (pyrene)) are used on the core samples to indicate potential trends in petrogenic versus pyrogenic PAH sources over time. Since all samples are from the same site, minimal variation in the number of PAH sources and similar degradation processes are assumed over the studied duration. Furthermore, both indices used here differentiate between pyrogenic and petrogenic sources only, without any specific source apportionment. The molecular ratios range from 0.2 – 0.5 for ANT/(ANT+PHE) and show little variation for FLA/(FLA+PYR) (0.48 – 0.55). Both ratios indicate that the PAH sources at this site are primarily pyrogenic likely originating from high-temperature combustion, e.g. vehicle exhaust and coal and biomass burning. A discernible trend emerges when comparing the 11 lower core samples to the 8 upper core samples closer to the surface: the deeper samples exhibit lower ANT/(ANT + PHE) ratios (0.2 – 0.3) and higher FLA/(FLA + PYR) ratios, while the surface samples demonstrate the opposite trend with higher ANT/(ANT + PHE) ratios (0.3 – 0.5) and slightly lower FLA/(FLA+PYR) values. All values are still within the pyrogenic range but could indicate a change in pyrogenic sources over time in the surrounding area.

The hormones, estrone (E1) and estradiol (E2) were found only in the upper 10 cm of the core. Estrone has a high surface concentration of 70 ng/g but decreases rapidly to between 15 ng/g and 22 ng/g. At a depth of 130 mm, the highest concentration of 85 ng/g was measured. Interestingly, a similar result was found for estrone in sediments from the river Ouse, UK, where estrone showed a large concentration peak in 15 cm depth of the core (Labadie *et al.*, 2007). The authors suggest that this peak might result from a change in sediment sorption properties or porewater velocity, causing the downward migration rate of estrone to exceed the degradation rate leading to a buildup (Labadie *et al.*, 2007). Here, the estrone peak also concurs with peaks in Cu and Ba and a decline in TOC, which could indicate both a spill event at that time and/ or change in sediment composition and subsequent accumulation.

Estradiol is only present in the upper 7 cm of the core, starting with a concentration of 28 ng/g and increasing slightly to 45 ng/g. It seems that the estradiol concentration here is opposed to the estrone trend in the core and could even indicate transformation from estrone to estradiol before further degradation. Several studies investigated both degradation efficiencies and pathways of steroidal hormones in the environment and though transformation from estradiol to

estrone is more common, the pathway from estrone to estradiol is possible as well (Lee and Liu, 2002; Shi *et al.*, 2013). Estrone seems to be more susceptible to biotic than abiotic removal such as photodegradation, but the presence of sediments in general seems to delay degradation mechanisms, shown by Biswas, Vellanki and Kazmi (2024). Furthermore, environmental factors including salinity and alkalinity play a role in the degradation efficiency of steroidal hormones (Suri, Singh and Abburi, 2010). Overall, the profiles for estrone and estradiol suggest transformation from estrone to estradiol in the upper layers of the core and potential accumulation of the remaining estrone in the deeper layers.

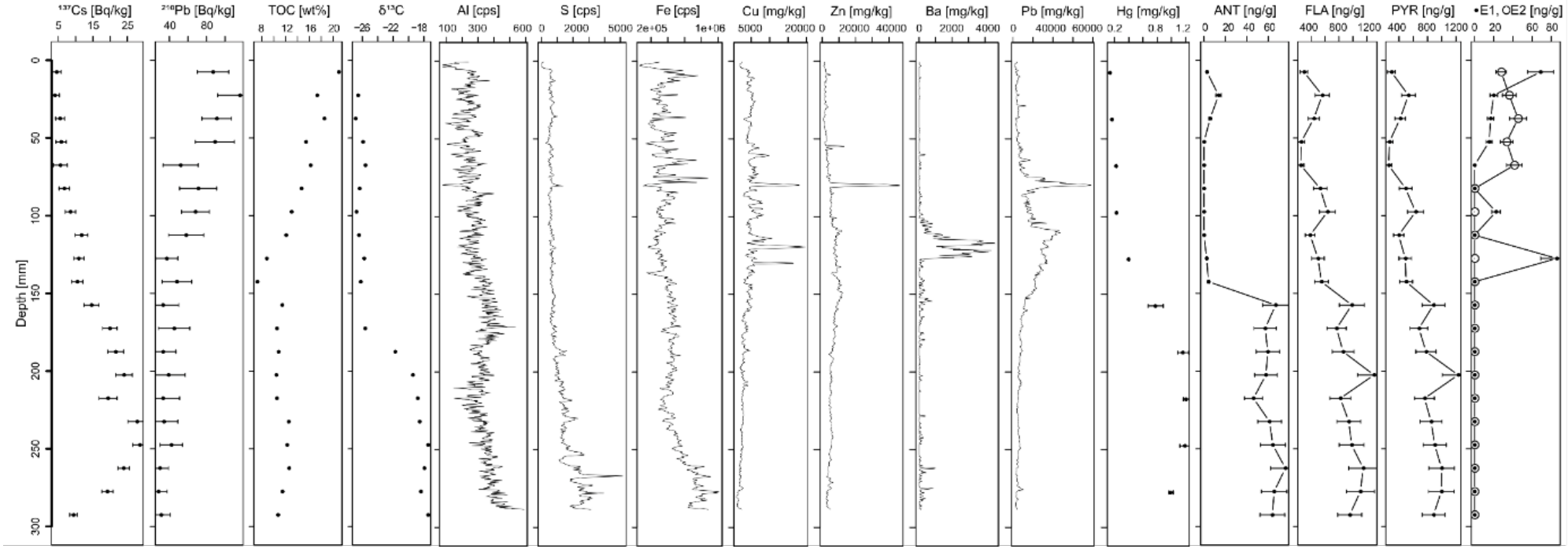

Figure 3.8: Southampton Water core profile. The y-axis is the depth in mm, with 0 mm being the surface of the core and 300 mm being the deep end of the core. Displayed are the radionuclides ^{137}Cs and ^{210}Pb in Bq/kg, the TOC in wt%, $\delta^{13}C$ in relation to the standard material VPDB, the major elements Al, S and Fe in counts per second [cps]. The trace elements Cu, Zn, Ba, Pb and Hg are in mg/kg, anthracene (ANT), fluoranthene (FLA) and pyrene (PYR), as well as estrone (E1) and estradiol (E2) are in ng/g sediment dry weight. The error bars for the PAHs and hormones are the relative standard deviation of the internal standards 9-bromo-phenanthrene and estrone-3-methylether, respectively.

3.4.5 2-dimensional GC-MS Non-Target Screening

Non-targeted analysis (NTA) using 2-dimensional GC-MS (GCxGC-MS) is a powerful tool to identify suspect compounds as well as unpredicted compounds in samples. However, environmental samples often have very complex matrices yielding thousands of potentially identifiable analytes, making data processing and compound identification difficult and time-consuming. Moreover, trace compounds can be drowned out by co-eluting matrix compounds and overlooked easily. NTA therefore requires thorough sample preparation and clean-up methods to eliminate as many interferences as possible, without simultaneously eliminating the compounds of interest.

NTA using GCxGC-MS was conducted with six of the core samples and six surface samples to investigate further contaminants and degradation products of estrone. The total ion current (TIC) chromatogram of the core samples was screened for the masses of ten potential estrone degradation and transformation products (Table B. 5). However, none of the suspected products were detected in the core samples and may indicate low or zero concentrations of predicted degradation products amongst a complex matrix.

Nevertheless, other anthropogenic compounds were found during the non-target screening. Analytes were identified by mass spectrum, retention time and comparison to a multi-contaminant standard mix (Table B. 6). In this study, NTA identified Bis(2-ethylhexyl) phthalate in all 12 samples, while two other phthalates (diethyl phthalate and dibutyl phthalate) were identified in all six surface samples and five core samples, respectively. While this study focused on steroidal hormones and therefore, exploration of further compounds by NTA was limited, the immediate identification of further contaminants such as phthalates shows the advantages of using NTA in contaminant screening.

Additionally, natural aromatic acids such as vanillic acid, ferulic acid, coumaric and fumaric acid increased with core depth. As degradation products of lignin and other plant-derived compounds, their accumulation, together with decreasing TOC with depth (Figure 3.8), indicates degradation of organic matter with depth.

3.5 Discussion

3.5.1 Spatial and Temporal Trends in Contaminant Distribution and Source Controls

This study offers a comprehensive overview of contamination in Southampton Water, addressing both spatial and temporal dimensions. Trace metals, PAHs and hormones were detected in relatively high concentrations in surface and core samples, clearly demonstrating

the presence of contamination hotspots around the estuary. Contaminant distribution was reflected by the presence of contaminant point sources, e.g. trace metals were particularly high close to the port, while hormones mainly occurred close to residential areas and the artificial hormone ethinylestradiol was only detected in proximity to wastewater treatment facilities or sewage discharge points. The sediment core analysis revealed distinct spill events for trace elements, such as Cu, Zn and Ba, along with increasing trends for e.g. Pb and PAHs with depth, indicating a decrease in usage over time. The hormones estrone and estradiol were present predominantly in the upper 10 cm of the core, with estrone showing a concentration peak at 13 cm depth, while estradiol followed an opposing trend, suggesting transformation from estrone to estradiol in the surface layers and subsequent accumulation of residual estrone associated with changes in sediment composition.

3.5.2 The Role of Sediment (and Organic Matter) Composition

The sediments in Southampton Water play a critical role in trapping various contaminant groups, as indicated by core profiles demonstrating the capacity of sediment to retain trace elements and PAHs over extended periods, potentially mitigating their impacts on the marine environment. However, other contaminants such as Hg and hormones may be more mobile and sedimentary retention in those cases not as effective.

Sediment composition, particularly the type and source of organic matter, plays an important role in contaminant retention, as suggested by PCA. In both the surface and the core samples, the organic compounds and Hg appear to be closely associated with TOC and TON values, which reflect the organic matter sources.

As anthropogenic pressures on estuaries continue to increase, understanding the interactions between contaminants and sediments remains crucial. Further research is needed to explore the specific roles and mechanisms by which different organic matter sources influence contaminant retention in sediments, particularly their origin and composition.

[Acknowledgements: The authors would like to thank the team at GAU-Radioanalytical Laboratories for their support in radiometric dating of the core and Hg analysis and the Chemistry Department at University of Southampton for providing access to the GCxGC-MS. We would also like to thank BOSCORF for their help with ITRAX core analysis and the School of Earth and Environment, University of Leeds for XRF analysis. This work is supported by the INSPIRE Doctoral Training Partnership funded by the Natural Environmental Research Council (grant number NE/S007210/1)].

Chapter 4 Controls on the Distribution and Sequestration of Steroidal Hormones, PAHs and Trace Metals in the Pearl River Delta, Southeast China

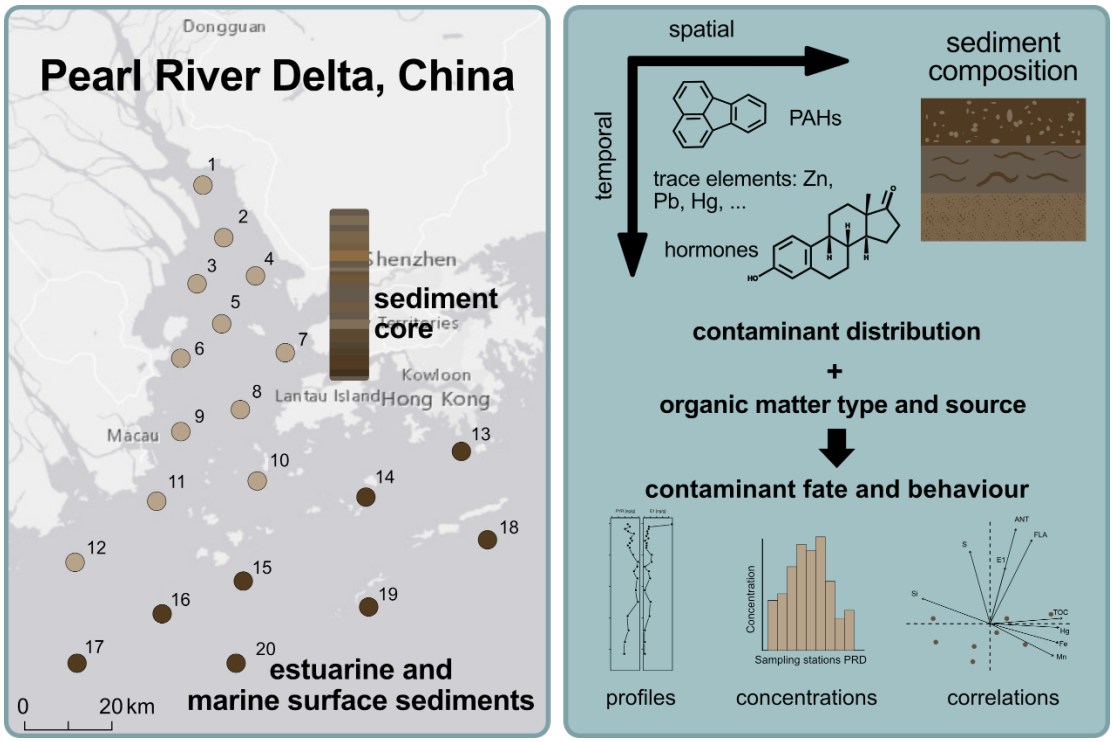

Figure 4.1: Graphic abstract for Chapter 4: Controls on the Distribution and Sequestration of Steroidal Hormones, PAHs and Trace Metals in the Pearl River Delta, Southeast China. The abstract was created with Affinity Designer 1.

This chapter is based on a manuscript intended for submission for peer review ("Controls on the Distribution and Sequestration of Steroidal Hormones, PAHs and Trace Metals in the Pearl River Delta, Southeast China", Appelt, J.-S., Bray, S., Whiteside, J.H., Wang, W., Cundy, A., *Environmental Pollution*) and has been reformatted to conform to University of Southampton guidelines for thesis submission.

Author contributions: JSA: Conceptualisation, data curation, formal analysis, investigation, methodology, validation, visualisation, writing - original draft; SB: Conceptualisation, methodology, resources, supervision, writing – review & editing; JHW: Conceptualisation, methodology, supervision, writing – review & editing; WW: Data curation, writing – review & editing; AC: Conceptualisation, data curation, funding acquisition, methodology, project administration, resources, supervision, writing – review & editing

4.1 Abstract

Understanding the distribution and fate of contaminants in estuarine sediments is essential for assessing long-term environmental risks. However, predicting contaminant behaviour in estuarine systems remains challenging due to the complex dynamics and processes that control their retention and transformation. This study investigates spatial and temporal patterns of trace metals, polycyclic aromatic hydrocarbons (PAHs), and steroidal hormones in the Pearl River Delta, China, one of the most urbanised estuarine systems in the world. Surface sediment samples reveal clear concentration gradients for trace metals and PAHs, decreasing seaward and indicating strong sedimentary retention near urban sources, with total trace metal concentrations ranging between 124 – 435 mg/kg, and 2 – 177 ng/g for PAHs. In contrast, estrone, the only detected hormone, showed no spatial trends (concentrations <LOD – 13 ng/g), suggesting more diffuse sources or greater mobility in the water column. Sediment core profiles provide a historical record of contaminant deposition, with increasing Cu and Zn inputs since ~1913, while other trace metal concentrations decline, likely reflecting successful environmental regulations in recent years. Estrone (E1) and estradiol (E2) are restricted to upper sediment layers, with surface maxima and rapid subsurface depletion, indicating ongoing inputs, transformation (E2 to E1), and degradation.

Principal component analysis (PCA) and sediment characteristics suggest that sediment properties such as total organic carbon (TOC), grain size, and $\delta^{13}C$ influence metal distributions but exhibit limited control over PAHs and estrone, likely due to different sources. This contrasts with prior findings and underscores the complexity of organic matter–contaminant interactions in estuarine environments. While sediments act as effective sinks for many contaminants, our results highlight the limited retention of hormones, likely linked to organic matter type and minimal spatial variability in its composition in this area. These findings emphasise the complex interactions between local sediment characteristics and contaminant inputs and suggest the need for deeper understanding of steroidal hormone behaviour in estuarine environments.

4.2 Introduction

Estuaries, which are located at the intersection of marine and terrestrial environments, serve as transitional aquatic environments where rivers enter the sea. These areas vary in salinity, transitioning from marine conditions at the river's mouth to more brackish and freshwater conditions further inland. The unique physicochemical properties allow estuarine sediments to act as sinks for various contaminants, preventing them from entering marine environments and mitigating their impacts on marine ecosystems through sediment trapping and the "estuarine filter" effect (Bianchi, 2006; Celis-Hernandez *et al.*, 2021). Consequently, estuaries are critical environments for assessing contaminant accumulation as well as sediment-contaminant interactions.

The main sources of conventional and emerging contaminant input into marine environments are anthropogenic activities. Hence, densely populated areas are particularly pressurised due to increased amounts of point and diffuse contaminant sources. The Pearl River Delta (PRD) in southern China is not only one of the largest estuarine systems in the world, but also one of the most heavily urbanised with a population exceeding 86 million people (Zhang, Gan and Yang, 2024). Since the 1980s, the region has undergone rapid economic growth and evolved into a critical global manufacturing hub. Consequently, this rapid development has resulted in severe deterioration of water and sediment quality in the region (Cundy *et al.*, 2022).

Estuarine sediments are key to understanding the fate, transport, and trapping of contaminants, as they provide a record of ongoing pollution inputs and a historical archive of contamination (Cundy *et al.*, 1997; Tamtam *et al.*, 2011; Cundy and Croudace, 2017). Understanding contaminant behaviour in sediments is critical, particularly in dynamic and heavily impacted estuaries like the PRD.

Due to its size, complexity, and the anthropogenic pressures it faces, the PRD has become a model study site for estuarine pollution and contaminant research (Wang and Rainbow, 2020). Studies have assessed the spatial distribution of conventional contaminants, such as trace metals, in surface sediments and sediment cores (Ip *et al.*, 2004; Fang and Wang, 2022; Shi *et al.*, 2022; Li *et al.*, 2024). PAHs have also been investigated in PRD sediments, and their ecological risks have been evaluated (Peng *et al.*, 2008; Li *et al.*, 2021; J. Zhang *et al.*, 2024). More recently, studies have looked at contaminants of emerging concern, including phthalate esters in sediments, and electrical waste contaminants (Liu *et al.*, 2014; Tao *et al.*, 2022).

While the fate and behaviour of conventional contaminants is well-documented in the PRD, knowledge gaps remain regarding contaminants of emerging concern (CECs), such as hormones.

Endocrine disruptors and steroidal hormones have been detected in various matrices from the PRD, including suspended particulate matter, wastewater effluents and water samples (Gong *et al.*, 2019; Deich *et al.*, 2021; Zhu *et al.*, 2024). However, their behaviour in sediments remains poorly understood and contradicting results were found. For instance, nonylphenol, an endocrine disruptor, has been detected in sediment cores at depths older than its widespread applications, indicating mobility within the sediments (Peng *et al.*, 2007). Similar findings have been reported from estuarine sediment cores in the United Kingdom, where estrogens, pharmaceuticals, bisphenol A (BPA) and per- and polyfluoroalkyl (PFAS) substances were also found to be mobile in estuarine sediments (Labadie *et al.*, 2007; Celis-Hernandez *et al.*, 2021). The partitioning, sequestration and degradation of CECs in PRD sediments remain largely understudied (Cundy *et al.*, 2022).

Another factor challenging the prediction of contaminant behaviour in sediments is the heterogeneous composition of sediments and the uncertainty about which sediment properties influence the contaminant fate. Close associations between contaminants and sedimentary organic matter have previously been established, e.g., for trace metals, PAHs and certain CECs (Yang *et al.*, 2011; Chien, Chen and Li, 2018; Luan *et al.*, 2022; Teixeira *et al.*, 2023; Lin *et al.*, 2024). However, the type and source of organic matter have often been overlooked, even though they may significantly influence contaminant retention mechanisms. Additionally, variations in organic matter composition with sediment depth can further complicate contaminant behaviour.

The unpredictability of contaminant fate underscores the necessity of addressing existing knowledge gaps and to better understand the potential of estuarine sediments as contaminant traps (Petrie, Barden and Kasprzyk-Hordern, 2015).

The PRD is of global economic significance, and the Chinese government is prioritising sustainable development through the “Greater Bay Area Plan”, which includes environmental conservation and contaminant mitigation strategies (Li *et al.*, 2022). Therefore, research focused on sediment-contaminant interactions and the role of organic carbon in contaminant sequestration is essential to inform remediation, risk management, and environmental policy (Cundy *et al.*, 2022).

In this study, we analysed surface samples and a sediment core from the PRD for trace metals, PAHs and steroidal hormones. Surface samples reflect the spatial distribution of various contaminants at one point in time, while the sediment core allows for the assessment of temporal contamination trends. Alongside contaminant concentrations, sediment properties including $\delta^{13}C$, TOC and TON values were determined to understand how sediment properties,

including organic matter characteristics, affect contaminant distribution and behaviour at both surface and deeper (buried) sediment levels.

4.3 Materials and Methods

In January 2021, twenty surface sediment samples were collected during a research cruise in the Pearl River Delta, China (Figure 4.2), conducted by the Chinese Academy of Sciences.

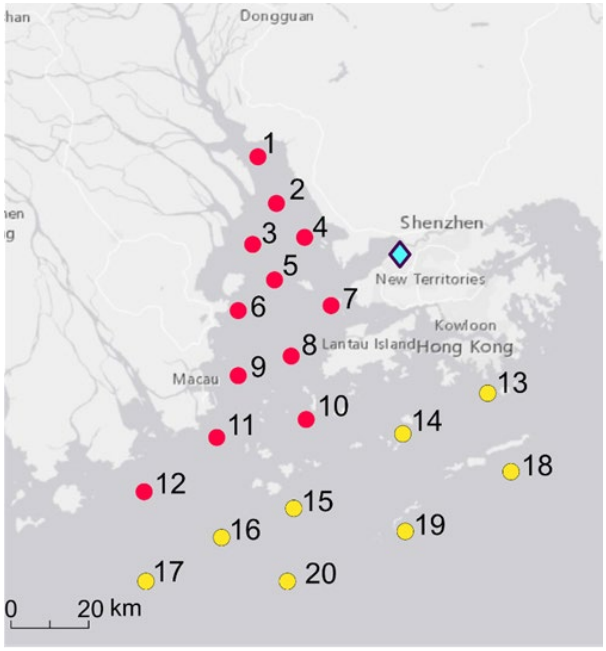

Figure 4.2: Sampling sites in the PRD for estuarine/coastal surface sediments (red circles) and marine surface sediments (yellow circles) from the South China Sea, as well as the core sampling site (purple/turquoise diamond).

Additionally, in May 2022, a 90 cm sediment core was obtained from the Mai Po wetland area of Shenzhen Bay. This core was then divided into vertical sections of 1.5 cm. Both the surface samples and core subsamples were freeze-dried and shipped to the UK for further analysis.

4.3.1 Inorganic Analysis

The determination of ^{210}Pb for dating of the sediment core and the sedimentation rate was described previously in Chapter 2. Mercury levels were measured following the procedures outlined in Chapter 2, along with the measurements of total inorganic carbon (TIC), carbon isotope ($\delta^{13}C$) analysis and the elemental concentrations of %C and %N of bulk organic matter.

For trace element analysis, 15 PRD surface and 19 core samples were digested with aqua regia using a CEM Mars6 Microwave Digestion System. The resulting solutions were analysed using an Agilent 8900 triple-quadrupole inductively coupled plasma mass spectrometer (QQQ-ICP-MS) in He mode. Major element concentrations were measured using wavelength dispersive X-ray

fluorescence (XRF) spectroscopy with a PANalytical Axios mAX spectrometer. Additional details and quality parameters related to these analyses are described in Chapter 2.

4.3.2 Organic Analysis

The method used for the organic analysis, as well as all the consumables involved, are outlined in Chapter 2. In brief, approximately 3 g of freeze-dried sediment were spiked with 1 ng of estrone-3-methylether and 9-bromo-phenanthrene as internal standards before extraction. The extraction process was conducted three times with 10 mL of DCM:MeOH (9:1) solution using ultrasonication. The combined extracts were concentrated in a vacuum centrifuge and subsequently fractionated using silica-gel columns, starting with hexane, followed by hexane:DCM (4:1), and finally DCM:MeOH (1:1). The resulting fractions were dried under a gentle nitrogen stream. The aromatic fraction was reconstituted in 200 µL of DCM, while the polar fraction was reconstituted in 200 µL DCM:BSTFA-TMCS (1:1) and derivatised at 50 °C for 40 min.

Analysis of all organic fractions was performed using a Thermo Scientific TRACE 1310 gas-chromatograph coupled with a Thermo Scientific TSQ 8000 Triple Quadrupole mass spectrometer. Mass spectrometric analysis used electron ionization (EI) at 70 eV, operating in single ion monitoring (SIM) mode. Identification of target compounds was based on their retention times and characteristic m/z ions. Quantitative analysis was performed using the peak areas of the compounds and an external calibration curve ($R^2 > 0.99$) for each compound. The identification features for each analyte can be found in Chapter 2, Table 2.4. For quality assurance, matrix-matched calibration samples, procedural blanks and solvent blanks were included with every GC-MS run. No target analytes were detected in solvent or procedural blanks.

Principal component analysis (PCA) was conducted using the open software R studio. Due to low variability of Hg, and missing estradiol values in the core samples, both variables were excluded from the core PCA.

4.4 Results and Discussion

4.4.1 Surface Sediment Characterisation: Organic Matter Content and Sources

General sources of organic matter in the PRD surface sediment were determined by plotting $\delta^{13}C$ against the total organic carbon to total nitrogen ratio (C_{org}/N_{total}) (Figure 4.3a)).

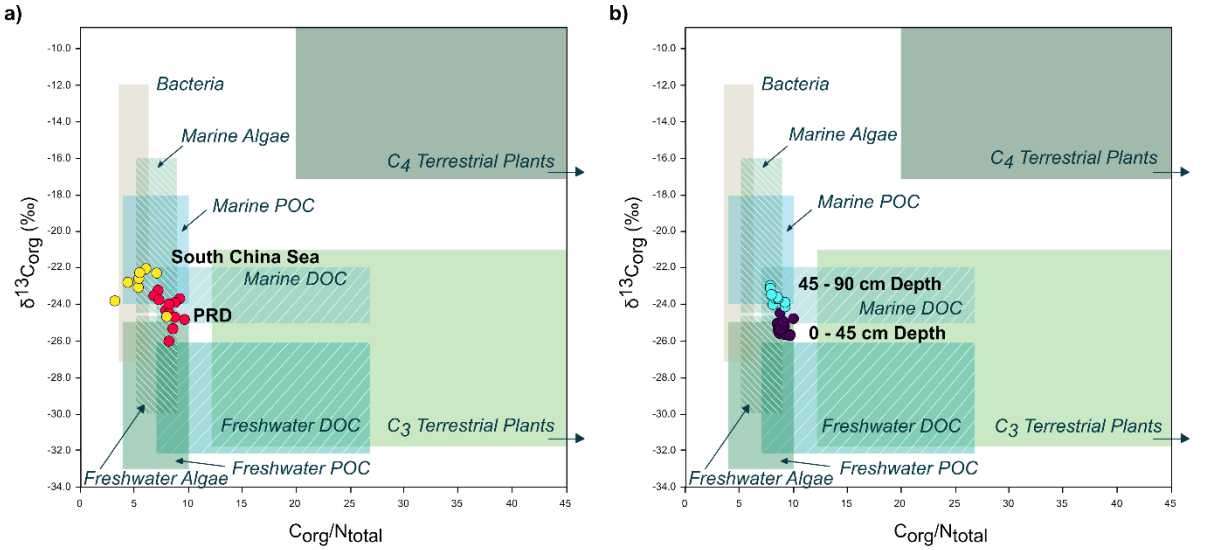

Figure 4.3: $\delta^{13}C$ vs. C_{org}/N_{total} ratio for a) 20 PRD surface sediment samples with estuarine/coastal sampling sites in the PRD (red) and marine sampling sites (yellow) from the South China Sea and b) 30 sediment core samples with the surface 45 cm of the core (purple) and the deepest core samples (turquoise) after Lamb, Wilson and Leng (2006).

All twenty surface samples have similar $\delta^{13}C$ values (between - 25.9 and -22.2 ‰) and comparable C_{org}/N_{total} ratios (3.0 – 9.44). The organic matter of all surface sampling sites originates predominantly from marine sources, such as marine algae and particulate organic carbon (POC). However, a few sites indicated contributions from freshwater sources, including freshwater algae or freshwater POC, which are characterised by lower $\delta^{13}C$ values. Despite the narrow range of $\delta^{13}C$ and C_{org}/N_{total} values, it is possible to differentiate between the sampling sites in the South China Sea (site 13 – 20, marked in yellow) and those within the PRD (site 1 – 12, marked in red) based on their sources of organic carbon. Given that some of these sampling locations are separated by over 100 km, the consistency of organic matter sources in the region is notable, especially when compared to other smaller estuarine systems (e.g. Southampton Water, see Chapter 3, Figure 3.3).

4.4.2 Contamination Analysis in PRD Surface Samples

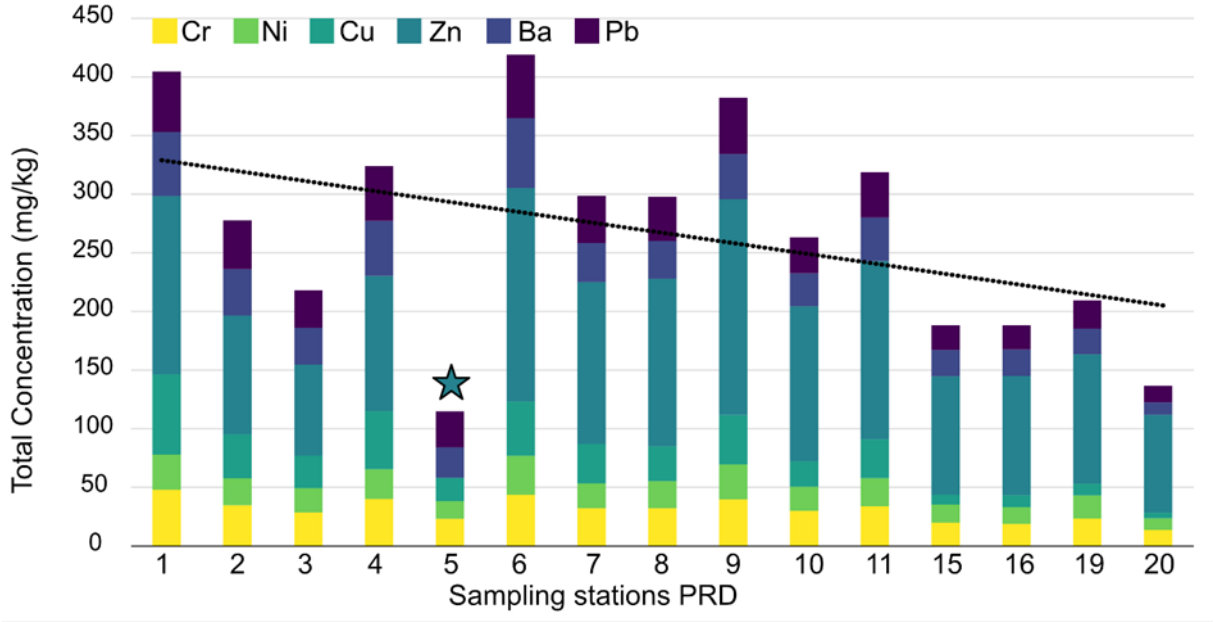

Figure 4.4: Sum of trace metal concentrations and contributions of each element (Cr, Ni, Cu, Zn, Ba and Pb) at each analysed PRD sampling site and a trendline, indicating a concentration decline from PRD 1 – 20. The star indicates an excluded value for Zn.

The sum of Cr, Ni, Cu, Zn, Ba and Pb concentrations ranged from 124 – 435 mg/kg at the PRD surface sampling sites (Figure 4.4). The individual contribution of each trace metal to the total concentration are also presented. Notably, the Zn concentration at station 5 was too high and outside the interquartile range and therefore excluded from this analysis. Among the trace metals, Zn exhibited the highest concentrations (78 – 184 mg/kg), followed by Pb (14 – 54 mg/kg) and Ba (11 – 60 mg/kg). The lowest concentrations were found for Ni (10 – 33 mg/kg). All trace elements analysed had a detection frequency of 100%. The highest total concentrations were observed at stations 6 and 1 (435 mg/kg and 417 mg/kg, respectively). Station 1 is located where the Pearl River feeds into the estuary after passing the cities of Guangzhou and Dongguan, carrying urban and industrial road runoff and wastewater that cause high contaminant concentrations. Station 6 is located near Qi'Ao Island and Zhuhai. Concentration levels display a clear trend, with elevated concentrations found within the estuary and lower concentrations recorded at the marine sampling stations further from urban and industrial influences (specifically, stations 15, 16, 19 and 20). This pattern is consistent with previous observations in the PRD (D. Zhang *et al.*, 2013).

Overall, the trace metal concentrations measured in this study are comparable to those reported in previous studies on the PRD: While Li et al. (2024) sampled closer to the river systems and shores and detected slightly higher concentrations of Cr, Cu, Pb and Zn, Ip et al. (2007) found average concentrations similar to those in this study, with comparable distribution

patterns. Factors influencing the trace element distribution in the estuary include temperature and the salinity gradient, which affect the deposition of dissolved metals into sediments (Fang and Wang, 2022; Li *et al.*, 2024). Salinity levels also determine whether sediments act as source or sink for trace elements; results indicate that sediments can release Zn into the water column under freshwater conditions while acting as sinks for Zn in brackish environments (Gao *et al.*, 2023). Furthermore, industrial activities have been identified as a significant anthropogenic influence on trace element distribution in the estuary, particularly electroplating factories as sources for Cr, Cu and Zn (Li *et al.*, 2024).

The concentrations of three PAHs in ng/g dry sediment are shown in Figure 4.5.

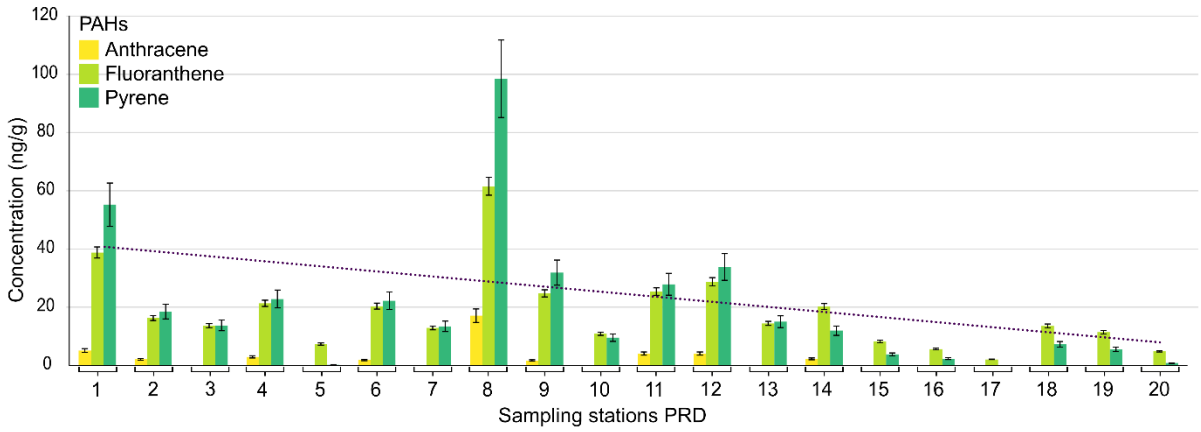

Figure 4.5: Concentration (ng/g) of three PAHs in PRD surface samples and the trendline for the total PAH concentration (purple). The error bars are the RSD of the internal standard 9-bromo-phenathrene across all surface samples and represent instrumental and procedural consistency.

The RSD of the internal standard 9-bromo-phenanthrene across all 20 surface samples was 13.5%, indicating stable instrument performance. The total PAH concentrations ranged from 2.1 – 177.2 ng/g (average 39.9 ng/g, median 28.4 ng/g). Among the PAHs measured, pyrene had the highest concentrations (<LOD – 98.5 ng/g), followed by fluoranthene (2.1 – 61.5 ng/g) and anthracene (<LOD – 17.1 ng/g). Pyrene and fluoranthene were the dominant PAHs detected, consistent with previous observations (Chapter 3). Fluoranthene was detected at each sampling site, while anthracene was detected in only 50% of the sites. The highest concentration of PAHs was recorded at sampling site 8, located near Lantau Island and Hong Kong airport. Despite Lantau Island being relatively green with a low population density, the presence of the airport and urban areas in Hong Kong may contribute to PAH pollution at this site (Wong and Fung, 2016). Generally, PAH concentrations decrease from lower-numbered stations, which are closer to the coast to higher-numbered stations located further outside the estuary in the South China Sea. Interestingly, the most remote sampling site (20), approximately 100 km from the most inland site (1) and around 40 km offshore, still showed detectable PAHs levels. This finding

is unexpected and suggests potential long-range transport of these compounds or the existence of alternative pollution sources. Previous studies have extensively documented PAH levels in Chinese riverine and estuarine sediments, with reported total concentrations reaching up to 1423 ng/g in the Huai River, 2000 ng/g in the Songhua River, and 208 ng/g in the Yangtze River estuary (Zhang *et al.*, 2019; Liu *et al.*, 2020; Mohammed *et al.*, 2021). In this study, only three PAHs were analysed, resulting in lower concentrations compared to those found in similar studies.

The concentrations of the only detected steroidal hormone, estrone, in ng/g dry sediment are illustrated in Figure 4.6 for the 20 surface samples collected in the PRD.

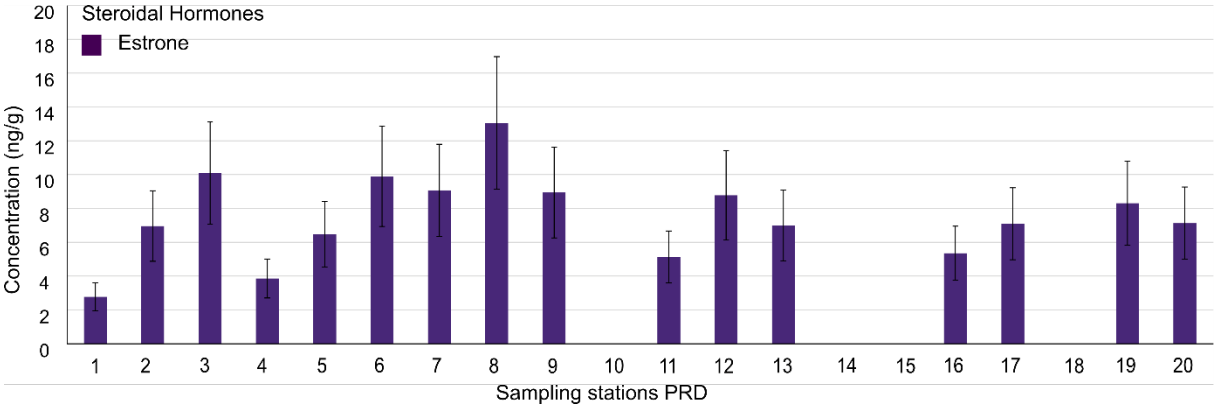

Figure 4.6 Concentration (ng/g) of the steroidal hormone estrone at 20 PRD surface samples. The error bars are the RSD of the internal standard 9-bromo-phenathrene across all surface samples and represent instrumental and procedural consistency.

The RSD of the internal standard estrone-3-methylether across 18 surface samples (excluding two statistical outlier) was 19.8%, indicating acceptable instrument performance. The average concentration across all sites was 7.5 ng/g. Estrone was detected in 80% of the sampling locations (16/20), with concentrations ranging from below the LOD to 13.1 ng/g. The highest concentration of estrone (13.1 ng/g) was found at sampling site 8, which also registered the highest PAH levels. There was no decreasing concentration trend visible towards the more remote sampling sites. The spatial distribution of hormones in the PRD suggests that diffuse sources, such as aquaculture and agricultural and urban wastewater runoff, rather than point sources, are responsible for their presence. Furthermore, estrogens, including estrone, are more hydrophilic than e.g. PAHs, allowing them to remain in the water column longer before being removed by binding to organic matter or fine particles. Given the highly dynamic nature of the PRD, characterised by strong tides and estuarine circulation, the estrogens in the water column can be efficiently redistributed and homogenised throughout the estuary, which explains their detection at more remote sites. Importantly, the potent estrogen estradiol, progesterone and the synthetic hormone ethinylestradiol were not detected at any of the

sampling locations. Previous studies have reported similar estrone concentrations in PRD sediments reaching levels up to 10.9 ng/g and 8.6 ng/g (Gong *et al.*, 2011; Zhao *et al.*, 2025).

A Principal component analysis (PCA) was performed using trace metal, PAH, and hormone concentrations from the surface sediment samples, along with sediment characteristics (Figure 4.7).

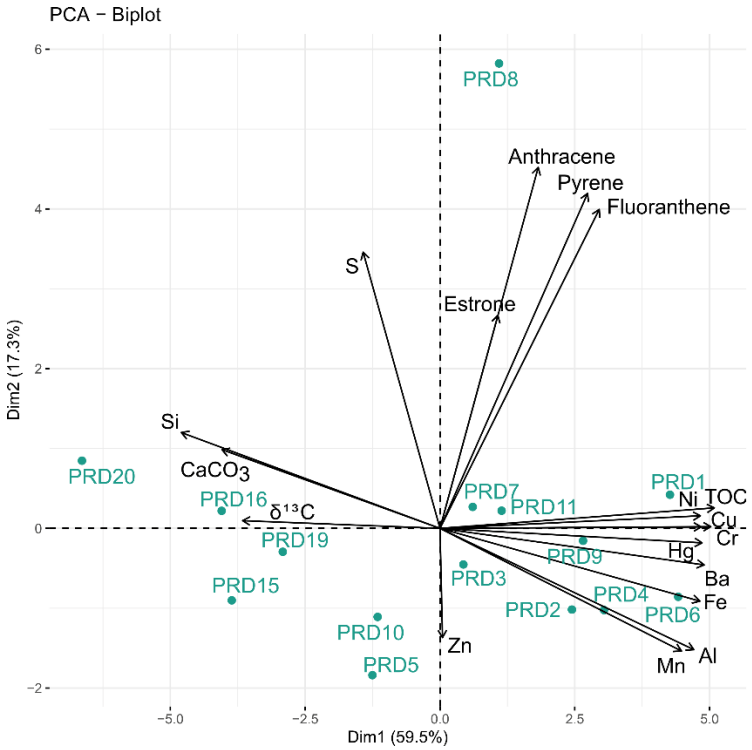

Figure 4.7: Biplot of the PCA conducted with contaminant concentrations and sediment properties of the PRD surface samples. The samples are in blue-green, the loadings of the measured variables are represented by black arrows.

The biplot reveals several distinct clusters. In the first (upper right) quadrant, the organic contaminants plot together, showing strong correlation with one another and with sampling site 8, where the highest concentrations of both PAHs and estrone were recorded. In the second (lower right) quadrant, most trace elements cluster together, except for Zn indicating a different source for Zn compared to the other trace metals. The PCA analysis suggests that organic contaminants and trace metals in the estuary originate from different sources or are strongly associated with different sediment fractions. The sampling stations closest to the river systems (1-11, excluding 5 and 10) cluster with the trace elements, as well as TOC and Al, indicating strong correlations between trace metals and sediment properties such as TOC and grain size. In contrast, previous studies in the PRD and other estuaries have reported different results (Gong *et al.*, 2011)(Chapter 2). However, trace metal concentrations in this study are generally consistent with reported background levels in the PRD (Pb: 40.6 mg/kg, Cu: 54.4 mg/kg, Zn 133 mg/kg, Cr: 109 mg/kg, Ni: 47.3 mg/kg) (Shi *et al.*, 2022). Therefore, sediment characteristics,

particularly grain size, may play a dominant role in controlling trace element distributions in this area, rather than anthropogenic inputs. The coastal sampling sites (15, 16, 19, 20) are clustered in the third and fourth quadrants, alongside Si and $CaCO_3$, indicating marine sediment properties. Meanwhile, stations 5 and 10 appear unrelated to any other variables, suggesting differing sediment characteristics. Overall, dimension 1 of the PCA reflects a gradient from marine influence on the left to anthropogenic and urban influence on the right, while dimension 2 differentiates between organic and inorganic variables.

4.4.3 Sediment Characterisation of the PRD Core

Similar to the surface samples, the $\delta^{13}C$ and C_{org}/N_{total} ratios for the subsampled PRD core samples were plotted to determine the source of organic carbon throughout the core (Figure 4.3b)). The ranges for $\delta^{13}C$ (-25.6 - -22.8 ‰) and C_{org}/N_{total} (7.6 – 9.7) are narrower than those for the surface samples. However, it is possible to distinguish between the top 45 cm of the core (indicated by purple circles) and the deepest 45 cm (indicated by turquoise circles) in terms of organic carbon sources. The surface samples exhibit lower $\delta^{13}C$ values (-25.6 – -24.3 ‰), suggesting a mixed origin of organic carbon from freshwater algae, freshwater POC and marine DOC. In contrast, the deepest layers of the core are predominantly derived from marine DOC and marine algae origin (-24 – -22.8 ‰). Additionally, Figure 4.9 indicates a slight decrease in TOC throughout the core, suggesting organic matter degradation (Middelburg, 1989).

The profiles describing sediment characteristics throughout the core are shown in Figure 4.9. The profile for the radionuclide ^{210}Pb displays a nearly uniform exponential decline with depth, allowing for the dating of the core and calculation of sedimentation rates using a constant flux: constant sedimentation rate model (CF:CS). The radionuclide ^{137}Cs was determined as well, but its activities were very low throughout the core (0.0012-0.0027 Bq/g), precluding an alternative calculation of sediment accumulation rates alongside ^{210}Pb. The deepest segment of the core corresponds to approximately the year 1913, with a sedimentation rate of 8.3 mm/year, which aligns well with previously determined sedimentation rates in the area (i.e. 8.6 mm/year (Zhang *et al.*, 2002)).

Aluminosilicates typically dominate the finer sediment (clay) fractions and are mostly unaffected by redox processes or early diagenesis. Therefore, Al concentration is often used as a proxy for sediment grain size, with higher Al concentrations reflecting a greater proportion of fine-grained material in sediments (Windom *et al.*, 1989; Loring, 1991). In this core, Al concentrations increase toward the bottom of the core, peaking at approximately 400 mm depth. Assuming that Al reflects grain-size variations at this site, this trend suggests an increase in fine-grained particles with depth. However, Al as grain-size proxy should be interpreted

cautiously. Regional geology and erosion processes can influence Al concentrations independently of grain size (Birch, 2020). Moreover, Al concentrations vary little within silt-sized sediments and are therefore more effective at distinguishing between clay and sand, than at clay and silt (Famera *et al.*, 2013).

The S and Fe profiles provide insight into the extent of early-diagenetic redox processes occurring within the core sediments (Spencer, Cundy and Croudace, 2003). In this case, the S and Fe profiles display opposing trends with sulphur spikes in the upper 20 cm declining with depth, while Fe increases with depth. The increase in Fe may be linked to changes in sediment composition and grain size, as suggested by the correlating profiles of $\delta^{13}C$ and Al. The lower S concentration in the deeper sections of the core indicate oxic or suboxic conditions, where sulphate reduction has not yet become the dominant redox process. The higher S concentrations at the surface may be related to associations with organic carbon or evaporative effects that concentrate salts, including sulphates, at the surface.

4.4.4 Geochronology of Contaminants in the PRD

Figure 4.9 describes the core profiles for trace element, PAH and hormone concentrations. Mercury concentrations remain relatively stable throughout the core, with only minor fluctuations near the surface and no notable increase with depth. An average concentration of 0.2 mg/kg indicates a consistent but small input (Figure 4.9). Cu and Zn are the only trace elements displaying a decreasing trend with depth, suggesting a constant increase in their inputs over time, with concentrations reaching 101 and 353 mg/kg, respectively. Ba, Pb and Cr exhibit greater fluctuations over time. Ba and Pb show broad maxima at around 42 cm depth, coinciding with a maximum in Al and a minor maximum in Hg. Cr and Pb show similar trends throughout the core, suggesting a common source. They are the only elements showing a decreasing trend over time, pointing to a decline in contaminant input, potentially due to stricter regulatory measures (e.g. the prohibition to use Pb as antiknock agent in fuels). Alternatively, the peaks in Ba, Pb and Cr could reflect accumulation in the core due to changing sediment properties, suggesting post-depositional redistribution driven by alterations in sediment characteristics, and subsequent re-adsorption depending on TOC degradation, changes in OM sources, and finer grain sizes indicated by higher Al concentrations. Pb and Cr show peaks in the deepest layers of the core, with concentrations of 80 mg/kg and 57 mg/kg respectively. There are also coinciding peaks for Cu, Ba, Pb and Cr at a depth of 14 cm, possibly indicating a discrete input event that released these metals into the environment.

Previous studies have found similar trends in temporal contaminant input into PRD sediments, with higher concentrations of Cu and Zn in surface layers compared to the depths of the core (Ip

et al., 2004). However, Ip et al. (2004) noted that different sampling locations can receive varying types of trace metal inputs. For example, a core from the western PRD showed decreasing concentrations in surface layers since 2010, suggesting a decline in trace metal inputs possibly due to stricter regulations (Shi *et al.*, 2022). While different locations display varying patterns in trace metal input, the reported concentration ranges are quite similar for both the western core and the eastern PRD core analysed in this study (Shi *et al.*, 2022). In stations closer to the rivers, core concentrations were higher for Cr, Cu and Zn (14-469 mg/kg, 14-257 mg/kg and 11-630 mg/kg, respectively) (Gao *et al.*, 2016).

PAHs were detected throughout all layers of the core, with average concentrations of 6.5 ng/g for anthracene (3.2 – 12 ng/g), 21.5 ng/g for fluoranthene (12.6 – 29 ng/g) and 28.2 ng/g for pyrene (18 – 38.4 ng/g). Fluoranthene and pyrene are the dominant PAHs, consistent with surface samples and previous findings (Chapter 2). All PAHs show peaks around 35 – 50 cm depth, with lower concentrations in the deepest samples. Assuming a constant sedimentation rate, these PAH peaks correspond to the period between 1962 and 1980, likely reflecting intensified coal and biomass combustion during a phase of socio-economic recovery in China. Similar PAH trends have been documented in other sediment cores from the PRD (Peng *et al.*, 2008; J. Zhang *et al.*, 2024). Despite analysing only a limited number of PAHs in this study, the total concentrations (34.9–72.9 ng/g) fall within the range reported in other regional studies (31–170 ng/g) (J. Zhang *et al.*, 2024). The core segment with relatively high concentrations may also be influenced by elevated aluminium content and the presence of finer-grained sediment, which could enhance the preservation of PAHs (Sun *et al.*, 2008; Duan *et al.*, 2022).

Molecular indices are commonly applied for PAH source attribution, because different PAH formation pathways produce characteristic molecular patterns ((Tobiszewski and Namieśnik, 2012; Potapowicz *et al.*, 2022). To assess temporal trends in PAH sources within the sediment core, two diagnostic ratios that distinguish between pyrogenic and petrogenic sources were applied (Figure 4.8).

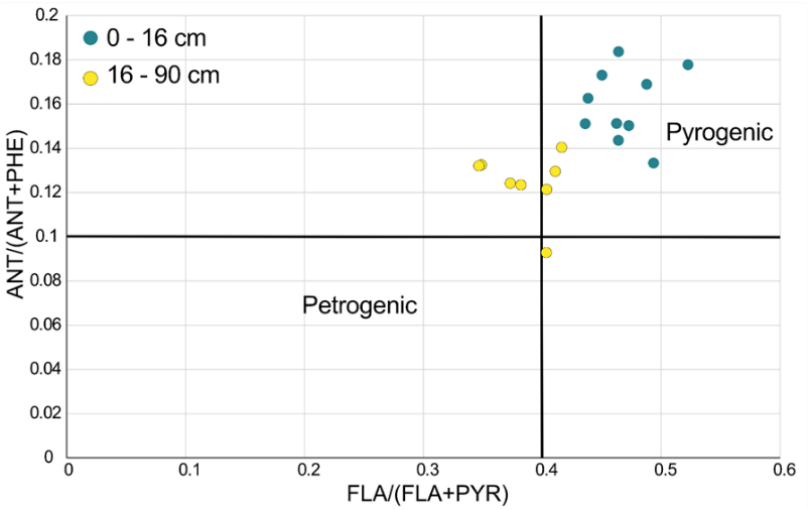

Figure 4.8: PAH molecular indices ANT/(ANT+PHE) vs. FLA/(FLA+PYR) to identify possible PAH sources (pyrogenic vs. petrogenic) in the sediment core. The core samples are divided into surface samples (upper 16 cm, blue) and deeper 74 cm (yellow).

Most core sections lie within the pyrogenic range of both indices with ANT/(ANT+PHE) values between 0.09 and 0.18 and FLA/(FLA+PYR) values from 0.3 to 0.5. The upper 16 cm of the core have higher ANT/(ANT+PHE) (0.13 – 0.18) and higher FLA/(FLA+PYR) ratios (0.43 – 0.52) compared to the deeper sections, indicating pyrogenic origin from high-temperature combustion such as fossil fuel or biomass burning, which aligns with increased industrial activity and urbanisation in China after the 1980s. In contrast, the deeper core samples present more diffuse ratios with ANT/(ANT+PHE) ranges between 0.09 and 0.16, and FLA/(FLA+PYR) ranging between 0.34 – 0.41 that complicate the source apportionment, likely due to mixed sources. Nonetheless, there is a marked trend shifting from more diffuse sources to petrogenic sources over time. Similar source-diagnostic trends have been observed in other sediment cores from the PRD (Peng *et al.*, 2008). In general, it should be noted that source apportionment of PAHs by molecular indices is not unambiguous, but rather indicative. As they are dependent on combustion conditions, environmental degradation processes and the mixing of different PAH sources, PAH indices should be treated with caution (Galarneau, 2008; Katsoyiannis, Sweetman and Jones, 2011).

Regarding steroidal hormones, only estrone (E1) and estradiol (E2) were detected (Figure 4.9), with the highest concentrations (8.8 ng/g for estrone and 2.8 ng/g for estradiol) found at the surface, followed by a rapid decline with depth. Estradiol was not detected below the top 10 cm of the core, while estrone showed some fluctuations in the upper 30 cm. The presence of estrone and estradiol at the sediment surface suggests recent or continuous inputs, potentially from wastewater or agricultural sources. The rapid decline of estradiol with depth, combined with the persistence of estrone in the upper 30 cm, implies a possible transformation from

estradiol to estrone and indicates degradation processes (Biswas, Vellanki and Kazmi, 2024; S. Zhang *et al.*, 2024).

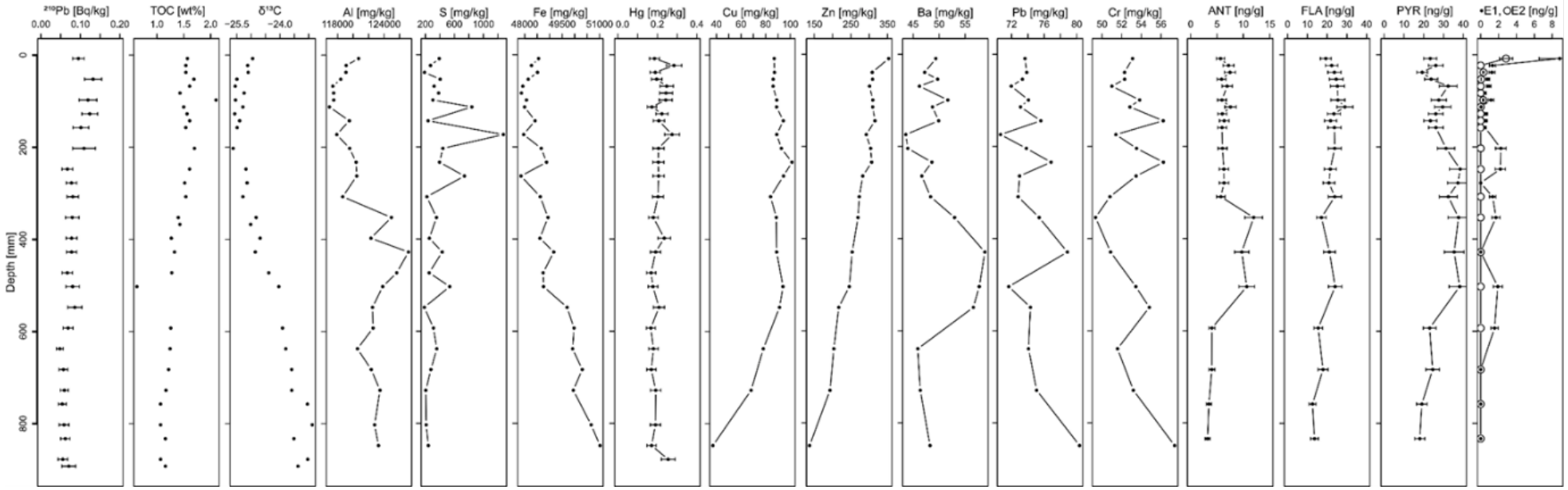

Figure 4.9: Pearl River Delta core profiles with the y-axis being the depth in mm (0 mm is the top of the core, and 300 mm is the depth of the core). Displayed are ^{210}Pb in Bg/kg, TOC in wt%, δ^{13}C in relation to VPDB, the major elements Al, S and Fe in mg/kg, trace elements Hg, Cu, Zn, Ba, Pb and Cr in mg/kg, anthracene (ANT), fluoranthene (FLA) and pyrene (PYR), as well as estrone (E1) and estradiol (E2) in ng/g sediment dry weight. The error bars for the PAHs and hormones are the relative standard deviation of the internal standards 9-bromo-phenanthrene and estrone-3-methylether, respectively.

The biplot from the PCA of core variables reveals more complex geochemical patterns compared to surface samples as seen in Figure 4.10:

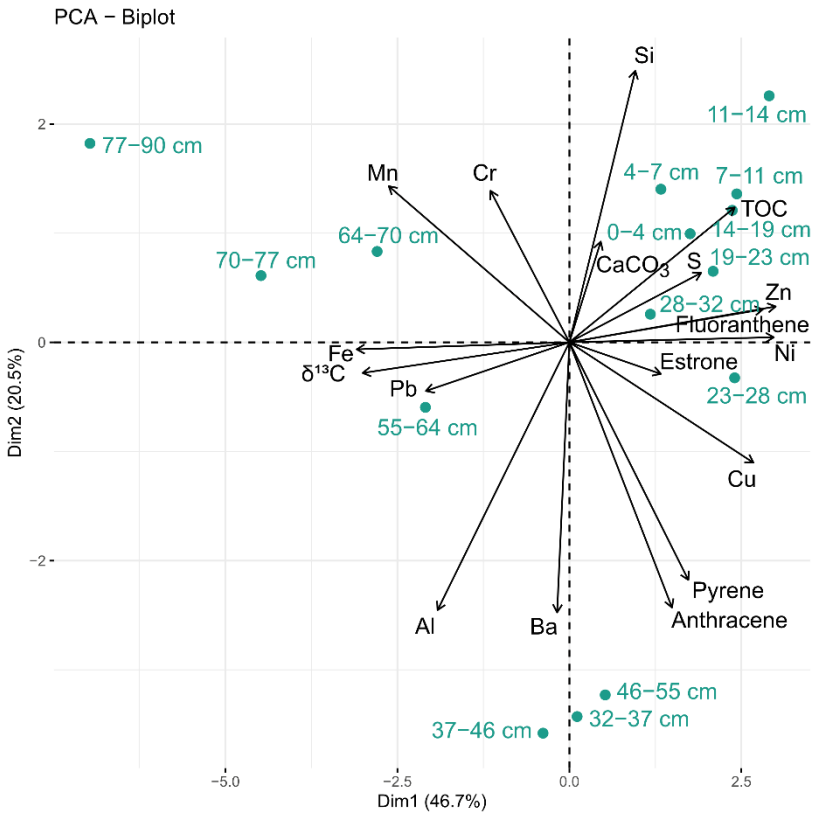

Figure 4.10: Biplot of PCA with all sediment core variables and their loadings indicated by black arrows, as well as the core samples in blue-green.

In the upper right quadrant, there is a clustering of the top 30 cm of the core, linked to TOC, $CaCO_3$, S and Si, as well as the contaminants Zn, Ni and fluoranthene. Previous studies have shown a strong correlation between TOC and Zn, Ni, and other trace metals in cores from Chinese rivers (Zhou *et al.*, 2014). Estrone and Cu appear to have a weak association with this cluster, suggesting recent contaminant input. While the surface samples indicate distinct sources for organic and inorganic contaminants, the PCA does not reveal specific source differentiation, potentially due to the limited contaminant sources available at the core location. Anthracene and pyrene are associated with the middle 30 – 50 cm of the core, reflecting their peak concentrations at this depth. The third and fourth (lower and upper left) quadrants show associations with the redox-sensitive elements Fe and Mn, as well as Cr, Pb and Al. These associations with the deeper layers of the core (55-90 cm), indicate a more natural signature, possibly influenced by redox conditions and the accumulation of Pb and Ba in finer-grained sediments, as indicated by Al as a grain size proxy. Pb is also associated with $\delta^{13}C$, which could suggest that the distribution and mobility of Pb are impacted by the type of organic carbon present. The biplot clearly differentiates the upper core layers, reflecting anthropogenic

activity and recent contamination, from the deeper layers that reflect more natural associations as well as the influence of sediment grain size on contaminants like Pb and Ba.

4.5 Conclusion and Outlook

4.5.1 Spatial and Temporal Trends in Contaminant Distribution and Source Control

This study examined spatial and temporal trends of contamination within one of the world's most urbanised estuaries. Trace metals and PAHs were detected throughout the estuary but displayed a notable decline in concentration towards more marine sampling sites. This indicates that sediments effectively trap contaminants near the source (e.g. urban and agricultural wastewater runoff), thereby reducing their influx into the marine environment. Estrone was the only hormone detected, and unlike PAHs and trace metals, its distribution did not reveal clear trends. This lack of clarity may be attributed to the hormone's longer residence time in the water column and subsequent dispersion, or to widespread diffuse sources rather than specific point sources. Overall, the concentration ranges for trace elements, PAHs and estrone were comparable with findings from prior studies.

Core profiles of trace elements and PAHs revealed historical input patterns dating back to approximately 1913, showing an increase in Cu and Zn concentrations, while other trace elements exhibited declining trends likely due to stricter environmental regulations over time. Estrone and estradiol were detected primarily in the upper layers, with peak concentrations at the surface and a rapid decline with depth, suggesting recent or ongoing inputs. The profiles also indicate the transformation of estradiol to estrone in the core, followed by the (bio)degradation of estrone. The core profiles illustrate the potential of sediments to retain some contaminants over extended periods, while allowing others to degrade (e.g., hormones) or become more mobile (e.g., Ba and Pb). PAH ratios further indicate a historical shift from diffuse to pyrogenic sources over time.

4.5.2 The Role of Sediment (and Organic Matter) Composition

The role of type and source of organic carbon in the surface samples and the core was investigated using PCA. Surface samples exhibited a clear distinction between the origin of organic and inorganic contaminants. Additionally, the distribution of trace metals in the PRD appears to be highly influenced by sediment properties such as TOC and grain size. However, no correlation was observed between organic contaminants and TOC, in contrast to previous findings (Chapter 3, (Dai *et al.*, 2022; Yu *et al.*, 2024)). For estrone, PCA indicated its co-occurrence with PAHs at one site, indicating a specific point source for both contaminant

groups. However, no correlation to sediment properties such as grain size, TOC, or $\delta^{13}C$ was established. In the sediment core, correlations are more complex. The upper 30 cm show signs of recent contaminant input, including hormones, while the deeper sections reflect more natural geochemical processes. These deeper layers correlate the distribution of Pb and Ba with grain size and organic carbon type.

Both surface and core samples demonstrate that sediments serve as selective sinks for various contaminant groups, including steroidal hormones, thereby limiting their widespread distribution within the open estuary. However, the findings suggest limited long-term preservation of hormones in this estuary, which contrasts with previous findings. This may be due to the source and type of organic matter, which exhibited minimal variation within the PRD. The contrasting influences of organic carbon and sediment properties (such as $\delta^{13}C$) in surface and core samples underline the necessity for further research into how organic matter controls the behaviour of contaminants.

These findings emphasise the complex interplay between contaminant inputs and sedimentary organic matter, highlighting the importance for further exploration into the mechanisms governing the retention and degradation of steroidal hormone in estuarine sediments.

[Acknowledgements: The authors would like to thank the team at GAU-Radioanalytical Laboratories for their support in radiometric dating of the core and Hg analysis. We also appreciate the contribution from the Southern Marine Science and Engineering Guangdong Laboratory (Guangzhou) in sampling support, site selection and sample provision. This work is supported by the INSPIRE Doctoral Training Partnership funded by the Natural Environmental Research Council (grant number NE/S007210/1) and via a collaborative research grant award from the Hong Kong Branch of the Southern Marine Science and Engineering Guangdong Laboratory (Guangzhou) (GML2019ZD0409) and (SMSEGL20SC01-V).]

Chapter 5 Influence of Organic Matter Type and Source on the Adsorption of Steroidal Hormones in Estuarine Systems

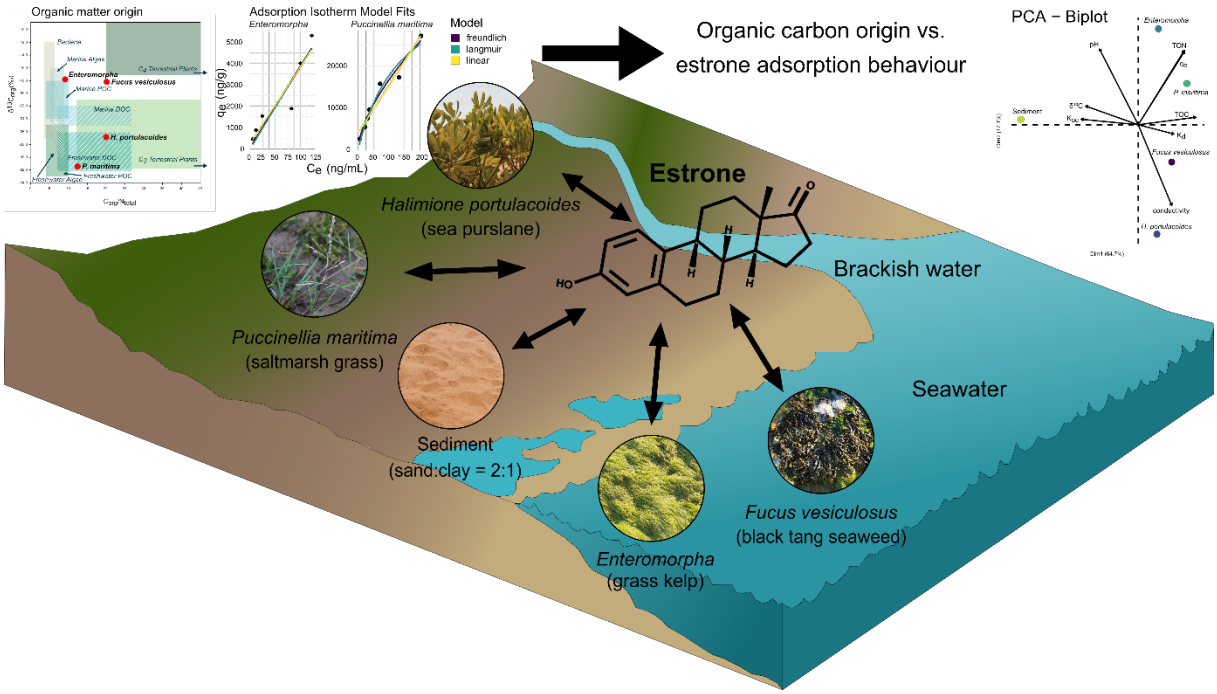

Figure 5.1: Graphic abstract of Chapter 5: Influence of Organic Matter Type and Source on the Adsorption of Steroidal Hormones in Estuarine Systems. The abstract was created using Affinity Designer 1.

This chapter is based on a manuscript intended for submission for peer review ("Influence of Organic Matter Type and Source on the Adsorption of Steroidal Hormones in Estuarine Systems", Appelt, J.-S., Bray, S., Whiteside, J.H., Cundy, A., *Environmental Science and Technology*) and has been reformatted to conform to University of Southampton guidelines for thesis submission.

Author contributions: JSA: Conceptualisation, data curation, formal analysis, investigation, methodology, validation, visualisation, writing - original draft; SB: Conceptualisation, methodology, resources, supervision, writing – review & editing; JHW: Conceptualisation, methodology, supervision, writing – review & editing; AC: Conceptualisation, data curation, funding acquisition, methodology, project administration, resources, supervision, writing – review & editing

5.1 Abstract

The fate of steroidal hormones in estuarine environments is strongly influenced by interactions with fine-grained, organic-rich sediments, yet the role of sedimentary organic matter type and source in controlling hormone adsorption remains poorly understood. This study investigates the adsorption behaviour of estrone on sorbents derived from various estuarine plant materials, each representing distinct organic matter sources. Adsorption experiments were conducted under brackish and marine salinities to simulate estuarine conditions using five different estuarine sorbents (freeze-dried samples of *Puccinellia maritima*, *Fucus vesiculosus*, *Halimione portulacoides*, *Enteromorpha* and organic matter-poor sediment). The adsorption isotherms revealed that sorption patterns varied by substrate: *Enteromorpha* and *Halimione portulacoides* exhibited linear adsorption, while *Puccinellia maritima* and estuarine sediment followed Freundlich-type behaviour. *Fucus vesiculosus* did not conform to common isotherm models, suggesting that its sorption mechanisms are more complex. Salinity variations between brackish and marine conditions did not significantly affect adsorption, suggesting a threshold effect at higher ionic strength. Although no direct correlation was found between sorption behaviour and the source of organic matter, total organic carbon (TOC) and particularly total organic nitrogen (TON) emerged as key drivers for estrone adsorption. These findings advance our understanding of the role of organic matter composition in hormone fate and behaviour in estuarine systems.

5.2 Introduction

Endocrine-disrupting chemicals (EDCs), including steroidal hormones, can interfere with endocrine processes and therefore pose significant risks to the environment and potentially human health (United Nations Environment Programme (UNEP) and World Health Organisation (WHO), 2013). Estuaries, often heavily urbanised areas, have been shown to act as sinks for a wide range of contaminants due to their unique properties as transitional environments, mitigating contaminant effects on marine environments. Fine-grained, organic-rich estuarine sediments in particular play an important role in the trapping of contaminants, and steroidal hormones have been detected in estuarine sediments globally, e.g. along the coast of Guangdong, China and in the Scheldt estuary, Belgium (Morais *et al.*, 2023; Jia *et al.*, 2024; Zhao *et al.*, 2025). The fate and behaviour of organic contaminants, including EDCs, have also been analysed on a temporal scale using estuarine sediment cores. Some studies have found that certain contaminants, e.g., antimicrobial agents in river sediments remain immobile (Tamtam *et al.*, 2011). In contrast, other organic pollutants, including pharmaceuticals, plasticisers and perfluoroalkyl substances, have been detected at sediment depths that predate their commercial introduction into the environment, suggesting mobility within sediments through processes like porewater diffusion and tidal flushing (Thiebault *et al.*, 2017; Celis-Hernandez *et al.*, 2021). In another study, the steroidal hormone estrone was found in undisturbed, over 120-year-old riverine clay sediments (Labadie *et al.*, 2007). Depending on the environmental context and specific contaminant, the effectiveness of estuarine sediment trapping varies widely and makes reliable predictions of contaminant fate and behaviour challenging.

Given the ubiquitous presence and potential toxicity of steroidal hormones in estuarine sediments, improved understanding of their adsorption mechanisms and the properties that influence adsorption behaviour is required to fully assess environmental risk. Bowman, Zhou and Readman (2002) investigated the sorption behaviour of estrogens under estuarine conditions and found that sediment concentration influenced the partition coefficient for estrone and estradiol, while salinity enhanced sorption of estrone, but not estradiol. Similarly, Casey et al. (2003) found that the adsorption affinity of estradiol depends on particle size and organic matter (OM) content and Sangster et al. (2015) investigated further and concluded that OM content has a greater influence on the sorption of various steroidal hormones than particle size. Additionally, pH influences the dissociation of hormones and sediment compounds, and therefore, plays an important role in adsorption behaviour as well (Neale, Escher and Schäfer, 2009). The adsorption mechanisms in marine sediments can also be complicated by the presence of competing compounds, such as bisphenol A (BPA) (Fei, Leung and Li, 2017).

Potential mechanisms and mobility for EDCs have also been assessed using quantitative structure-property relationship models, suggesting strong mobility in sediments (Li *et al.*, 2014).

Due to the complexity of adsorption processes under environmental conditions, results can vary and indicate contradicting results; while some studies found specific and hydrophobic interactions to be the predominant mechanisms taking place for different EDCs, other studies suggest that hydrophobic interactions are not the predominant sorption mechanism (Lee *et al.*, 2003; Yamamoto *et al.*, 2003; Yang, Lin, Zhang, *et al.*, 2020).

While the importance of OM content in hormone adsorption is well-established, variations in the type and source of OM are often underexplored, with sedimentary organic carbon frequently treated as a homogenous adsorbent. Several studies indicate that the sedimentary organic carbon nature and source control the speciation of trace elements like Hg, but studies concerning the impact of OM source on organic contaminant sequestration are still scarce (Hissler and Probst, 2006; Chakraborty *et al.*, 2015; Fernandes *et al.*, 2016). For example, Nybom et al. (2024) evaluated the relationship between organic carbon composition in sediments and the sorption of polycyclic aromatic hydrocarbons (PAHs) and polychlorinated biphenyls (PCBs) and concluded that stronger sorption reflected a change in OM composition. Regarding hormones and other EDCs, studies have found different adsorption capacities for estrogens on dissolved organic matter (DOM), suspended particulate matter (SPM), colloids and sediments and soils (Ma and Yates, 2018; Song *et al.*, 2024). The effect of specific sediment compounds, such as humic acids, alginic acids and tannic acids on EDC adsorption has been investigated by several researchers (Yamamoto and Liljestrand, 2003; Yamamoto *et al.*, 2003; Neale, Escher and Schäfer, 2009). Chen et al. (2012) in particular studied the adsorption of estrogens on sediments from different sources and noted that the sorption coefficients varied by sediment origin (e.g, agricultural, industrial or domestic discharges). However, they did not delve into the differences on a molecular basis. Despite extensive research emphasising the importance of organic matter in contaminant retention, the molecular origins and composition driving these variations are frequently overlooked.

This study aims to investigate the adsorption capacities of estuarine carbon from differing sources for hormones under changing salinities. We measured total organic carbon (TOC), total organic nitrogen (TON), as well as the carbon isotopic composition ($\delta^{13}C$) of estuarine plant materials (*Fucus vesiculosus, Enteromorpha, Halimione portulacoides, Puccinellia maritima*, sediment) to determine the sources of organic carbon. Adsorption experiments were conducted with the steroidal hormones estrone and progesterone in each estuarine substrate at varying concentrations in brackish water and maintaining a constant concentration in saltwater to simulate estuarine conditions. Results are fitted to linear and nonlinear adsorption isotherms to

evaluate adsorption behaviour and distribution coefficients K_d and carbon-normalised partition coefficient K_{OC} are determined from experimental data.

5.3 Materials and Methods

5.3.1 Chemicals

Methanol (MeOH) and ethyl acetate (EtOAc) were purchased from Rathburn Chemicals, UK. Analytical standards for estrone and progesterone were sourced from Merck, while other chemicals were purchased as described in Chapter 2. For extraction, we used Oasis HLB solid-phase extraction (SPE) cartridges (6cc/200mg) from Waters, UK. A standard stock solution for estrone and progesterone was prepared in DCM (100 ng/µL) and stored at -18°C, with a working solution (10 ng/µL) prepared from this stock.

5.3.2 Adsorption Experiments

Estuarine plant materials — *Halimione portulacoides* (sea purslane), *Fucus vesiculosus* (black tang seaweed), *Ulva intestinalis* (grass kelp/*Enteromorpha*), and *Puccinellia maritima* (saltmarsh grass) —were collected from the Hamble estuary, UK, in September 2024. The plants were washed with deionized water and freeze-dried to reduce sample volumes and variations in water content while preserving surface chemical characteristics. A blank sediment (with a sand:clay ratio of 2:1, furnaced at 400 °C) was also used as substrate. Filtered saltwater (salinity of 31 g/kg, measured with a HANNA Instruments Salinity analyser) was sourced directly from Southampton Water via taps located within the institution's research aquarium, and brackish water (salinity 15 g/kg) was prepared by mixing seawater with tap water. To prevent microbial activity, the seawater was sterilised in a Boxer 300/100LR Autoclave at 120 °C for 60 min. The freeze-dried plant material was coarsely ground to homogeneity using a mortar and pestle.

To determine adsorption isotherms, 0.2 – 2 g of dried substrate was weighed into a glass vial and spiked with seven different concentrations of the estrone and progesterone working solutions (100 - 2000 ng for *Halimione portulacoides*, *Fucus vesiculosus*, *Enteromorpha*, and sediment; 400 - 6000 ng for *Puccinellia maritima*; details in Table D. 1). Triplicate samples were prepared for one of the concentrations. After allowing the samples to dry, 10 mL of brackish water was added. The samples were sealed in containers and agitated on a Stuart SSL1 orbital shaker for 72 h to reach equilibrium adsorption. A separate set of triplicate samples from each substrate was prepared, spiked with 400 ng of estrone and progesterone, and treated with 10 mL of seawater before shaking for 72 h prior to extraction. The same procedure was applied to

freshwater samples. A sketch of the method described here, and the used substrates can be found in Figure 5.2.

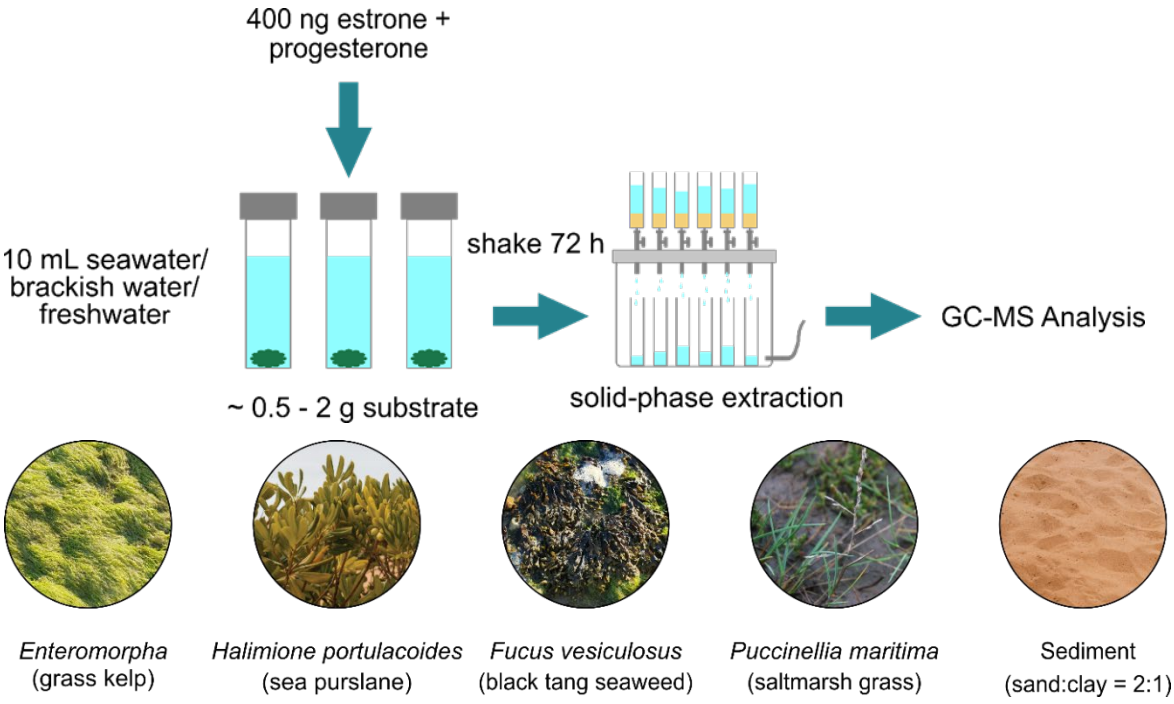

Figure 5.2: Diagram of the method for batch adsorption experiments on the top and pictures of estuarine materials used as substrates at the bottom.

5.3.3 Sorbent Characterisation

An Elementar Vario Isotope Select Elemental Analyser coupled with an Isoprime GeoVisION continuous flow isotope ratio mass spectrometer (IRMS) (Isoprime 100) was used for $\delta^{13}C$ analysis and to determine the elemental concentrations of %C and %N in bulk organic matter. The isotopic ratios were referenced against the Vienna PeeDee Belemnite (VPDB) standard for $\delta^{13}C$ and atmospheric N_2 was used as a reference for $\delta^{15}N$. Additional details are described in Chapter 2.

The pH for each substrate was measured after 72 h equilibration at each salinity using a Mettler Toledo pH-meter and conductivity was determined for each substrate in freshwater using a portable EC/TDS meter (HANNA Instruments).

5.3.4 Extraction and GC-MS Analysis

All samples were extracted using solid-phase extraction (SPE) after Kumirska et al. (2013). In brief, cartridges were preconditioned with 3 mL EtOAc, 3 mL MeOH and 3 mL distilled water. Samples were then loaded into the cartridges, washed with 10 mL MeOH:H_2O (1:9) and dried under vacuum for 1 h. Elution was performed using 8 mL of MeOH. The eluates were dried using a GeneVac EZ-2 vacuum centrifuge and transferred to GC-MS vials with MeOH. Extracts were

then dried under a gentle nitrogen stream and reconstituted in 200 µL of a DCM:BSTFA-TMCS (1:1) solution before derivatisation at 50 °C for 40 min. Sample analysis was conducted using a Thermo Scientific TRACE 1310 gas-chromatograph coupled to a Thermo Scientific TSQ 8000 Triple Quadrupole mass spectrometer. Specifications are described in Chapter 2. Target compounds were analysed based on retention times and characteristic m/z ions, and quantitative analysis was performed using peak areas of the quantitative compounds. Identification features for each analyte are provided in Table 2.4, Chapter 2.

Recovery rates for estrone in freshwater calibration samples were consistently low (around 2%) due to low retention in the SPE cartridges (Figure D. 4). To enhance analyte–sorbent interactions, freshwater samples were acidified to pH 4 with HCl to increase ionic strength; however, recoveries remained too low for quantification of estrone in freshwater (Figure D. 4). Additionally, progesterone analysis showed substantial variability across substrates, which could not be explained by the measured sediment properties (Figure D. 5). Consequently, progesterone results are not discussed further, nor are results from freshwater samples. Only estrone data from brackish and seawater are discussed in the following sections.

5.3.5 Quality Control

Matrix-matched calibration curves were prepared by spiking brackish and seawater samples (no sorbent material) with estrone at concentrations of 200 ng, 400 ng and 1000 ng, which were extracted using the same SPE method to account for any recovery losses. Each substrate in saltwater and one concentration per substrate in brackish water were prepared in triplicate to ensure reproducibility. Blanks for all substrates and seawater were prepared and analysed with GC-MS in selected ion monitoring (SIM) mode to ensure no additional hormone contributions were present. Additionally, procedural blanks were created for each sample batch to track any contamination during preparation, and no steroidal hormones were detected in any blank samples (Figure D. 3).

5.3.6 Adsorption Isotherms and Coefficient Determination

The concentrations were measured in the liquid phase, and the amount $\boldsymbol{q_e}$ of analyte adsorbed (ng/g) was calculated using the following equation:

$$\boldsymbol{q_e} = \frac{(\boldsymbol{m_0} - \boldsymbol{m_{aq}^{ads}})}{\boldsymbol{m}} \qquad \text{(eq. 3)}$$

Where $\boldsymbol{m_0}$ is the mass of the analyte at the beginning of the test (ng), *m* is the mass of sorbent (g) and $\boldsymbol{m_{aq}^{ads}}$ is the measured mass of analyte in the aqueous solution.

The partition coefficient $\boldsymbol{K_d}$ (L/kg) was determined using the equation:

$$K_d = \frac{m_s^{ads}}{m_{aq}^{ads}} \cdot \frac{V}{m} = \frac{q_e}{C_{aq}^{ads}} \qquad \text{(eq. 4)}$$

Where m_s^{ads} is the mass of the analyte adsorbed in the solid phase (ng), *V* is the initial volume (mL) of the sea/brackish water and C_{aq}^{ads} (ng/mL) is the concentration in the aqueous phase at equilibrium.

The organic carbon normalised adsorption coefficient K_{OC} (L/kg) was calculated from the partition coefficient and the TOC of the substrate as follows:

$$K_{OC} = K_d \cdot \frac{100}{\%TOC} \qquad \text{(eq. 5)}$$

In addition, the adsorption data in brackish water (q_e vs. C_{aq}^{ads}) were plotted and fitted to linear (eq. 6), Freundlich (eq. 7) and Langmuir (eq. 8) isotherm models, to determine the model that best describes the adsorption behaviour by comparing the correlation coefficient R^2 using R Studio. The linear, Freundlich and Langmuir models are described by the following equations:

$$q_e = K_d \cdot C_{aq}^{ads} \qquad \text{(eq. 6)}$$

$$q_e = K_F \cdot C_{aq}^{ads\frac{1}{n}} \qquad \text{(eq. 7)}$$

Where K_F is the Freundlich adsorption coefficient and *n* the regression constant.

$$q_e = \frac{q_{max} \cdot K_L \cdot C_{aq}^{ads}}{1 + K_L \cdot C_{aq}^{ads}} \qquad \text{(eq. 8)}$$

For the Langmuir model, q_{max} represents the maximum adsorption capacity (g/kg) and K_L is the Langmuir equilibrium constant (L/kg).

5.4 Results and Discussion

5.4.1 Substrate Characteristics

To characterise the organic carbon properties of the plant substrates, we analysed the $\delta^{13}C$ and total organic carbon (TOC) and nitrogen (TON). Figure 5.3 shows the origin of organic carbon in each substrate (Lamb, Wilson and Leng, 2006).

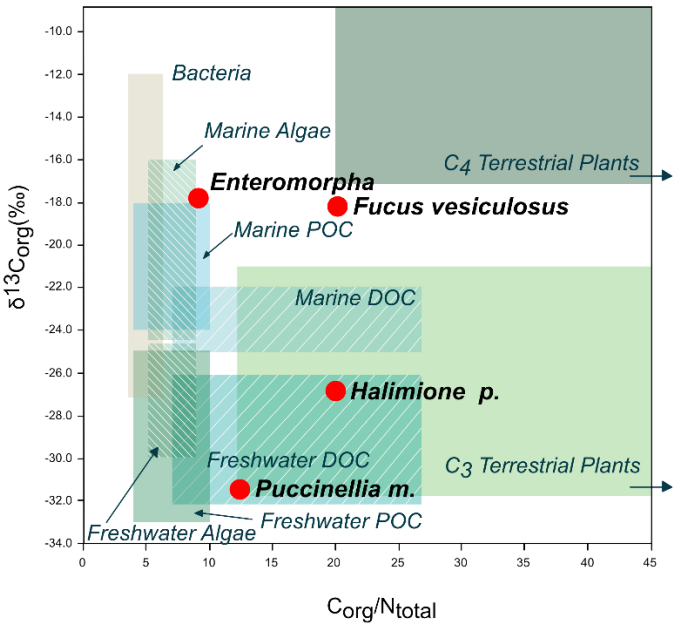

Figure 5.3: Organic matter origin of substrates ($\delta^{13}C$ vs. C_{org}/N_{total} after Lamb, Wilson and Leng (2006)).

We can clearly differentiate between the marine substrates, e.g., *Enteromorpha* and *Fucus vesiculosus*, which have less negative $\delta^{13}C$ values and the more terrestrial substrates, including *Puccinellia maritima* and *Halimione portulacoides*, where organic matter is derived from freshwater dissolved organic carbon (DOC) and C_3 terrestrial plants. The sediment used as substrate was furnaced and free of any organic material.

Across both salinities, pH levels of the aqueous phases derived from suspensions of plant material ranged from 5.8 – 7.8 following the order *Fucus vesiculosus* < *Puccinellia maritima* < *Halimione portulacoides* < *Enteromorpha* < sediment. Conductivity was highest for the marine substrates; *Halimione portulacoides* and *Fucus vesiculosus* had values of 2000 µS/cm and 1930 µS/cm, respectively, likely due to the presence of marine salts incorporated in their matrix. In contrast, the sediment had the lowest conductivity at 370 µS/cm.

5.4.2 Adsorption Isotherms and Sorption Parameters

Adsorption isotherms for estrone on estuarine substrates in brackish water are shown in Figure 5.4.

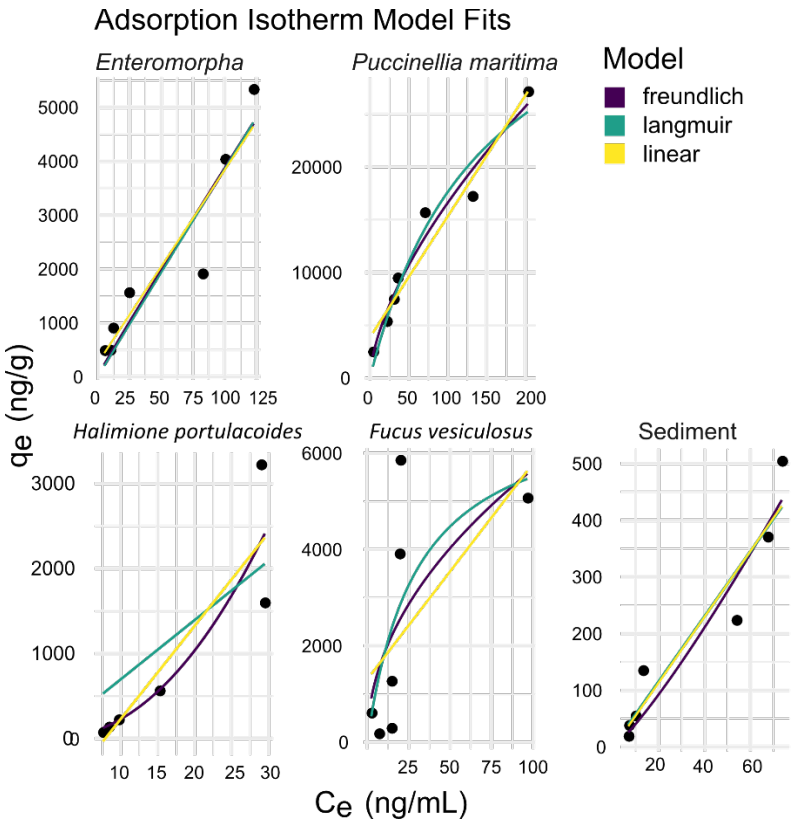

Figure 5.4: Adsorption isotherms (adsorbed amount q_e (ng/g) vs. C_{aq}^{ads} (ng/mL) for five different substrates in brackish water (black dots) and three different model fits: Freundlich model (purple fit), Langmuir model (blue-green fit) and linear model (yellow).

Enteromorpha, Puccinellia maritima, and sediment exhibit similar linear adsorption behaviours, whereas *Fucus vesiculosus* and *Halimione portulacoides* show distinct, non-linear patterns, which are also evident in the differences observed in model fits (Figure 5.4). The linear adsorption model best fits the data for *Enteromorpha* (R^2 = 0.89), while for *Puccinellia maritima*, sediment and *Halimione portulacoides*, the Freundlich model provides the best fit data (R^2 = 0.97, 0.92 and 0.81, respectively) (Table 5.1). The root mean square error (RMSE) for each model corroborates the R^2 values. However, none of the models discussed effectively describe adsorption mechanisms for *Fucus vesiculosus*. This may be due to the highly variable composition of the sorbent, or the presence of multiple sorption mechanisms.

Table 5.1: Model parameters for linear, Freundlich and Langmuir model, R^2 and RMSE for estrone adsorption to each substrate in brackish water.

	Enteromorpha	***Puccinellia maritima***	***Halimione portulacoides***	***Fucus vesiculosus***	**Sediment**
Freundlich K_F	43.9	904.8	1.5	585.6	2.6
Freundlich n	1.0	1.6	0.5	2.0	0.8
Langmuir K_L	0.00	0.01	0.00	0.03	0.00
Langmuir q_{max}	1165567	43333	3515418	7161	132654
R^2 Linear	**0.89**	0.95	**0.81**	0.36	0.91
R^2 Freundlich	0.88	**0.97**	**0.81**	0.45	**0.92**
R^2 Langmuir	0.88	0.95	0.67	0.51	0.91
RMSE Linear	590.3	1838.2	499.0	1800.5	50.8
RMSE Freundlich	613.9	1473.4	495.3	1667.6	49.7
RMSE Langmuir	614.7	1683.6	653.7	1565.4	50.9

Table 5.2: Adsorption parameters (q_e, K_d, K_{OC}, $logK_{OC}$) for estrone in brackish water and seawater at an initial concentration of C_0= 40 ng/mL.

	Brackish water				**Seawater**			
Substrate	**q_e (ng/g)**	**K_d (L/kg)**	**K_{oc} (L/kg)**	**$logK_{oc}$**	**q_e (ng/g)**	**K_d (L/kg)**	**K_{oc} (L/kg)**	**$logK_{oc}$**
Enteromorpha	1533.1	62.93	198.70	2.30	1673.5	77.07	243.34	2.39
Puccinellia maritima	2334.0	629.60	1448.34	3.16	1421.6	75.65	174.02	2.24
Halimione portulacoides	544.2	35.69	115.42	2.06	563.3	48.63	157.29	2.20
Fucus vesiculosus	1233.8	84.74	248.51	2.40	1337.2	188.55	552.94	2.74
Sediment	132.1	10.08	14393.64	4.16	133.7	10.26	14656.76	4.17

Assuming linear adsorption within a small concentration range, we calculated the distribution coefficient (K_d) for each substrate in both brackish and seawater at a concentration of 40 ng/mL estrone (Table 5.2). In brackish water, the amount of estrone adsorbed ranges from 132.1-2334 ng/g with *Puccinellia maritima* having the highest adsorption, followed by *Enteromorpha* (1533.1 ng/g) and *Fucus vesiculosus* (1233.8 ng/g). The partition coefficient K_d displays a similar

pattern: 629.6 L/kg for saltmarsh *Puccinellia maritima*, 84.7 L/kg for *Fucus vesiculosus*, 62.9 L/kg for *Enteromorpha*, 35.9 L/kg for *Halimione portulacoides* and 10.1 L/kg for sediment. Sorption values for the same compound can vary over several orders of magnitude across different sorbents (Li, Carter and Boxall, 2020). Some studies have reported negative correlations between sorption coefficient and sand content for estrone, with K_d values ranging from 11 – 119 L/kg and 1.1 – 75.1 L/kg, which may explain the lowest K_d observed for sediment (Caron *et al.*, 2010; Sangster *et al.*, 2015). Moreover, the sediment used here is free of organic matter, which likely further limits estrone sorption.

To eliminate the effects of varying organic matter content and facilitate better comparison with existing literature, we determined the organic carbon–normalised adsorption coefficient $\log K_{OC}$. This trend diverges from that of K_d: *Halimione portulacoides* (2.06) < *Enteromorpha* (2.3) < *Fucus vesiculosus* (2.4) < *Puccinellia maritima* (3.2) < sediment (4.2.). These values suggest that estrone has a moderate affinity for organic carbon in *Halimione portulacoides*, *Enteromorpha* and *Fucus vesiculosus*. *Puccinellia maritima* demonstrates a high affinity for estrone, indicating strong hydrophobic interactions. The highest $\log K_{OC}$ value was recorded for sediment, which likely results from its very low organic carbon content; here, sorption may be driven by the high surface area of clay particles or minerals. With the exception of *Halimione portulacoides*, our $\log K_{OC}$ values calculated here are in good agreement to reported $\log K_{OC}$ values for estrogens (2.77 – 3.90) (Dai *et al.*, 2022).

In seawater, the partition coefficients K_d differed from those in brackish water, following this order: sediment (10.3 L/kg) < *Halimione portulacoides* (48.6 L/kg) < *Puccinellia maritima* (75.7 L/kg) < *Enteromorpha* (77.1 L/kg) < *Fucus vesiculosus* (188.6 L/kg). While *Puccinellia maritima* and *Enteromorpha* show similar adsorption capacities, *Fucus vesiculosus* exhibits the highest affinity for estrone in seawater based on K_d. Except for sediment, which displayed the lowest adsorption capacity, the trends for adsorbed amount q_e and K_d varied between seawater and brackish water.

For $\log K_{OC}$, the trends also differed between the two water types. In seawater, sediment again shows the highest $\log K_{OC}$ due to its low organic carbon content. Estrone exhibits the highest affinity for organic carbon in *Fucus vesiculosus* (2.74), followed by *Enteromorpha* (2.39), while *Puccinellia maritima* and *Halimione portulacoides* have similar values (2.24 and 2.20, respectively).

Regarding the influence of organic matter origin on estrone sorption behaviour, *Enteromorpha* and *Puccinellia maritima* demonstrate the highest adsorbed amounts q_e among all substrates at both salinities. Both matrices have the lowest C_{org}/N_{total} ratio but differ widely in their $\delta^{13}C$ values (-31‰ for *Puccinellia maritima*, -17.4 ‰ for *Enteromorpha*) (Figure 5.). Consequently, it

appears that the adsorption behaviour of estrone is primarily controlled by TOC and TON, rather than the origin of the organic carbon.

5.4.3 Effect of Salinity on Adsorption

Salinity is a crucial environmental factor that affects the adsorption behaviour of contaminants, particularly in estuaries where strong salinity gradients can occur. Previous studies have shown that the adsorption of estrone increases with higher salinity, attributed to the reduced solubility of the compound in the presence of salts (Lai *et al.*, 2000; Bowman, Readman and Zhou, 2003; J. Zhang *et al.*, 2013). Figure 5.5 shows the differences in the amount of estrone adsorbed by each substrate in both brackish and seawater, with an initial concentration of 40 ng/mL.

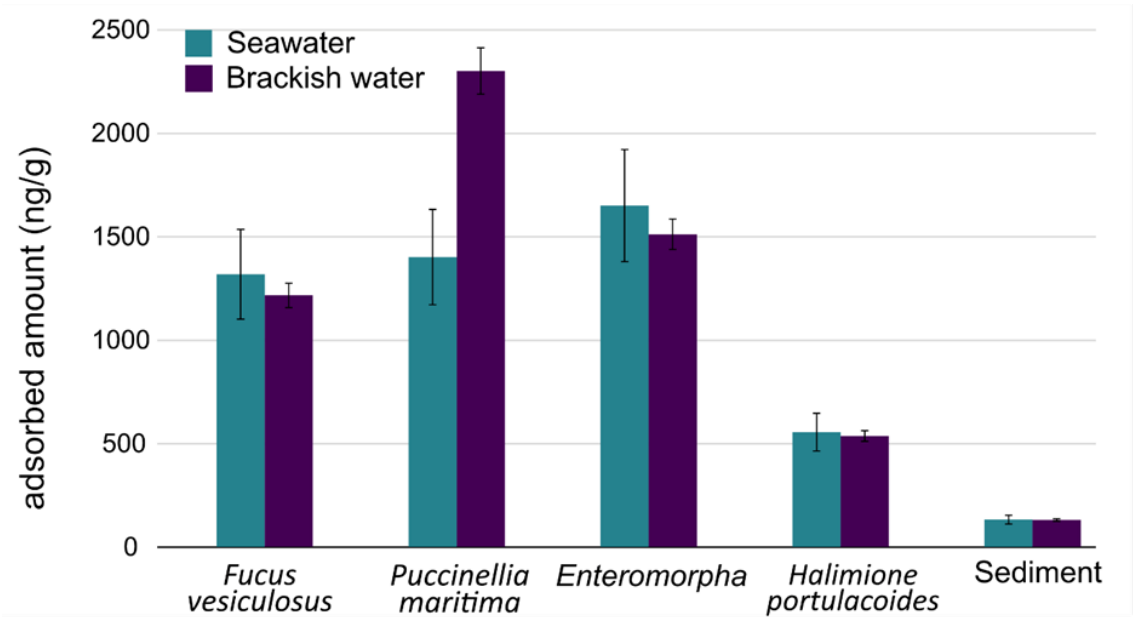

Figure 5.5: Comparison of adsorbed amount (ng estrone / g adsorbent) in each substrate for brackish water and seawater at the same concentration (40 ng/mL). Error bars are the RSD (%) of triplicates for each substrate.

In seawater, the adsorbed amounts range from 134-1674 ng/g, with the lowest adsorption found in sediment, followed by *Halimione portulacoides* at 563 ng/g (Figure 5.5). *Fucus vesiculosus* and *Puccinellia maritima* show similar adsorption levels in seawater (1337 ng/g and 1422 ng/g, respectively), while *Enteromorpha* exhibited the highest adsorption as a sorbent (1674 ng/g). In brackish water, the adsorption pattern is similar, with sediment and *Halimione portulacoides* showing the lowest adsorption levels (132 ng/g and 544 ng/g, respectively), followed by *Fucus vesiculosus* (1234 ng/g). Here, *Puccinellia maritima* reached the highest adsorption at 2334 ng/g. While the varying trends for partition coefficients K_d and $\log K_{OC}$, indicate some influence of salinity, the adsorbed amount q_e of estrone across most substrates in both

seawater and brackish water does not exhibit a statistically significant difference ($p>0.05$). Previously, contradicting results were found and increasing salinity was thought to increase the adsorption of organic compounds due to the "salting out" effect (Lai *et al.*, 2000; J. Zhang *et al.*, 2013). Moreover, it has been suggested previously that the dominant sorption mechanism of estrogens is hydrophobic partitioning to organic matter, which is independent of salinity (Yang, Lin, Dai, *et al.*, 2020; Dai *et al.*, 2022). Other studies indicate that the salinity effect might not be as pronounced for moderately hydrophobic compounds such as estrone (Bowman, Zhou and Readman, 2002). One possible explanation is that the relatively high salinity levels (15 and 31 g/kg) may have reached a threshold beyond which further increases do not significantly impact sorption behaviour, as suggested by (Neale *et al.*, 2010). Consequently, stronger salinity effects might be more apparent in freshwater environments. Notably, only for *Puccinellia maritima* did the adsorbed amount differ, showing higher adsorption in brackish water.

5.4.4 Controls on Adsorption Behaviour

To assess the correlations between substrate properties, salinity and adsorption of estrone, principal component analysis (PCA) was conducted for each salinity (Figure 5.6).

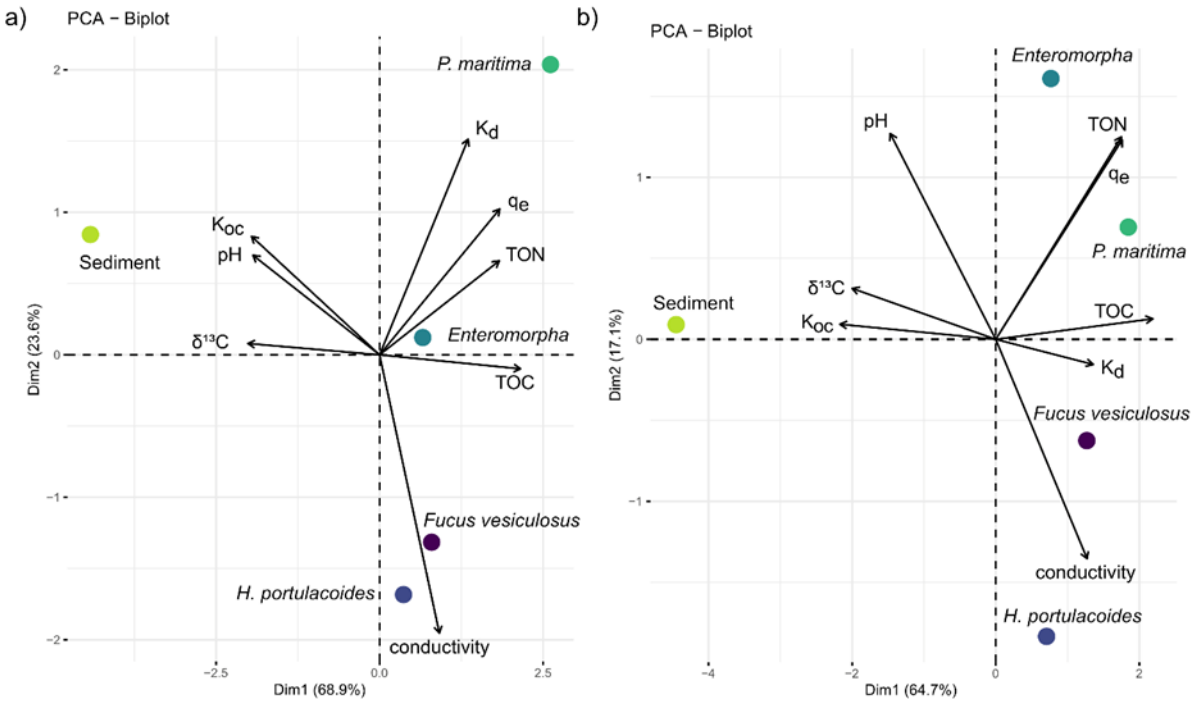

Figure 5.6: Biplot of the PCA for estrone and each substrate in a) brackish water and b) seawater. Each substrate is indicated by a different coloured dot; the loadings of the substrate properties are black arrows.

Figure 5.6a) visualises the results in brackish water: *Puccinellia maritima* and *Enteromorpha* are clustered in the upper right quadrant, where they are linked with the partition coefficient K_d, the

adsorbed amount q_e, and total organic nitrogen (TON). *Enteromorpha* also shows an association with total organic carbon (TOC). In the second (lower right) quadrant, *Fucus vesiculosus* and *Halimione portulacoides* plot closely with conductivity, likely reflecting their high salt content which contributes to elevated conductivity measurements. Sediment is clustered in the fourth (upper left) quadrant, associated with pH, K_{OC} and $\delta^{13}C$. The link with high K_{OC} values and sediment is attributed to its very low organic matter content, indicating that adsorption in the sediment may mainly be driven by pH.

In Figure 5.6b), *Puccinellia maritima* and *Enteromorpha* again cluster in the first quadrant, though their positions are reversed compared to Figure 5.6a). Here, the adsorbed amount q_e shows a strong correlation with TON, and *Puccinellia maritima* is closely associated with TOC. *Fucus vesiculosus* in the second quadrant is associated with K_d, while *Halimione portulacoides* plots again, nearest to conductivity. Conductivity and pH are negatively correlated, and the correlation between sediment and pH appears weaker in seawater compared to brackish water.

Sediment is distinct from plant-based substrates due to its lack of organic matter, indicating that different sorption mechanisms influence estrone retention in sediment versus organic-rich plant matrices. TON seems to strongly influence estrone adsorption, possibly because nitrogen-containing functional groups in the sediment organic matter, such as amines and amides, can act as hydrogen bond donors or acceptors. These groups enhance interactions with moderately hydrophobic compounds like estrone, promoting sorption through hydrogen bonding. Consequently, sediments with higher nitrogen content tend to retain more estrone. Both *Enteromorpha* and *Puccinellia maritima* demonstrate the strongest adsorption in brackish and seawater and exhibit higher TON levels than the other substrates, reinforcing the idea that TON controls adsorption behaviour. The influence of conductivity on sorption appears to diminish with increasing salinity. Conductivity, an indicator of ionic strength, generally enhances the sorption of organic compounds by reducing their water solubility through the “salting out” effect (J. Zhang *et al.*, 2013). However, as mentioned before, under marine conditions, salinity and conductivity levels are already high, which may limit their further influence on adsorption (Neale *et al.*, 2010). Instead, adsorption in this context seems more strongly governed by sediment properties, particularly TON and TOC.

5.5 Conclusion

This study investigated the influence of different organic matter sources on the adsorption behaviour of the steroidal hormone estrone under estuarine conditions. The sorbents used were derived from estuarine plant materials and have varying origins of organic matter, which allows

for an evaluation of how these sources impact estrone adsorption. Additionally, different salinities were used to replicate estuarine conditions.

The adsorption isotherms for each of the five substrates displayed distinct sorption patterns: *Enteromorpha* and *Halimione portulacoides* show linear adsorption, while *Puccinellia maritima* and sediment align with the Freundlich adsorption model. *Fucus vesiculosus* does not fit any of the common models, suggesting a more complex or mixed adsorption mechanism. The partition coefficients K_d and $\log K_{OC}$ were consistent with those reported in previous studies. Highest adsorption was achieved for *Enteromorpha* and *Puccinellia maritima* in both seawater and brackish water.

While it was proposed that the origin of organic carbon might affect the adsorption capacity, results show no direct correlations between adsorption behaviour and the source of organic carbon. Instead, TOC and particularly TON emerge as the primary factors driving estrone adsorption. To our knowledge, this is the first study to identify TON as a significant driver of estrone adsorption. As TOC and TON ratios reflect the organic carbon source, the origin appears to play only an indirect role.

Furthermore, our findings reveal that salinity at brackish and seawater levels does not significantly influence estrone adsorption, possibly due to a threshold effect at elevated ionic strengths. It should be noted that comparisons with freshwater were not possible using this method. In particular, further laboratory investigations into the mechanistic controls of steroidal hormones in SPE laboratory procedures could advise future monitoring schemes tracking contaminants of this type in freshwater environments.

Overall, this study provides new insights into the role of organic matter type and source in controlling the fate of steroid hormones such as estrone in estuarine environments and contributes to a better understanding of the factors influencing hormone-sediment interactions under varying salinity conditions.

[Acknowledgements: This work is supported by the INSPIRE Doctoral Training Partnership funded by the Natural Environmental Research Council (grant number NE/S007210/1)]

Chapter 6 Conclusion

6.1 Summary and Key Findings

This thesis investigates the fate of three chemically and behaviourally distinct contaminant groups (trace metals, PAHs and hormones) in estuarine systems, specifically focusing on the role of estuarine sediments in contaminant sequestration. Two estuaries, the Pearl River Delta in China and Southampton Water in the UK, were chosen for this study due to their differences in climate, sediment composition and urbanisation. The research assessed the spatial and temporal distribution of these contaminants and their association with the characteristics of organic matter. This approach enables comparison of regionally varying geochemical and environmental influences on contaminant behaviour and retention. Additionally, adsorption experiments were conducted in both brackish and seawater using estuarine plant material with varying organic matter origins to examine the adsorption behaviour of the steroidal hormone estrone under estuarine conditions. Together, these three studies systematically explore the role of organic matter type and source in contaminant sequestration, with particular focus on hormones as contaminants of emerging concern. This work enhances understanding of the role of organic matter in contaminant dynamics within estuarine sediments. The synthesis will discuss key findings, implications, limitations of the studies, and future research recommendations.

6.1.1 Sedimentary Controls on Contaminant Distribution in Southampton Water, UK and the Pearl River Delta, China.

Chapters 3 and 4 present a comprehensive analysis of two contrasting estuarine systems, Southampton Water in the UK and the Pearl River Delta in China, focusing on the distribution and behaviour of trace elements, PAHs, and steroidal hormones in surface sediments and sediment cores. Additionally, sediment organic matter properties were assessed, including total organic carbon (TOC), total organic nitrogen (TON), and stable carbon isotopes ($\delta^{13}C$). The extensive characterisation of the estuaries required a broad range of analytical methodologies and involved, among others, gas chromatography mass-spectrometry (GC-MS), X-ray fluorescence analysis (XRF), γ-ray spectrometry and continuous flow isotope ratio mass spectrometry.

Despite substantial differences in size, climate, sediment composition, and degree of urbanisation, both estuaries exhibited similar spatial trends for trace metals and PAHs: elevated concentrations near urban and industrialised areas, such as the port in Southampton Water and

cities like Guangzhou in the Pearl River Delta (PRD), and lower levels at more remote and marine sites. At the sampling sites closest to the port of Southampton Water, concentrations for Cu (2570 mg/kg), Zn (5560 mg/kg) and Pb (810 mg/kg), as well as PAHs ($\sum \mathrm{PAHs}$: 240 mg/kg) were the highest detected in the sample set. In contrast, the sampling sites furthest away from the shore showed lowest overall contaminant concentrations. Similar trends were observed for the PRD, where the sum of trace metal concentration declined from 435 mg/kg close to the shore to 142 mg/kg offshore. These trends suggest effective sedimentary trapping of contaminants in depositional zones, and a reduction in contaminant transport to offshore environments. Historical contamination patterns for trace metals (e.g., Zn, Cu, Pb) and PAHs, were successfully recorded in sediment core profiles, highlighting the long-term retention capacity of estuarine sediments.

In Southampton Water, sedimentary organic matter sources showed a high variability with $\delta^{13}C$ values ranging between -29‰ and -21‰ and carbon to nitrogen ratios (C/N) between 7.2 and 27.6, indicating mixed terrestrial and marine sources. Steroidal hormones were detected throughout the estuary, with the highest concentrations observed near residential areas and wastewater treatment plants (WWTPs) with up to 18 ng/g estrone, 15 ng/g estradiol and 66 ng/g progesterone. The synthetic hormone ethinylestradiol was only found near WWTPs (11 – 38 ng/g), indicating insufficient removal during wastewater treatment. Natural estrogens, such as estrone and estradiol, were detected at the top of the sediment core with concentrations up to 85 ng/g for estrone and 45 ng/g for estradiol, suggesting limited retention and potential degradation over time.

Principal Component Analysis (PCA) and core profiles revealed strong associations between PAHs, hormones, and Hg with TOC, TON, and $\delta^{13}C$ values, highlighting the influence of organic matter composition in contaminant distribution. These results underscore the need for organic matter characterisation when evaluating contaminant fate and transport in estuarine sediments.

Non-target analysis (NTA) using two-dimensional gas chromatography-mass spectrometry (GCxGC-MS) was employed to identify potential degradation products of estrone. Although no degradation products were detected, additional anthropogenic contaminants, such as phthalates, were found in both surface and core samples.

NTA has the potential to identify a wide spectrum of known and unknown contaminants, including transformation products and emerging contaminants, but its effective application requires intensive resources and demands substantial analytical expertise. In this study, limitations in project capacity prevented a thorough exploration of estrone degradation products and other potential contaminants. However, such information, together with detailed

analysis of estuarine characteristics presented in this study, would greatly enhance the understanding of hormone fate and persistence in estuarine sediments.

The Pearl River Delta displayed more uniform sediment properties, particularly in terms of organic matter composition. C/N ratios varied between 3.0 – 9.44, while $\delta^{13}C$ values ranged between - 25.9 and -22.2 ‰. Estrone was the only hormone detected with up to 13.1 ng/g, showing no clear spatial patterns, which suggests diffuse sources or extended residence time in the water column leading to widespread deposition. Unlike Southampton Water, there were no clear correlations observed between organic contaminants and sediment properties. However, trace metal distributions in surface and core samples showed correlations with TOC and grain size, indicating sedimentary controls on their behaviour. PCA suggested point sources for both PAHs and estrone in surface sediments, as well as recent contamination inputs in the upper core layers.

The Pearl River Delta is located in tropical to subtropical climate and is heavily influenced by seasonal monsoons, which likely affect contaminant transport and sediment dynamics. However, in this study, the sampling was conducted exclusively during the dry season, thereby excluding the influence of monsoons. Future studies incorporating seasonal sampling, particularly during peak monsoon periods, would provide a more comprehensive understanding of contaminant behaviour under varying environmental conditions.

In direct comparison, contaminant concentrations in Southampton Water are higher than those observed in the PRD, irrespective of contaminant group. For instance, the combined concentrations of Cu, Zn, Ba and Pb in Southampton Water range from 106 - 10078 mg/kg, whereas concentrations of the same metals in the PRD range from 112 to 908 mg/kg. Similarly, the average combined concentration of fluoranthene, anthracene and pyrene in the PRD is 40 ng/g, while in Southampton Water, the average combined PAH concentration is 27540 ng/g. Regarding steroidal hormones, average estrone concentrations are comparable between both estuaries. However, in Southampton Water, not only estrone was detected, but also estradiol, progesterone and ethinylestradiol, whereas these hormones were not detected in the PRD.

Given the higher degree of urbanisation and greater population density of the PRD, higher levels of contamination might be expected relative to Southampton Water. However, the PRD is a considerably larger and more open estuarine system, which promotes enhanced hydrodynamic mixing and dilution of contaminants, resulting in lower sedimentary concentrations. In addition, the PRD shows lower variability in the sediment composition than Southampton Water. Since sedimentary adsorption of contaminants is dependent on sediment composition, the type and greater uniformity of sediment in the PRD basin may limit the adsorption capacity. As established in Chapter 5, the source of organic matter, particularly TOC and TON influence the

adsorption capacity of sediments. Sediments from the PRD show lower C/N ratios (average 6.9) compared to those from Southampton Water (average 11.6), due to slightly lower TON (average 0.1 wt%) and lower TOC values (average 0.7 wt%). These characteristics may lead to reduced contaminant retention in the sediments and may explain the generally lower contaminant concentrations in the PRD compared to Southampton Water.

Overall, both studies emphasise the critical role of organic matter composition and environmental context in understanding contaminant dynamics under varying estuarine systems.

6.1.2 Influence of Organic Matter Type and Source on the Estrone Adsorption in Estuarine Systems

The third study explores how varying organic matter sources affect the adsorption behaviour of the steroidal hormone estrone under estuarine conditions. Adsorption isotherms were fitted using common models for five substrates of differing organic matter origin, showing different sorption mechanisms: Linear adsorption was observed for *Enteromorpha* and *Halimione portulacoides*, while the Freundlich model best described adsorption onto *Puccinellia maritima* and sediment. In contrast, *Fucus vesiculosus* indicated a more complex adsorption behaviour and did not fit any of the common models tested. Salinity levels in brackish and seawater did not significantly affect estrone adsorption, possibly due to a threshold effect at higher ionic strengths. The results indicated no direct correlation between adsorption behaviour of estrone and the varying sources of organic carbon. However, TOC and particularly TON emerged as key factors controlling estrone adsorption, suggesting that the organic matter origin, reflected by TOC and TON ratios, has only an indirect effect.

This study provides new insights into the factors controlling estrone adsorption. However, some limitations need to be considered in the experiment setup. Firstly, laboratory adsorption experiments cannot fully replicate the complex biogeochemical interactions that occur in the environment, including microbial activity, redox reactions and natural organic matter heterogeneity, all of which can influence adsorption behaviour. Additionally, the processes of washing and freeze-drying the estuarine plant materials as sorbents may have altered their surface characteristics and reactive sites, leading to discrepancies between laboratory results and natural sorption behaviour. While TOC, TON and $\delta^{13}C$ were used as proxies for organic matter quality and source, the chemical composition of the sorbent materials, from humic compounds to molecular-scale functional groups, polarity and aromaticity, were not assessed. Moreover, the analyte here was studied (almost) in isolation, neglecting any effects caused by compound mixtures including competition for sorption sites. Previous research has shown that

even contaminants within the same chemical family can exhibit different behaviours, meaning the sorption behaviour of estrone observed here may not reflect the behaviour of other steroidal hormones under the same conditions, due to their different chemical structure and octanol-water partitioning coefficients (K_{ow} values).

Isolating the effect of the different factors controlling sedimentary adsorption of hormones in estuarine systems is a historically complex proposal. This thesis improves the ability to predict the trapping of estrone in estuarine systems, particularly in direct comparison with another comparable estuary with known sedimentary properties. This thesis shows that a more thorough knowledge of the geochemistry and sediment properties of a sampling site may explain the retention of different contaminant groups at that site. Additionally, when comparing two estuarine sediments, higher retention of estrone may be expected in the estuary with higher TOC and TON values. The local vegetation can provide an indication of the sediment composition underneath if its TOC and TON contents are known as well, but vegetation is not the only contributor of TOC and TON that plays a role; proxies for organic matter source using TON and TOC to explain contaminant behaviour still require contextual regional perspectives for interpretation.

6.2 Limitations and Future Work

This thesis has investigated the influence of different organic carbon sources on the distribution and adsorption behaviour of trace metals, PAHs, and hormones in estuarine systems through both field studies and laboratory-based adsorption experiments. Although the three studies presented here provided new insights, they also revealed several limitations that point towards directions for future research.

In this thesis, particularly in Chapters 3 and 4, several proxies were used to explain and compare environmental conditions and processes. All proxies have strengths that justify their use and caveats that limit their application. One assumption used was that aluminium (Al) serves as a proxy for grain size. This is a widely established approach in geochemistry because Al is predominantly associated with the aluminosilicates in the fine clay fraction and mostly insensitive to degradation or diagenesis. However, there are limitations to the use of Al as grain size proxy that should be considered. Al may vary with the mineralogical composition independent of grain size and does not capture variations within the fine sediment fractions, for example clay versus silt, which might affect adsorption behaviour. To improve the reliability of Al as grain-size proxy in this thesis, future work should focus here on experimental validation by direct grain-size measurements.

The geochemical indices EF and I_{geo} can detect trace metal enrichment and pollution, but the results are very sensitive to the baseline concentrations used to calculate these factors. In this study, local background concentrations were used where available to make the results more reliable and future works in this area should conscientiously strive to determine local concentrations in applicable cases.

To explain potential PAH sources, PAH molecular indices were used in the core samples. Different formation pathways yield distinctive molecular PAH patterns, which can be used to discriminate between high temperature pyrogenic and lower temperature petrogenic processes. However, PAH indices need to be treated with caution, because varying degradation processes, combustion conditions and mixing of several sources can influence the ratio and subsequent source attribution. Therefore, two PAH diagnostic indices were combined in this thesis to strengthen source attribution. These indices were applied only to core samples, under the assumptions that PAH emission sources at a given site have remained relatively constant over time and that degradation pathways affect different PAH compounds in a similar manner within the same depositional environment. Future work could include the assessment of local PAH emitters, but also integration of compound-specific stable isotope analysis, e.g. $\delta^{13}C$ in PAHs, which would provide additional information for source attribution.

Proxies are important tools to interpret and explain often complex environmental conditions. However, they are most powerful when their underlying assumptions are well understood and when solidified by combining them with additional proxies or independent evidence. The application of proxies should be appropriate to the specific research question and environmental setting, and their limitations should be carefully considered before interpretation. For all proxies, reliability increases with a thorough understanding of their appropriate application and limitations.

One key limitation of this thesis the extensive laboratory analysis of organic and inorganic components. Each contaminant group covered in this thesis requires its own sample preparation and analysis technique, which increases time and complexity. For trace metals, sample preparation and analysis using XRF or ICP-MS are widely established, validated and reliable techniques, and are preferred methods for the rapid and simultaneous detection of numerous elemental species. In contrast, the analysis of organic contaminants is more challenging due to excessive sample preparation, development of bespoke and targeted methodologies for individual analytes, dedication of instrument time, and complex data analysis. In particular, PAHs and hormones require separate preparative methods due to their distinct chemical properties, and as such PAHs and hormones ideally require different

extraction approaches to achieve efficient recovery and accurate quantification, which is more time-consuming.

The instrument used for analysis provides an additional challenge. Hormones and PAHs can both be analysed using GC-MS, but hormones require derivatisation, which adds further time and can reduce analyte recovery. Furthermore, environmental samples often contain complex matrices, including natural phytohormones which might interfere with the target analytes when using single-ion monitoring. Where available, tandem mass spectrometry (MS-MS) provides higher selectivity and sensitivity and would be the preferable alternative to single-quadrupole GC-MS for the accurate qualification and quantification of hormones in complex matrices in future studies. Hormone analysis in these environments is novel, and future works could focus on continuing the development of robust preparative and instrumental techniques to maximise detection in estuarine systems.

Instead of the extensive and varying analysis techniques, non-targeted screening approaches could be a critical tool for the analysis of a wider range of contaminant groups, including emerging contaminants and transformation products. Including these techniques in future studies could reduce the time needed for sample preparation and enable assessment of a broader spectrum of contaminants. Therefore, the understanding of contaminant degradation pathways, particularly in complex environments such as estuaries could be improved.

The field studies revealed region-specific differences in contaminant behaviour, likely driven by variations in environmental and geochemical conditions. These findings underscore the need for comprehensive sediment and environmental characterisation alongside contaminant analysis. For both Southampton Water and the Pearl River Delta, further molecular-level characterisation of sediments focusing on organic matter composition could help identify additional factors controlling the fate and behaviour of trace elements, PAHs and hormones.

Given the seasonal variability of the Pearl River Delta, future research should focus on sampling across multiple seasons to better capture changes in contaminant dynamics. This would allow for a more comprehensive understanding of how seasonal changes in hydrology and biogeochemical conditions affect the distribution, transformation, and persistence of contaminants.

While batch adsorption experiments provide valuable insights into the factors controlling estrone adsorption on estuarine substrates, they are limited in their ability to replicate the complexity of natural environmental systems. To bridge the gap between laboratory and field observations, future research should incorporate detailed molecular-level characterisation of substrates, including the identification of specific functional groups such as phenolics or

carboxylic acids, which may play critical roles in hormone–substrate interactions. Such in-depths characterisations will improve our understanding of observed adsorption processes in controlled settings and their applicability in real-world systems. Additionally, it is recommended that future batch experiments include structurally related hormones to determine whether the adsorption behaviour observed is specific to estrone or applicable across broader chemical classes.

Overall, this research has provided important insights into the complex interactions between organic carbon sources and contaminant behaviour, in particular hormones, in estuarine systems. Given the broad research area and pressing relevance in context of environmental pollution and human exposure risks, future studies that integrate advanced analytical techniques, seasonal variability, and molecular-level characterisation will be essential to fully understand the processes that influence contaminant fate and behaviour in dynamic environments such as estuaries.

Appendix A Supplementary Information for Chapter 2: Methods and Method Development

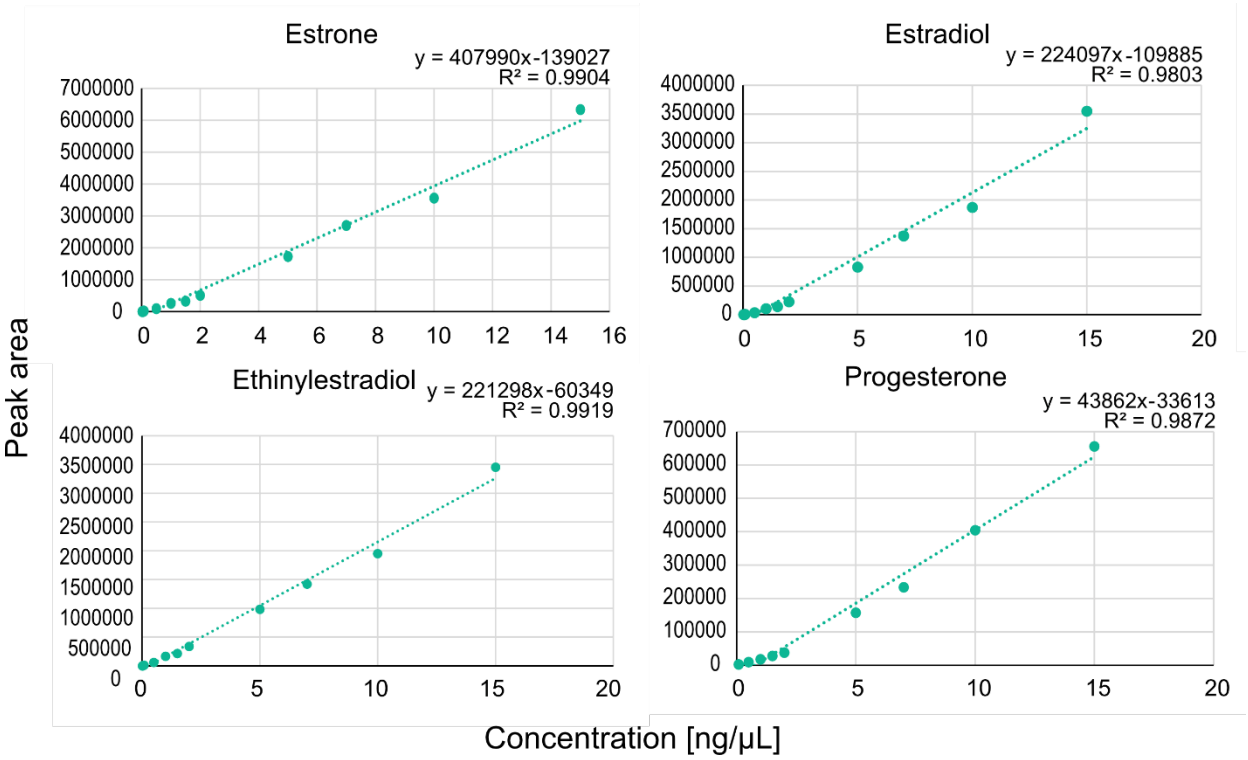

Figure A. 1: Twelve-point calibration curves from 0.02 – 15 ng/µL for each targeted steroidal hormone with the calibration equations and linearity R^2 value.

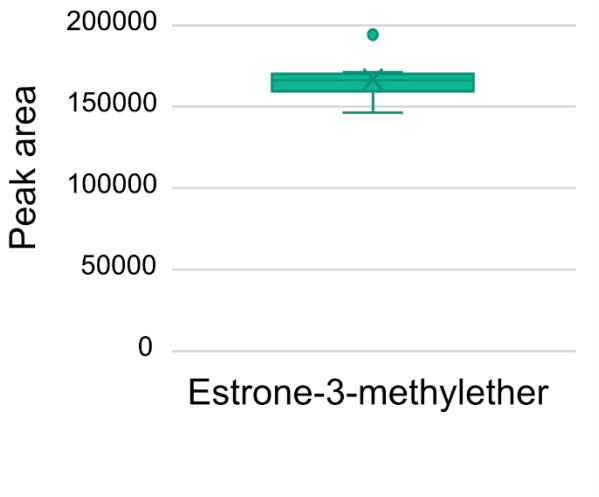

Figure A. 2: Boxplot of the internal standard estrone-3-methylether over eight samples with an RSD of 7.1%.

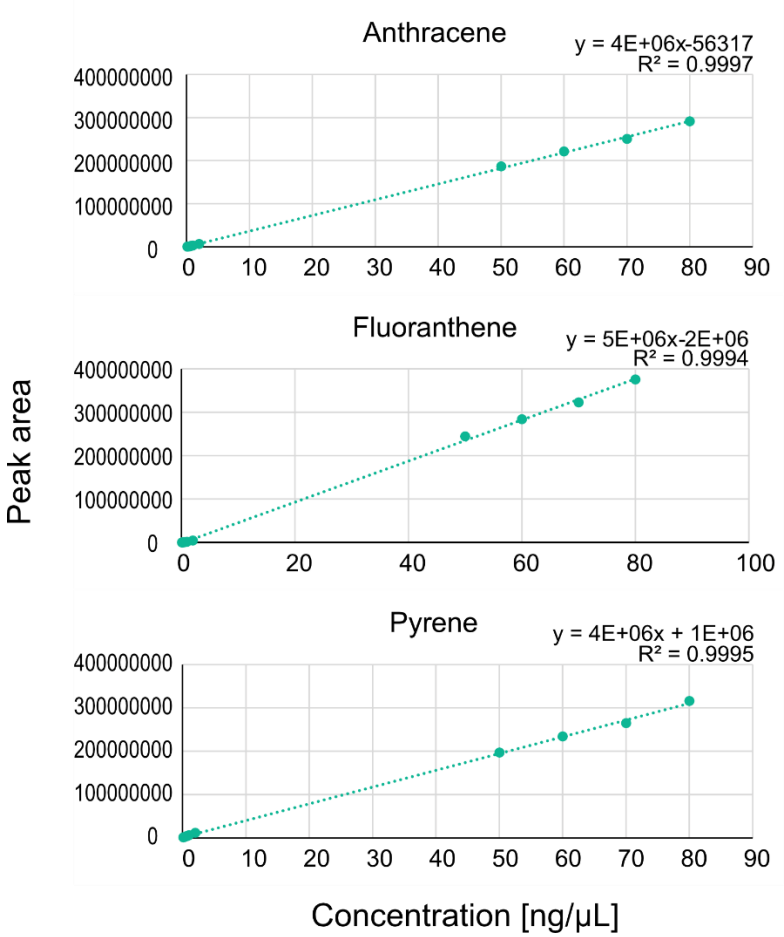

Figure A. 3: Eleven-point calibration curves for each targeted PAH with calibration equations and linearity R^2 values.

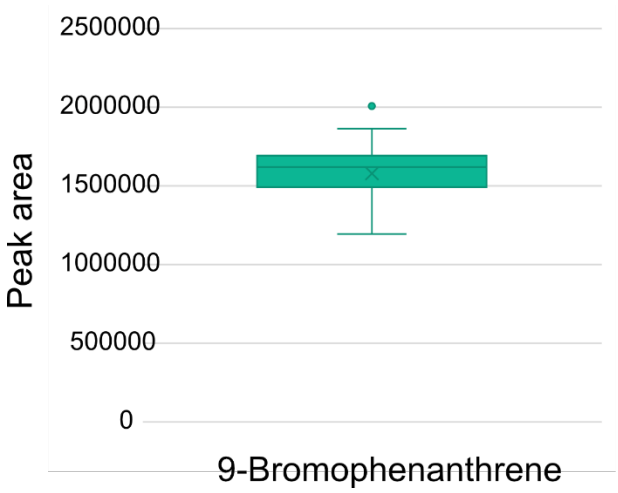

Figure A. 4: Boxplot of the internal standard 9-bromophenanthrene over ten samples with an RSD of 15%.

Appendix B Supplementary Information for Chapter 3: Spatial and Temporal Trends in Trace Metal, PAH and Steroidal Hormone Contamination in a Major Urban and Industrial Estuary: Southampton Water, UK

B.1 GC-MS Data

Several hundred chromatograms were produced during the completion of the methodological and experimental work presented in this thesis. Given that this body of work is dependent on the interpretation of these chromatograms, representative chromatograms are presented below and include a representative procedural blank. All chromatograms produced are not presented but raw data files are available upon request.

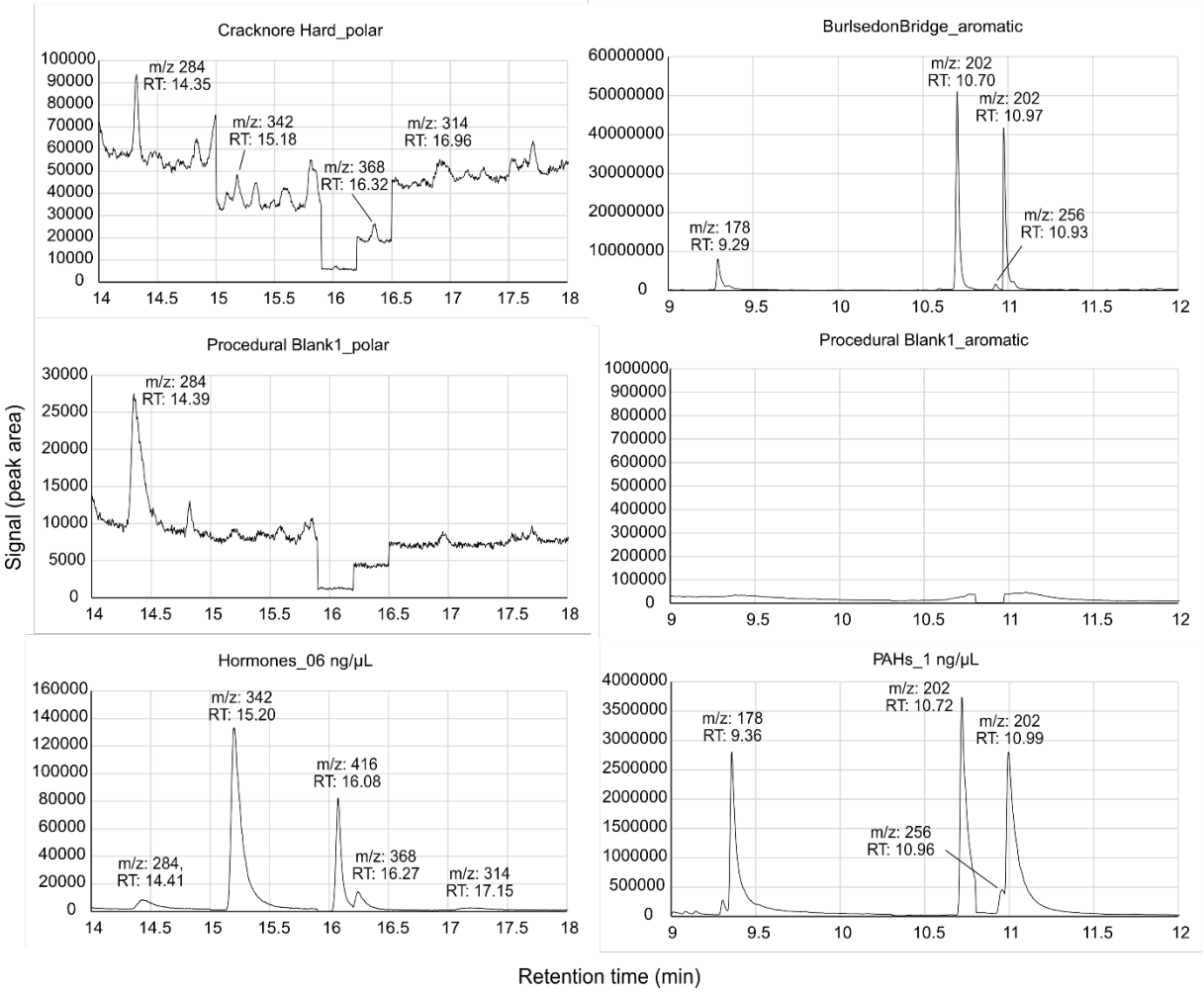

Figure B. 1: Example chromatograms from SIM mode for Southampton Water surface samples with peaks for targeted hormones: estrone-3-methylether (m/z: 284), estrone (m/z: 342), estradiol (m/z: 416), ethinylestradiol (m/z: 368), progesterone (m/z: 314) and targeted PAHs: anthracene (m/z: 178), fluoranthene (m/z: 202), pyrene (m/z: 202) and 9-bromo-phenanthrene (m/z: 256). On the left side: polar fractions for a sample example (Cracknore Hard) at the top, a procedural blank (middle) and a hormone standard (bottom left); on the right side: aromatic fraction for Bursledon Bridge as example (top), a procedural blank (middle) and a PAH standard (bottom right).

B.2 Geochemical Indices

Enrichment factor (EF), with TE being the respective trace element concentration:

$$\mathrm{EF} = \frac{\frac{\mathrm{TE}}{\mathrm{Al}_{\mathrm{Sediment}}}}{\frac{\mathrm{TE}}{\mathrm{Al}_{\mathrm{Background}}}} \qquad \text{(eq. B1)}$$

Geo-accumulation index I_{geo}: with TE being the respective trace element concentration and B the background concentration of the same trace element:

$$I_{geo} = \log_2\left(\frac{TE}{1.5 \cdot B}\right) \qquad \text{(eq. B2)}$$

Table B. 1: Southampton Water sediment surface samples raw data for all analysed parameters.

	Ashlett Creek	Bitterne Park	Bunny Meadows	Bursledon	Calshot	Cracknore Hard	Eling	Hamble CP	Hythe	SWAC	Vespasian Rd	Warsash
S* (wt%)	0.60	0.62	0.60	1.11	1.07	1.08	1.63	1.66	1.25	1.61	1.29	0.55
Fe_2* (wt%)	3.80	2.98	2.25	3.02	3.76	1.90	1.68	2.62	1.76	2.99	2.29	1.90
Mn* (wt%)	< LOD	< LOD	0.10	0.17	0.17	0.17	0.23	0.24	<LOD	<LOD	<LOD	0.02
Al* (wt%)	6.11	4.13	3.13	3.34	6.24	1.77	1.37	2.62	2.65	2.67	2.53	2.20
Cu/Al	229	337	473	946	524	1831	2572	1370	16	191	106	15
Zn/Al	845	1308	1655	2092	1116	3932	5564	2873	48	260	264	62
Ba/Al	362	347	723	434	237	677	1118	375	<LOD	553	403	331
Pb/Al	64	102	140	217	123	469	813	401	42	466	184	63
Hg (mg/kg)	0.10	0.12	0.10	2.42	0.08	0.80	0.19	0.05	0.16	0.88	0.72	0.03
$CaCO_3$ (wt%)	6.88	45.46	14.41	4.65	12.86	1.72	1.04	0.32	0.91	4.06	11.36	2.05
TON (wt%)	0.25	0.20	0.15	0.24	0.28	0.10	0.07	0.00	0.08	0.26	0.60	0.06
TOC (wt%)	2.05	2.28	1.19	2.77	2.00	1.01	0.87	0.53	0.87	7.28	7.17	0.45
$\delta^{13}C$ (‰)	-21.90	-28.47	-21.94	-25.87	-21.08	-24.07	-24.71	-25.86	-22.21	-24.03	-27.69	-22.13
Estrone (ng/g)	3.40	4.24	1.75	18.20	2.66	1.47	1.54	0.85	3.70	6.15	4.21	2.39
Estradiol (ng/g)	2.02	3.76	1.30	4.07	1.26	1.29	< LOD	1.30	2.47	15.14	5.59	1.29
Ethinylestradiol (ng/g)	< LOD	<LOD	<LOD	<LOD	<LOD	14.63	11.42	<LOD	<LOD	38.29	24.51	<LOD
Progesterone (ng/g)	25	21	<LOD	145	26	28	53	18	22	74	66	<LOD
Anthracene (ng/g)	<LOD	<LOD	67	133	<LOD	967	1503	6.8	155	29196	470	121
Fluoranthene (ng/g)	171	78	1238	2556	195	11396	18025	168	3800	100783	6318	1071
Pyrene (ng/g)	183	79	942	1752	186	10194	19419	212	2824	108962	6301	1048
* Corrected for O												

Min-max scaling:

$$x_{scaled} = \frac{x - x_{min}}{x_{max} - x_{min}} \qquad \text{(eq. B3)}$$

Table B. 2: Southampton Water core sediment samples raw data for all analysed parameters. ‘x’ means samples were not measured.

	^{137}Cs	^{210}Pb	TOC	TON	δ^{13}C	Al	Si	S	Mn	Fe	Cu	Zn	Ba	Pb	Hg	Estrone	Estradiol	ANT	FLA	PYR
Depth (mm)	(Bq/kg)		(wt%)		(‰)	(wt%)					(mg/kg)					(ng/g)				
7.5	4.5	87	20.93	1.36	x	242	379	148	513	287391	2541	1493	< LOD	3628	0.14	68.9	27.8	2.8	296	293
22.5	4	116	17.28	1.25	-26.6	219	1110	605	1030	284371	3860	1569	< LOD	3098	x	20.0	36.2	14	559	532
37.5	5.5	91	18.5	1.19	-26.9	283	1623	604	1161	331160	5414	2335	< LOD	4777	0.17	16.7	45.4	5.8	438	416
52.5	5.8	89	15.42	1.02	-26.0	280	1665	489	1101	330022	4412	2373	< LOD	4404	x	15.2	33.5	0.10	257	265
67.5	5.6	52	16.18	1.06	-25.6	145	1122	634	961	218474	7630	2897	357	5632	0.23	<LOD	41.5	0.05	251	253
82.5	6.7	71	14.65	0.97	-26.4	279	816	636	934	764205	6301	3282	< LOD	27113	x	<LOD	<LOD	0.05	530	492
97.5	8.5	68	12.98	0.95	-26.8	234	1679	607	1239	326957	7527	4512	2	14732	0.23	22.4	<LOD	0.05	634	633
112.5	11.7	58	12.07	0.88	-26.5	280	2707	415	1290	366408	3664	6315	450	18554	x	<LOD	<LOD	0.05	386	395
127.5	10.9	37	8.81	0.68	-25.8	254	4392	873	741	171220	17644	6686	1420	33102	0.40	85.8	<LOD	2.5	499	488
142.5	10.5	48	7.23	0.52	-26.2	250	2239	583	1189	341007	5110	9151	50	27737	x	<LOD	<LOD	4.3	547	500
157.5	14.6	33	11.41	0.90	x	365	2351	808	1373	414649	4235	11714	< LOD	17487	0.78	<LOD	<LOD	67	984	884
172.5	19.9	45	10.51	0.86	-25.7	339	2970	578	1430	461571	3015	7103	211	8549	x	<LOD	<LOD	57	765	680
187.5	21.6	33	10.79	0.86	-21.8	365	2351	872	1275	417809	2866	6414	49	8067	1.17	<LOD	<LOD	60	859	779
202.5	24	39	10.41	0.85	-19.5	297	2456	908	1302	448099	2510	5169	63	6219	x	<LOD	<LOD	58	1303	1230
217.5	19.4	33	10.5	0.85	-18.9	229	1592	1430	790	376466	3013	4527	< LOD	6377	1.21	<LOD	<LOD	46	819	758
232.5	27.8	34	12.5	0.95	-18.6	285	1630	1705	883	363290	2909	4709	< LOD	4390	x	<LOD	<LOD	61	941	850
247.5	28.6	42	12.24	0.93	-17.5	391	3026	1359	1340	505803	2522	5922	72	5582	1.20	<LOD	<LOD	64	981	901
262.5	23.9	29.6	12.57	0.90	-18.0	392	2897	1366	1412	590613	2190	4986	74	5268	x	<LOD	<LOD	76	1148	998
277.5	19.2	28.1	11.47	0.88	-18.5	397	2671	1838	1641	704940	1908	4818	65	4114	0.99	<LOD	<LOD	65	1107	994
292.5	9.4	31	10.7	0.83	-17.5	466	3332	2561	1550	676299	1238	2990	27	2580	x	<LOD	<LOD	64	954	885

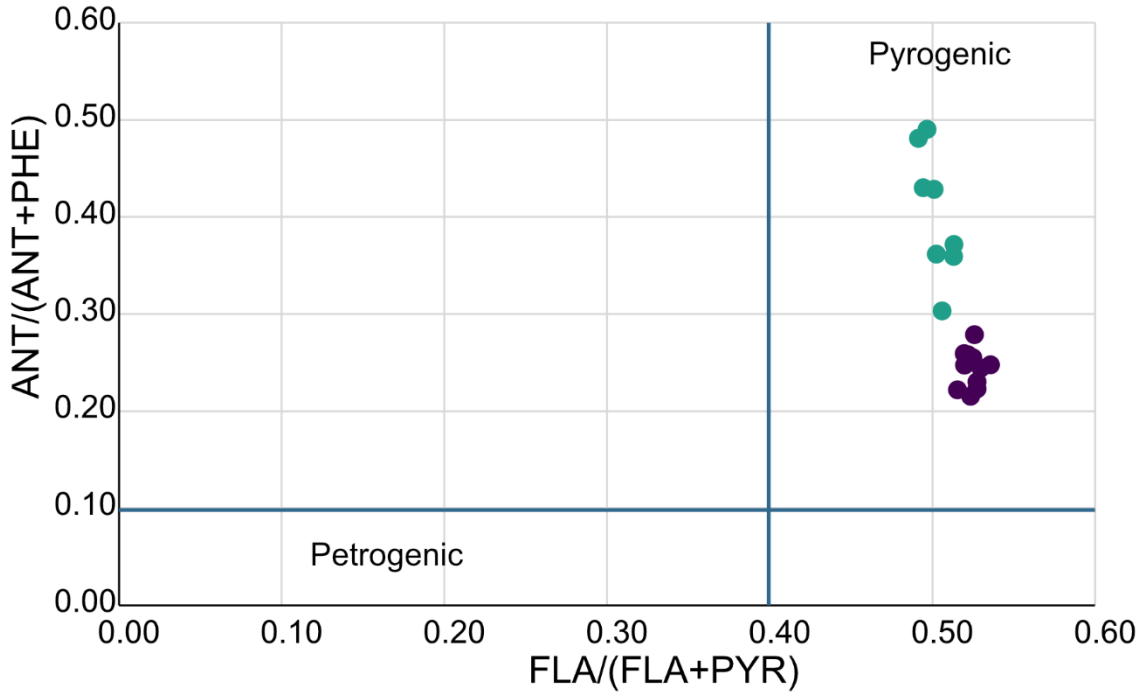

Figure B. 2: PAH molecular indices of the sediment core samples: ANT/(ANT+PHE) plotted against FLA/(FLA+PYR). Turquoise circles: upper 8 samples (0 – 143 cm); Purple circles: 11 lowest core samples (143 – 229 cm).

Table B. 3: Potential degradation products of estrone with formula, nominal mass and nominal mass for TMS-derivates.

Compound	**Formula**	**Molar Mass**	**TMS molar mass**	**TMS Groups**	**Reference**
4-Hydroxyestrone	$C_{18}H_{22}O_3$	286.371	432.751	2	(Chen *et al.*, 2018)
Estrolactone	$C_{18}H_{22}O_3$	286.371	359.561	1	(Yu *et al.*, 2019)
6-Ketoestrone	$C_{18}H_{20}O_3$	284.355	357.545	1	(Yu *et al.*, 2019)
Estro-g-Lactone	$C_{17}H_{20}O_3$	272.349	345.539	1	(Yu *et al.*, 2019)
Pyridinestrone acid	$C_{18}H_{21}O_3N$	299.369	372.559	1	(Chen *et al.*, 2018)
16α-Hydroxyestrone	$C_{18}H_{22}O_3$	286.371	432.751	2	(Pratush *et al.*, 2020)
Estriol	$C_{18}H_{24}O_3$	288.381	507.951	3	(Du *et al.*, 2022)
2-Hydroxyestrone	$C_{18}H_{22}O_3$	286.371	432.751	2	(Pratush *et al.*, 2020)
2-Methoxyestrone	$C_{19}H_{24}O_3$	300.397	373.587	1	(Pratush *et al.*, 2020)
4-Methoxyestrone	$C_{19}H_{24}O_3$	300.397	373.587	1	(Pratush *et al.*, 2020)

Table B. 4: List of analytes in multianalyte standard for GCxGC-MS analysis.

Compound	**Molar Mass**	**TMS groups**	**TMS Molar mass**
Anthracene	178.234	0	178.234
Pyrene	202.256	0	202.256
Fluoranthene	202.256	0	202.256
1.2-Dimethyl-naphthalene	156.22	0	156.22
9-Bromophenanthrene	257.13	0	257.13
Cholesterol	386.65	1	459.84
Estrone	270.366	1	343.556
Estradiol	272.38	2	418.76
Ethinylestradiol	296.41	2	442.79
Progesterone	314.469	0	314.469
Dibutyl phthalate	278.348	0	278.348
Bis(2-ethylhexyl)-phthalate	390.564	0	390.564
Bisphenol A	228.291	2	374.671
Nicotine	162.236	0	162.236
2.4-Dichlorophenol	163	1	236.19

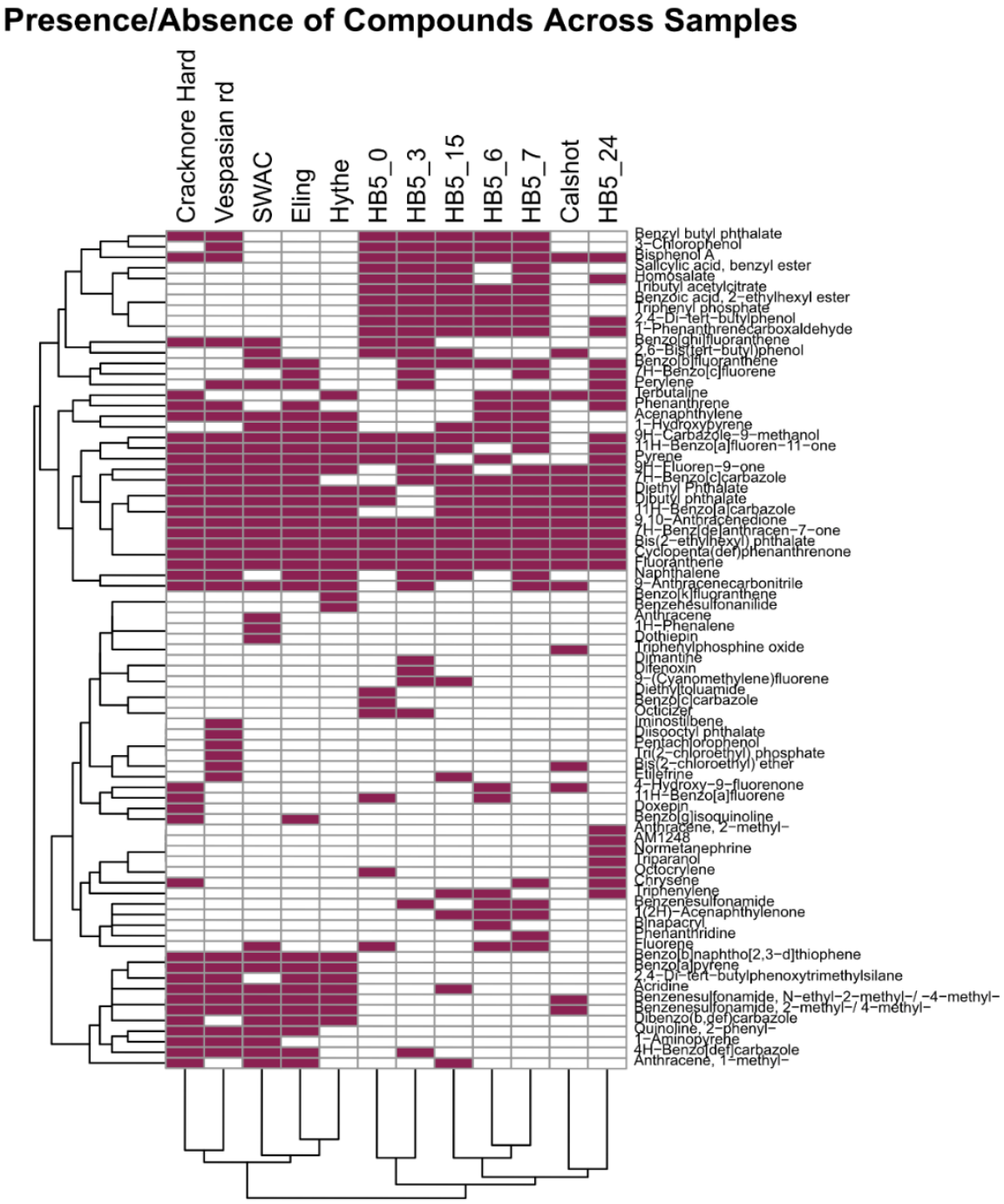

Figure B. 3: Presence (red cell) and absence (empty cell) of different contaminants in twelve Southampton Water samples found using non-target screening with GCxGC-MS.

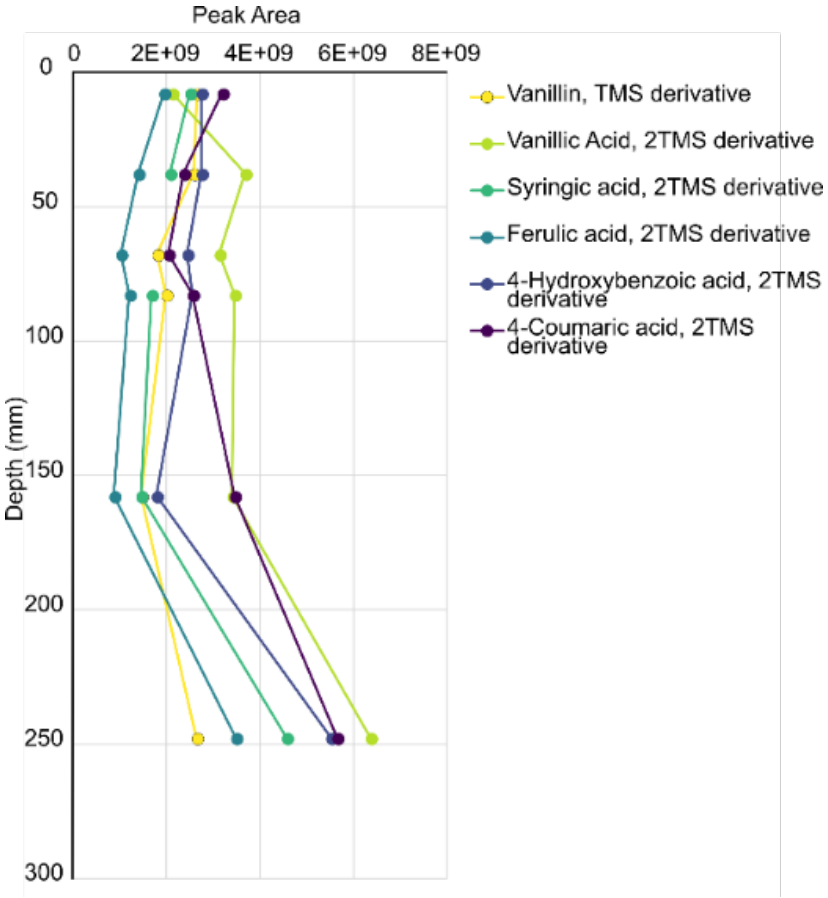

Figure B. 4: Peak area of a range of organic matter degradation products (Vanillin, Vanillic Acid, Syringic acid, ferulic acid, 4-hydroxybenzoic acid, 4-coumaric acid) vs. core depth (mm). All compound intensities increase with depth.

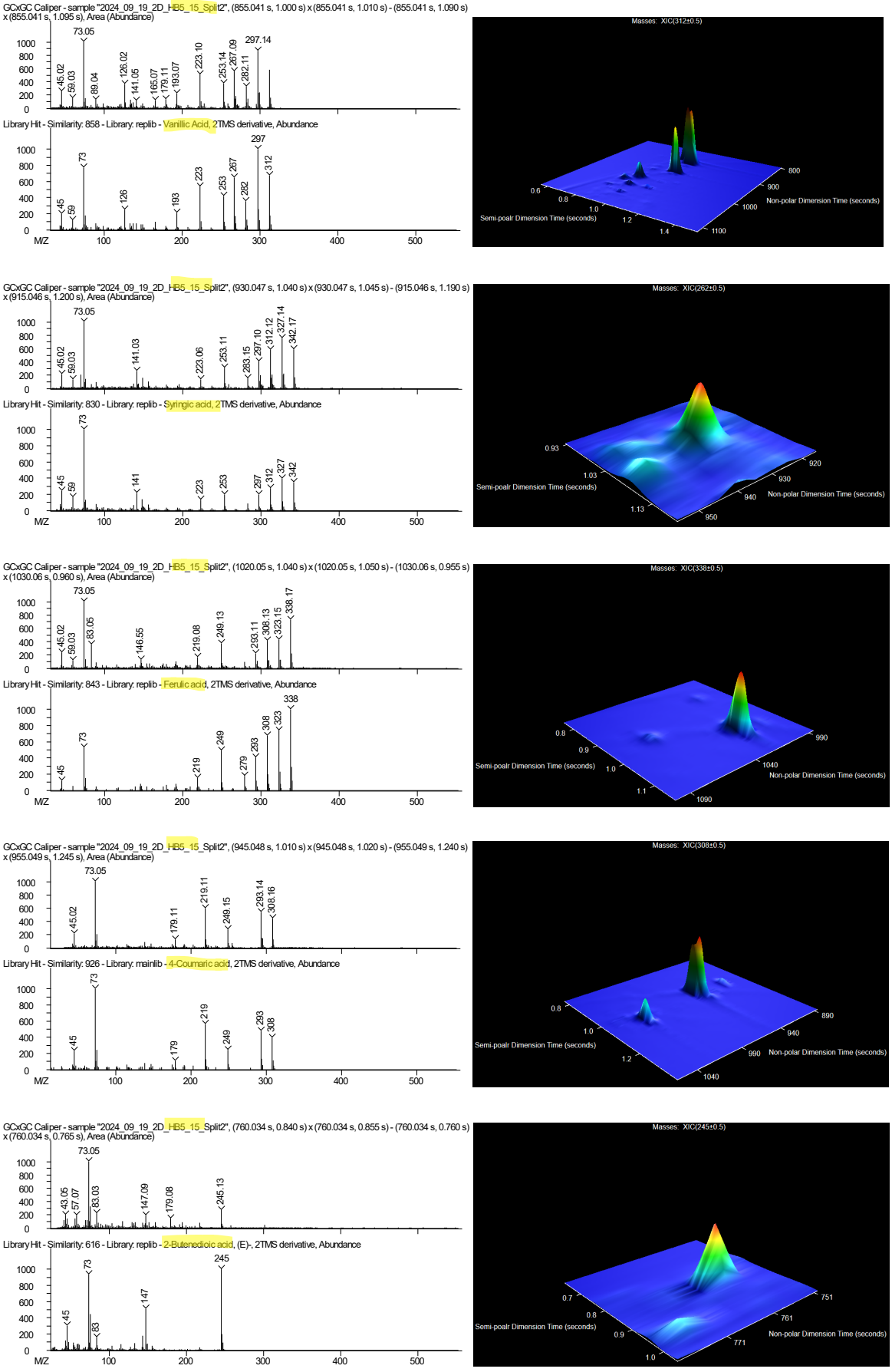

Figure B. 5: Sample spectra (top left) and library spectra (bottom left) of different organic matter degradation compounds with corresponding chromatogram peak (right side). Sample and compounds name are highlighted in yellow.

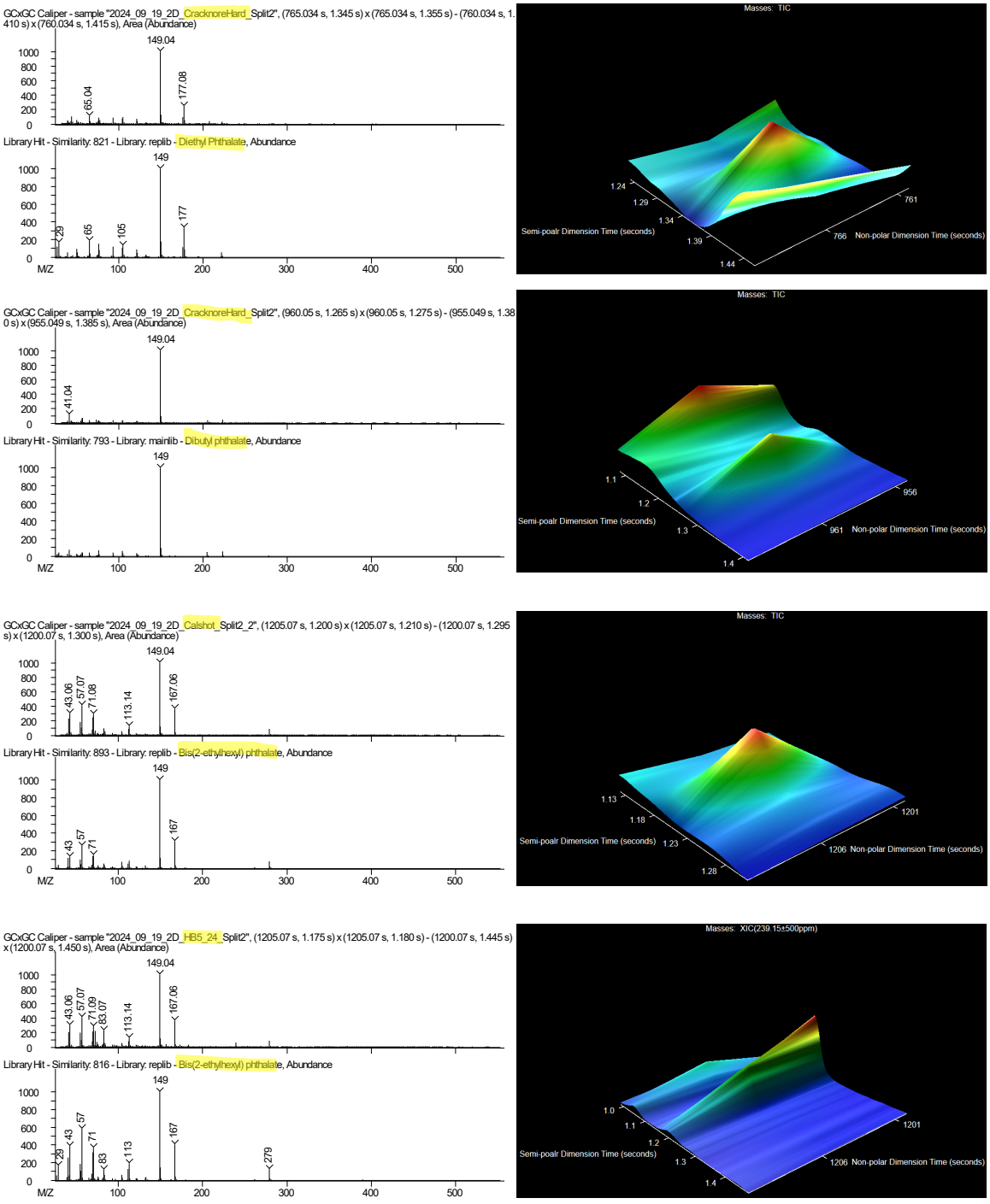

Figure B. 6: Examples of contaminant mass spectra from samples (top left) and library spectra (bottom left) with corresponding GCxGC-MS chromatogram peaks (right side). Sample and compound name are highlighted in yellow.

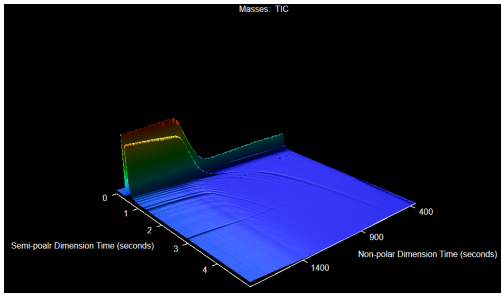

Figure B. 7: 2-D total ion current (TIC) chromatogram of a DCM:BTSFA-TMCS solvent blank.

Appendix C Supplementary Information for Chapter 4: Controls on the Distribution and Sequestration of Steroidal Hormones, PAHs and Trace Metals in the Pearl River Delta, Southeast China

Representative chromatograms of Chapter 4 are presented below and include a representative procedural blank. Raw data files for chromatograms produced are available upon request.

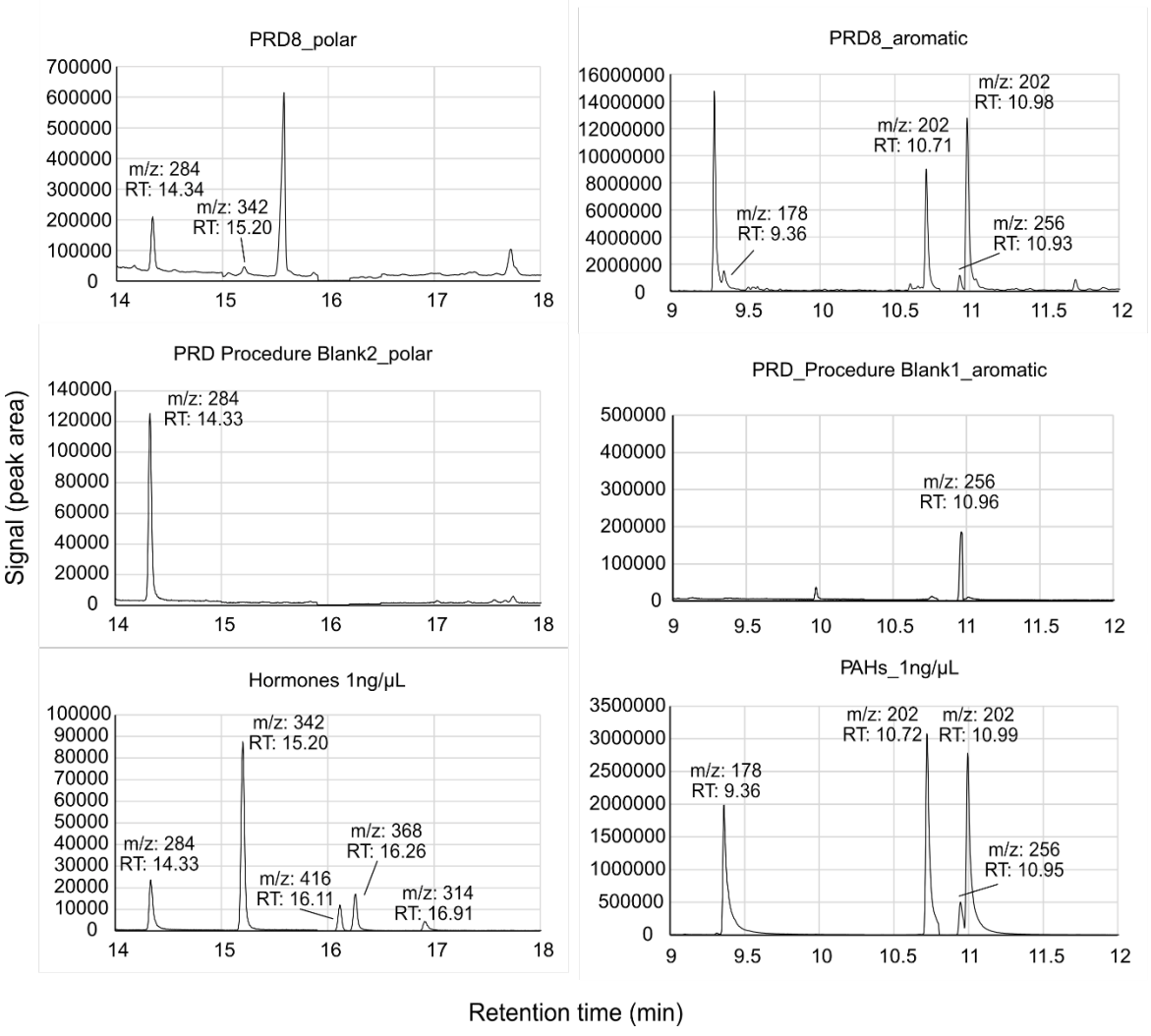

Figure C. 1: Example chromatograms of SIM mode for the polar fraction (on the left side) and aromatic fraction (on the right side), with a sample example (PRD8) (top panel), a procedural blank (middle) and a standard mix (bottom). Target hormones are estrone-3-methylether (m/z: 284), estrone (m/z: 342), estradiol (m/z: 416), ethinylestradiol (m/z: 368), progesterone (m/z: 314). Targeted PAHs are anthracene

(m/z: 178), fluoranthene (m/z: 202), pyrene (m/z: 202) and 9-bromo-phenanthrene (m/z: 256)

Table C. 1: All measured variables of 20 Pearl River Delta surface samples (stations 1-20). 'x' means samples were not measured.

Sample ID		1	2	3	4	5	6	7	8	9	10	11	12	13	14	15	16	17	18	19	20
Si	mg/kg	270890	264053	275759	250506	301155	254193	276960	306298	273640	301096	290878	277136	353753	262391	329925	351579	400944	263860	304583	366054
S		168	336	656	289	263	378	1958	1759	347	537	685	366	1366	660	348	1258	483	831	418	1134
Fe		42729	46781	46931	46539	38792	53399	42016	37664	49692	37380	43079	45974	16758	40797	26853	24797	12892	38674	31940	18941
Mn		627	869	574	817	566	971	661	495	727	572	777	949	336	638	420	359	218	671	515	282
Al		100759	108265	92876	113999	84961	108236	91891	71167	93759	72165	79211	88086	43122	94297	60827	51085	28475	87394	72411	41702
Cr	mg/kg	48	35	29	40	23	44	32	32	40	30	34	x	x	x	20	19	x	x	24	14
Co		12	11	11	12	9.1	16	11	12	14	11	13	x	x	x	7.0	7.5	x	x	8.4	4.9
Ni		30	23	21	25	15	33	21	23	30	21	24	x	x	x	15	14	x	x	20	10
Cu		68	38	28	49	20	46	33	30	42	22	33	x	x	x	8.6	10	x	x	9.8	4.7
Zn		152	101	78	115	832	182	138	143	184	132	152	x	x	x	101	102	x	x	110	83
Ba		54	40	31	47	26	59	33	32	38	28	37	x	x	x	23	23	x	x	22	11
Pb		52	41	32	47	31	54	40	38	48	31	38	x	x	x	21	21	x	x	24	14
Hg	ng/g	144	126	106	120	100	143	109	103	147	94	143	127	21	115	30	36	11	39	31	16
$CaCO_3$	wt%	0.13	0.44	0.83	0.63	0.21	0.75	1.05	1.28	0.89	1.43	1.40	1.16	3.18	2.21	1.78	1.67	1.07	2.80	2.84	5.37
TON		0.12	0.11	0.10	0.12	0.09	0.13	0.09	0.10	0.12	0.10	0.10	0.12	0.06	0.16	0.09	0.05	0.03	0.14	0.10	0.05
TOC		0.96	0.92	0.76	0.95	0.63	1.10	0.84	0.89	1.02	0.65	0.79	0.84	0.30	0.92	0.46	0.38	0.09	0.93	0.51	0.20
$\delta^{13}C$	‰	-25.93	-25.24	-24.24	-24.38	-23.13	-24.61	-24.74	-23.59	-23.80	-23.44	-23.90	-23.65	-22.98	-21.95	-22.48	-24.58	-23.71	-22.19	-22.17	-22.69
E1	ng/g	2.76	6.96	10.08	3.85	6.47	9.90	9.07	13.05	8.94	< LOD	5.12	8.78	6.99	< LOD	< LOD	5.35	7.09	< LOD	8.31	7.13
ANT		5.1	2.1	< LOD	2.9	< LOD	1.9	< LOD	17	1.7	< LOD	4.1	4.1	< LOD	2.2	< LOD	< LOD	< LOD	< LOD	< LOD	< LOD
FLA		39	16	14	21	7.4	20	13	62	25	11	25	29	14	20	8.2	5.6	2.1	14	11	4.9
PYR		55	19	14	23	0.2	22	13	99	32	9.5	28	34	15	12	3.8	2.3	< LOD	7.2	5.5	0.8

Table C. 2: Data of all measured sediment properties of Pearl River Delta core samples. 'x' means samples were not measured.

Depth	^{137}Cs	^{210}Pb	TOC	TON	$CaCO_3$	$\delta^{13}C$	Al	Si	S	Mn	Fe
mm	Bq/kg		wt%			‰	mg/kg				
7.5	<LOD	0.095	1.57	0.19	0.10	-24.95	120702	251596	391	511	48554
22.5	x	x	1.54	0.18	<LOD	-25.12	119104	250774	270	544	48273
37.5	x	x	1.54	0.18	<LOD	-25.10	119072	249569	187	564	48510
52.5	0.001	0.132	1.69	0.20	0.08	-25.49	118397	250357	404	544	48141
67.5	x	x	1.61	0.18	0.08	-25.55	117369	251144	320	515	47924
82.5	x	x	1.43	0.16	<LOD	-25.24	117477	251036	382	509	47866
97.5	0.001	0.119	2.10	0.22	<LOD	-25.54	117487	252366	303	516	48069
112.5	x	x	1.50	0.18	0.11	-25.29	116928	250934	841	531	47993
127.5	0.002	0.124	1.56	0.16	3.08	-25.57	x	x	x	x	x
142.5	x	x	1.61	0.18	0.08	-25.40	119498	247885	237	514	48414
157.5	<LOD	0.101	1.54	0.17	0.15	-25.49	x	x	x	x	x
172.5	x	x	x	x	x	x	117881	246259	1277	487	47955
202.5	<LOD	0.109	1.70	0.18	0.10	-25.63	119542	245604	441	506	48661
232.5	x	x	x	x	x	x	120385	246405	395	458	48874
247.5	<LOD	0.067	1.61	0.19	0.15	-25.18	x	x	x	x	x
262.5	x	x	x	x	x	x	120454	246113	738	446	47848
277.5	0.002	0.077	1.52	0.17	0.18	-25.14	x	x	x	x	x
307.5	<LOD	0.081	1.54	0.18	0.09	-25.29	118653	248359	220	530	48621
352.5	0.001	0.079	1.40	0.16	0.18	-24.83	124939	242637	352	528	48932
367.5	x	x	1.43	0.16	0.09	-25.02	x	x	x	x	x
397.5	0.001	0.078	1.27	0.13	0.16	-24.69	122296	243536	255	514	48607
427.5	0.001	0.078	1.33	0.15	0.20	-24.86	127147	240760	432	473	49160
472.5	<LOD	0.067	1.28	0.15	0.22	-24.39	125631	243960	252	467	48738
502.5	0.002	0.080	0.63	0.07	0.16	-24.04	123816	248013	536	469	48750
547.5	0.002	0.086	x	x	x	x	122505	245391	185	532	49696
592.5	0.002	0.069	1.26	0.16	0.16	-23.91	122574	246052	311	552	49974

637.5	0.002	0.048	1.24	0.14	1.21	-23.80	120553	244651	357	607	49918
682.5	0.002	0.057	1.22	0.15	0.15	-23.59	122337	248114	276	589	50304
727.5	0.002	0.059	1.17	0.14	0.14	-23.59	123466	245827	206	601	49946
757.5	0.002	0.054	1.07	0.14	0.13	-23.05	x	x	x	x	x
802.5	0.003	0.059	1.07	0.14	0.10	-22.88	122771	247906	211	639	50659
832.5	0.002	0.062	1.16	0.14	0.13	-23.51	x	x	x	x	x
847.5	x	x	x	x	x	x	123272	247930	240	696	51016
877.5	0.003	0.056	1.07	0.14	0.10	-23.04	x	x	x	x	x
892.5	0.003	0.071	1.16	0.15	0.20	-23.37	x	x	x	x	x

Table C. 3: Data of all measured trace elements and organic contaminants for Pearl River Delta core samples. ‘x’ means samples were not measured.

Depth	**Cr**	**Co**	**Ni**	**Cu**	**Zn**	**Ba**	**Pb**	**Hg**	**E1**	**E2**	**ANT**	**FLA**	**PYR**
mm	mg/kg								ng/g				
7.5	53	11	30	87	353	49	74	0.19	8.84	2.83	5.7	19	23
22.5	x	x	x	x	x	x	x	0.28	1.33	<LOD	7.2	22	26
37.5	52	11	30	87	308	47	74	0.19	1.25	0.32	7.5	24	19
52.5	52	11	30	86	309	50	73	0.20	0.79	0.04	5.9	25	24
67.5	51	11	29	86	301	46	72	0.25	0.91	<LOD	6.9	25	32
82.5	x	x	x	x	x	x	x	0.24	0.49	<LOD	x	x	x
97.5	54	11	31	89	310	52	74	0.24	1.16	0.29	5.9	25	28
112.5	53	11	30	89	309	49	73	0.17	0.05	<LOD	7.6	29	30
127.5	x	x	x	x	x	x	x	0.22	0.60	<LOD	6.0	23	26
142.5	56	11	35	94	316	50	76	0.21	0.58	<LOD	6.4	22	23
157.5	x	x	x	x	x	x	x	x	0.50	<LOD	6.0	24	26
172.5	51	10	29	89	292	44	71	0.27	x	x	x	x	x
202.5	54	10	31	93	304	44	74	0.21	2.25	<LOD	6.0	24	31
232.5	56	11	33	101	307	49	77	0.20	x	x	x	x	x
247.5	x	x	x	x	x	x	x	x	2.20	<LOD	6.3	22	38

262.5	53	10	31	94	283	47	73	0.21	x	x	x	x	x
277.5	x	x	x	x	x	x	x	x	<LOD	x	6.3	21	37
307.5	51	11	30	84	273	48	73	0.20	1.3	<LOD	5.7	24	32
352.5	49	10	28	89	269	53	75	0.18	1.7	<LOD	12	17	38
367.5	x	x	x	x	x	x	x	x	x	x	x	x	x
397.5	x	x	x	x	x	x	x	0.23	x	x	x	x	x
427.5	51	11	29	89	254	59	79	0.19	<LOD	<LOD	9.7	21	35
472.5	x	x	x	x	x	x	x	0.17	x	x	x	x	x
502.5	53	11	29	94	246	58	72	0.18	1.9	<LOD	11	24	38
547.5	55	11	29	91	217	57	74	0.21	x	x	x	x	x
592.5	x	x	x	x	x	x	x	0.17	1.6	<LOD	4.0	16	23
637.5	52	11	26	78	203	46	74	0.18	x	x	x	x	x
682.5	x	x	x	x	x	x	x	0.17	<LOD	<LOD	4.0	18	25
727.5	53	11	25	68	193	46	75	0.19	x	x	x	x	x
757.5	x	x	x	x	x	x	x	x	<LOD	<LOD	3.5	13	19
802.5	x	x	x	x	x	x	x	0.19	x	x	x	x	x
832.5	x	x	x	x	x	x	x	x	<LOD	<LOD	3.2	14	18
847.5	57	12	24	37	137	48	80	0.17	x	x	x	x	x
877.5	x	x	x	x	x	x	x	0.25	x	x	x	x	x
892.5	x	x	x	x	x	x	x	x	x	x	x	x	x

Appendix D Supplementary Information for Chapter 5: Influence of Organic Matter Type and Source on the Adsorption of Steroidal Hormones in Estuarine Systems

Table D. 1: Mass (ng) of estrone and progesterone spiked for adsorption isotherms in brackish water.

Substrate	Estrone/Progesterone spike (ng)
Enteromorpha	100, 140, 200, 400, 1000, 1400, 1800
Puccinellia maritima	400, 1000, 1400, 1800, 3000, 4000, 6000
Halimione portulacoides	100, 140, 200, 400, 1000, 1800
Fucus vesiculosus	100, 140, 200, 400, 1000, 1400, 2000
Sediment	100, 140, 200, 400, 1000, 1800

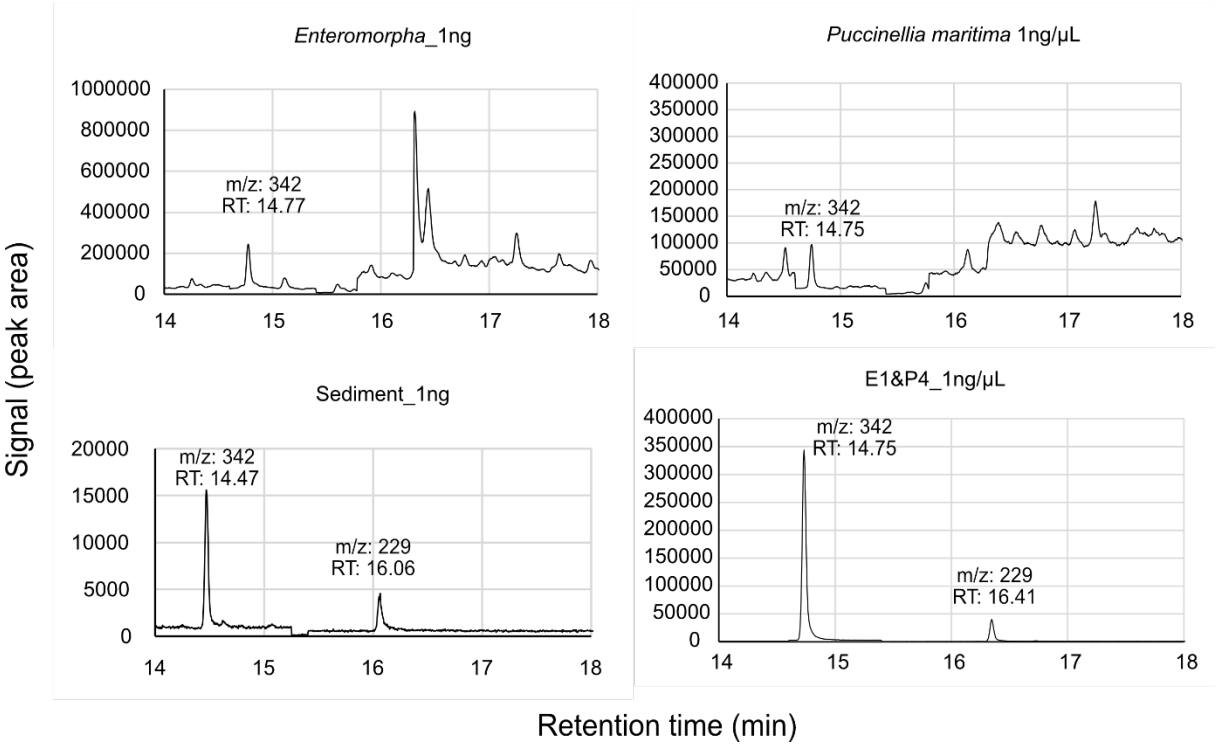

Figure D. 1: Example SIM-chromatograms of substrates in brackish water and one standard mix containing estrone and progesterone for comparison. Annotated peaks show the target hormones estrone (m/z: 342) and progesterone (m/z: 229).

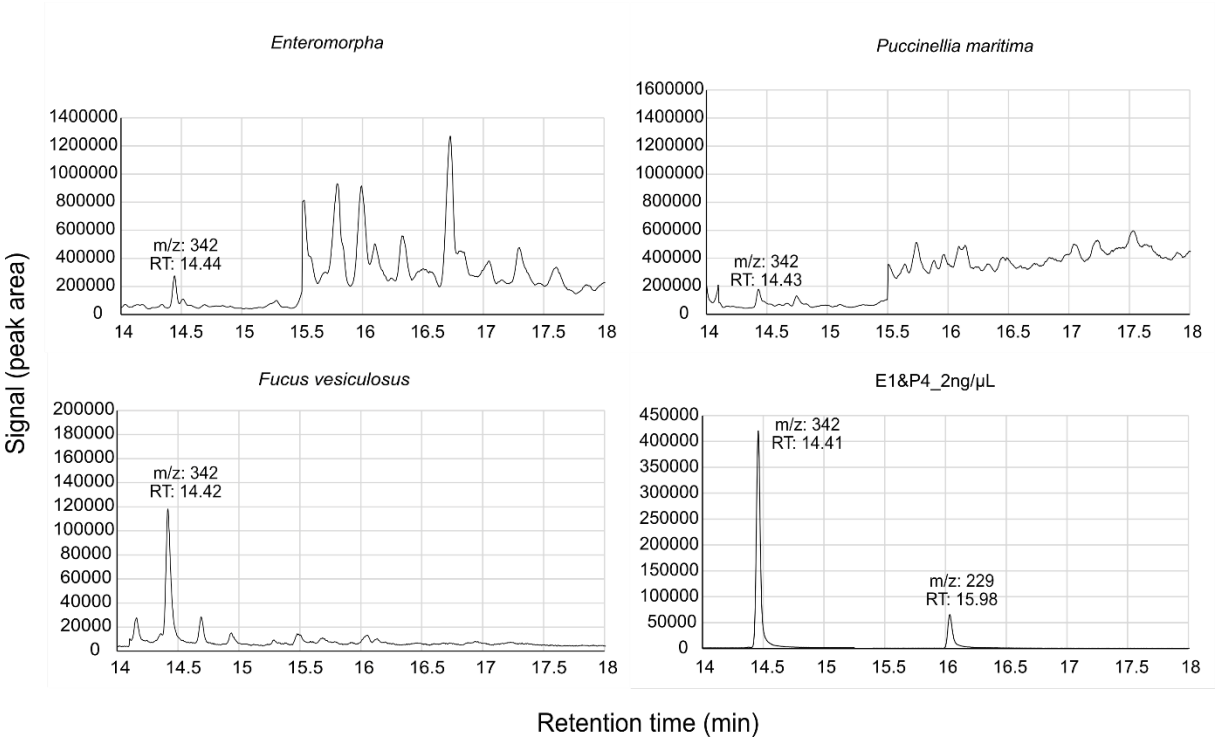

Figure D. 2: Example SIM-chromatograms for substrates in seawater and one hormone mix (estrone and progesterone) for comparison. Annotated peaks show the target hormones estrone (m/z: 342) and progesterone (m/z: 229).

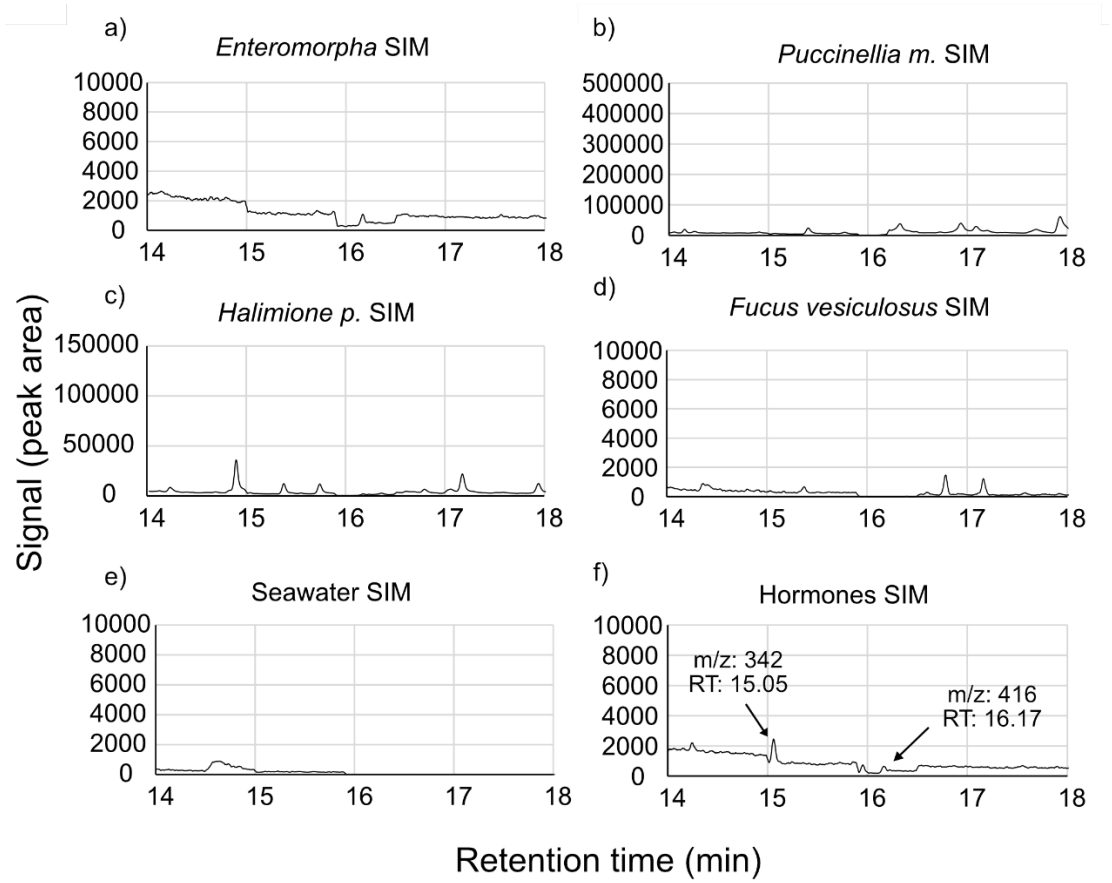

Figure D. 3: GC-MS SIM-chromatograms of each substrate (a) – d)) without hormone spikes to ensure no target analytes are present in any of the sorbent matrices (blanks). e): seawater blank and f): hormone standard in solvent for comparison.

Table D. 2: Data for characterisation of substrates.

Substrate	$\delta^{13}C$ (‰)	TOC (wt%)	TON (wt %)	pH (substrate in brackish water)	pH (substrate in seawater)	Conductivity (µS/cm)
Fucus vesiculosus	-17.81	34.1	1.74	6.10	5.53	1930
Puccinellia maritima	-31.02	43.47	3.67	6.34	5.82	700
Enteromorpha	-17.42	31.67	3.7	7.87	6.41	1200
Halimione portulacoides	-26.42	30.92	1.59	6.20	6.03	2000
Sediment	0	0.07	0	8.01	7.50	370

Table D. 3: Experimental parameters for estrone isotherms in brackish water with volume V (mL), mass of substrate (m (g)), initial concentration C_0 (ng/mL), concentration in equilibrium $\boldsymbol{C_{aq}^{ads}}$ (ng/mL)), adsorbed amount q_e (ng/g).

Substrate	V (mL)	m (g)	C_0 (ng/mL)	C_{aq}^{ads} (ng/mL)	q_e (ng/g)
Fucus vesiculosus	10.00	0.2095	10	7.00	143.21
	10.00	0.2018	14	2.42	573.86
	10.00	0.2118	20	14.56	257.04
	10.00	0.2062	40	14.56	1233.78
	10.00	0.2079	100	19.41	3876.55
	10.00	0.2064	140	19.86	5820.63
	10.00	0.2054	200	96.57	5035.62
Puccinellia maritima	10.00	0.1555	40	3.71	2333.95
	10.00	0.1509	100	21.36	5211.23

	10.00	0.1499	140	30.27	7320.36
	10.00	0.1552	180	35.20	9329.99
	10.00	0.1481	300	70.09	15523.94
	10.00	0.1574	400	131.32	17069.78
	10.00	0.1472	600	202.70	26990.66
Enteromorpha	10.00	0.1053	10	5.17	458.27
	10.00	0.0946	14	9.60	464.63
	10.00	0.0942	20	11.74	876.56
	10.00	0.102	40	24.36	1533.07
	10.00	0.0942	100	82.28	1881.08
	10.00	0.0998	140	100.01	4007.34
	10.00	0.1086	180	122.40	5303.95
Halimione portulacoides	10.00	0.4418	10	7.59	54.63
	10.00	0.4792	14	8.39	117.05
	10.00	0.5049	20	9.72	203.57
	10.00	0.4548	40	15.25	544.21
	10.00	0.4465	100	29.48	1579.36
	10.00	0.4714	180	28.99	3203.44

Sediment	10.00	1.9864	10	6.79	16.17
	10.00	1.9851	14	6.99	35.29
	10.00	1.9502	20	9.85	52.03
	10.00	2.0356	40	13.11	132.10
	10.00	2.0911	100	53.83	220.78
	10.00	1.9735	140	67.45	367.62
	10.00	2.1207	180	73.68	501.36

Table D. 4: Experimental parameters for estrone in brackish water and calculated partition coefficient K_d (L/kg), K_{OC} (L/kg) and logK_{OC}.

	V (mL)	**m (g)**	**C_0 (ng/mL)**	**C_{aq}^{ads} (ng/mL)**	**q_e (ng/g)**	**K_d (L/kg)**	**K_{oc} (L/kg)**	**LogK_{oc}**
Fucus vesiculosus	10.0	0.2062	40	14.56	1233.78	84.74	248.51	2.40
Puccinellia maritima	10.0	0.1555	40	3.71	2333.95	629.60	1448.34	3.16
Enteromorpha	10.0	0.1020	40	24.36	1533.07	62.93	198.70	2.30
Halimione portulacoides	10.0	0.4548	40	15.25	544.21	35.69	115.42	2.06
Sediment	10.0	2.0356	40	13.11	132.10	10.08	14393.64	4.16

Table D. 5: Experimental parameters for estrone in seawater and calculated partition coefficient K_d (L/kg), K_{OC} (L/kg), logK_{OC}.

	V (mL)	m (g)	C_0 (ng/mL)	C_{aq}^{ads} (ng/mL)	q_e (ng/g)	K_d (L/kg)	K_{oc} (L/kg)	logK_{oc}
Fucus vesiculosus	10.0	0.2439	40	7.43	1337.15	188.55	552.94	2.74
Puccinellia maritima	10.0	0.1487	40	18.88	1421.57	75.65	174.02	2.24
Enteromorpha	10.0	0.1092	40	21.74	1673.48	77.07	243.34	2.39
Halimione portulacoides	10.0	0.5012	40	11.77	563.31	48.63	157.29	2.20
Sediment	10.0	2.0157	40	13.05	133.71	10.26	14656.76	4.17

Table D. 6: Model parameters for linear, Freundlich and Langmuir Model.

	Linear Model		Freundlich Model		Langmuir Model		R^2		
	Intercept	C_e	K_F	n	K_L	q_{max}	Linear	Freundlich	Langmuir
Enteromorpha	253.67	35.86	43.94	1.03	0.00	1165566.83	**0.88**	0.88	0.87
Puccinellia maritima	3853.52	114.84	904.83	1.58	0.01	43332.81	0.95	**0.96**	0.95
Halimione portulacoides	-863.53	109.47	1.53	0.46	0.00	3515417.79	0.81	**0.81**	0.67
Fucus vesiculosus	1303.94	44.81	585.61	2.03	0.03	7161.34	0.36	0.45	0.51
Sediment	-2.91	5.81	2.63	0.84	0.00	132653.60	0.91	**0.92**	0.91

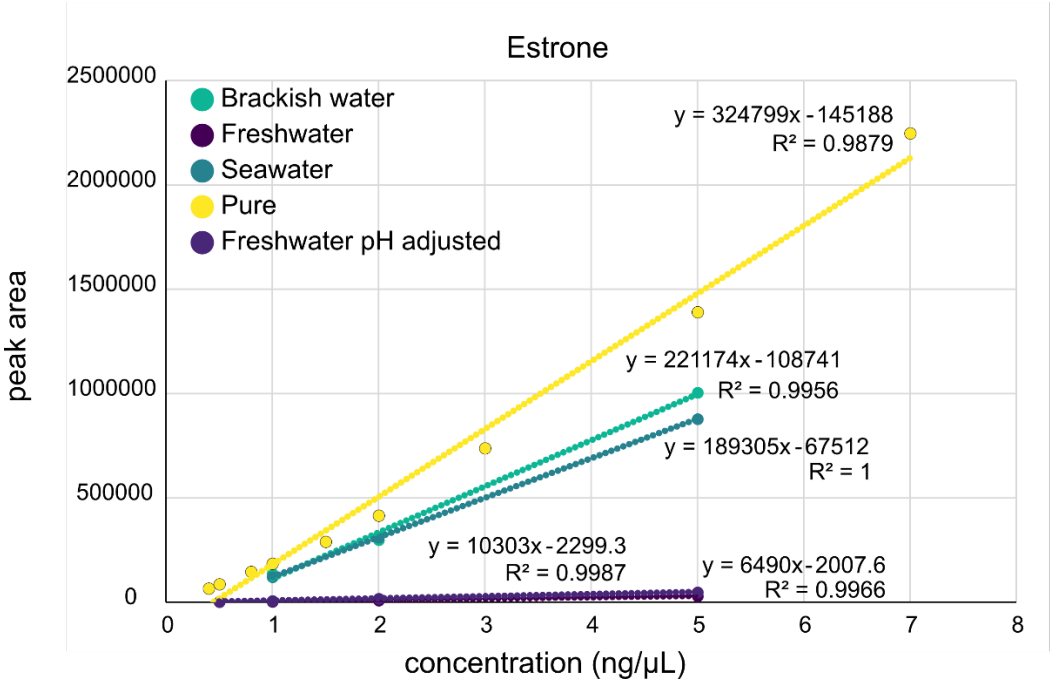

Figure D. 4: Calibration curves (spiked concentration in ng/µL vs. peak area) for estrone directly injected ("Pure", yellow), in brackish water (green), freshwater (dark purple), freshwater with adjusted pH (light purple), and seawater (blue-green).

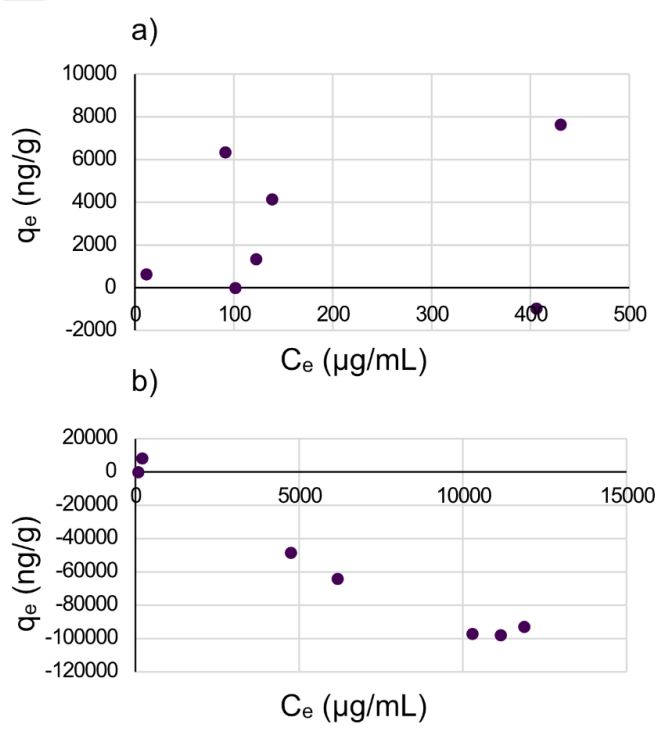

Figure D. 5: Adsorption behaviour of progesterone in brackish water: adsorbed amount q_e (ng/g) vs. equilibrium concentrations (C_e (µg/mL)) for a) *Fucus vesiculosus* and b) *Enteromorpha* as example substrates. The results for progesterone are highly variable and show release of progesterone from the substrates in some cases (b)).

List of References

Abril-Hernández, J.M. (2023) '210Pb-dating of sediments with models assuming a constant flux: CFCS, CRS, PLUM, and the novel χ-mapping. Review, performance tests, and guidelines', *Journal of Environmental Radioactivity*, 268–269. doi:10.1016/j.jenvrad.2023.107248.

Adeel, M. *et al.* (2017) 'Environmental impact of estrogens on human, animal and plant life: A critical review', *Environment International*. Elsevier Ltd, pp. 107–119. doi:10.1016/j.envint.2016.12.010.

Armstrong, B. *et al.* (2004) 'Lung cancer risk after exposure to polycyclic aromatic hydrocarbons: A review and meta-analysis', *Environmental Health Perspectives*. Public Health Services, US Dept of Health and Human Services, pp. 970–978. doi:10.1289/ehp.6895.

Barron, M.G., Heintz, R. and Rice, S.D. (2004) 'Relative potency of PAHs and heterocycles as aryl hydrocarbon receptor agonists in fish', in *Marine Environmental Research*, pp. 95–100. doi:10.1016/j.marenvres.2004.03.001.

Baste, I.A. and Watson, R.T. (2022) 'Tackling the climate, biodiversity and pollution emergencies by making peace with nature 50 years after the Stockholm Conference', *Global Environmental Change*. Elsevier Ltd. doi:10.1016/j.gloenvcha.2022.102466.

Bianchi, T.S. (2006) *Biogeochemistry of Estuaries*. Oxford University Press USA. Available at: https://books.google.co.uk/books?hl=de&lr=&id=3no8DwAAQBAJ&oi=fnd&pg=PR11&dq=Bianchi,+T.+S.+Biogeochemistry+of+Estuaries.+(Oxford+University+Press,+2006)&ots=DJdRgb_Dhi&sig=V_Oh2Vf3B5AqkIeVPUU6A_3G7zw&redir_esc=y#v=onepage&q&f=false (Accessed: 15 June 2025).

Birch, G.F. (2020) 'An assessment of aluminum and iron in normalisation and enrichment procedures for environmental assessment of marine sediment', *Science of the Total Environment*, 727. doi:10.1016/j.scitotenv.2020.138123.

Biswas, P., Vellanki, B.P. and Kazmi, A.A. (2024) 'Investigating biotic and abiotic degradation of emerging contaminants in surface water-sediment batch systems', *Journal of Cleaner Production*, 467. doi:10.1016/j.jclepro.2024.143019.

Boffetta, P., Jourenkova, N. and Gustavsson, P. (1997) 'Cancer risk from occupational and environmental exposure to polycyclic aromatic hydrocarbons', *Cancer Causes and Control*, 8, pp. 444–472.

Bowman, J.C., Readman, J.W. and Zhou, J.L. (2003) 'Sorption of the Natural Endocrine Disruptors, Oestrone and 17β-Oestradiol in the Aquatic Environment', *Environmental Geochemistry and Health*, 25, pp. 63–67.

Bowman, J.C., Zhou, J.L. and Readman, J.W. (2002) 'Sediment-water interactions of natural oestrogens under estuarine conditions', *Marine Chemistry*, 77, pp. 263–276. Available at: www.elsevier.com/locate/marchem.

Bryan, G.W., Langston, W.J. and Langston, J. (1992) 'Bioavailability, accumulation and effects of heavy metals in sediments with special reference to United Kingdom estuaries: a review', *Environmental Pollution*, 76, pp. 89–131.

Burban, P.Y., Lick, W. and Lick, J. (1989) 'The flocculation of fine-grained sediments in estuarine waters', *Journal of Geophysical Research*, 94(C6), pp. 8323–8330. doi:10.1029/JC094IC06P08323.

Caron, E. *et al.* (2010) 'Sorption of four estrogens by surface soils from 41 cultivated fields in Alberta, Canada', *Geoderma*, 155(1–2), pp. 19–30. doi:10.1016/j.geoderma.2009.11.017.

Casey, F.X.M. *et al.* (2003) 'Fate and transport of 17β-estradiol in soil-water systems', *Environmental Science and Technology*, 37(11), pp. 2400–2409. doi:10.1021/es026153z.

Celis-Hernandez, O. *et al.* (2021) 'Assessing the role of the "estuarine filter" for emerging contaminants: pharmaceuticals, perfluoroalkyl compounds and plasticisers in sediment cores from two contrasting systems in the southern U.K.', *Water Research*, 189. doi:10.1016/j.watres.2020.116610.

Celis-Hernandez, O. *et al.* (2022) 'Environmental risk of trace metals and metalloids in estuarine sediments: An example from Southampton Water, U.K.', *Marine Pollution Bulletin*, 178. doi:10.1016/j.marpolbul.2022.113580.

Chakraborty, P. *et al.* (2015) 'Organic matter - A key factor in controlling mercury distribution in estuarine sediment', *Marine Chemistry*, 173, pp. 302–309. doi:10.1016/j.marchem.2014.10.005.

Chapman, P.M. and Wang, F. (2001) 'Assessing sediment contamination in estuaries', *Environmental Toxicology and Chemistry*. SETAC Press, pp. 3–22. doi:10.1002/etc.5620200102.

Chaturvedi, P. *et al.* (2021) 'Prevalence and hazardous impact of pharmaceutical and personal care products and antibiotics in environment: A review on emerging contaminants', *Environmental Research*. Academic Press Inc. doi:10.1016/j.envres.2020.110664.

Chen, C.F. *et al.* (2020) 'Distribution, sources, and behavior of PAHs in estuarine water systems exemplified by Salt River, Taiwan', *Marine Pollution Bulletin*, 154. doi:10.1016/j.marpolbul.2020.111029.

Chen, F. *et al.* (2011) 'Distribution and accumulation of endocrine-disrupting chemicals and pharmaceuticals in wastewater irrigated soils in Hebei, China', *Environmental Pollution*, 159(6), pp. 1490–1498. doi:10.1016/j.envpol.2011.03.016.

Chen, T.C. *et al.* (2012) 'Sorption of estrogens estrone, 17β-estradiol, estriol, 17α-ethinylestradiol, and diethylstilbestrol on sediment affected by different origins', *Journal of Environmental Science and Health - Part A Toxic/Hazardous Substances and Environmental Engineering*, 47(12), pp. 1768–1775. doi:10.1080/10934529.2012.689225.

Chen, Y.L. *et al.* (2018) 'Estrogen degraders and estrogen degradation pathway identified in an activated sludge', *Applied and Environmental Microbiology*, 84(10). doi:10.1128/AEM.00001-18.

Chien, S.W.C., Chen, S.H. and Li, C.J. (2018) 'Effect of soil pH and organic matter on the adsorption and desorption of pentachlorophenol', *Environmental Science and Pollution Research*, 25(6), pp. 5269–5279. doi:10.1007/s11356-017-9822-7.

Combalbert, S. and Hernandez-Raquet, G. (2010) 'Occurrence, fate, and biodegradation of estrogens in sewage and manure', *Applied Microbiology and Biotechnology*, pp. 1671–1692. doi:10.1007/s00253-010-2547-x.

Cosby, A.G. *et al.* (2024) 'Accelerating growth of human coastal populations at the global and continent levels: 2000–2018', *Scientific Reports*, 14(1). doi:10.1038/s41598-024-73287-x.

Croudace, I.W. and Cundy, A.B. (1995) 'Heavy Metal and Hydrocarbon Pollution in Recent Sediments from Southampton Water, Southern England: A Geochemical and Isotopic Study', *Environmental Science and Technology*, 29(5), pp. 1288–1296. doi:10.1021/es00005a021.

Cundy, A.B. *et al.* (1997) 'Reliability of Salt Marshes as "Geochemical Recorders" of Pollution Input: A Case Study from Contrasting Estuaries in Southern England', *Environmental Science and Technology*, 31, pp. 1093–1101. Available at: https://pubs.acs.org/sharingguidelines.

Cundy, A.B. *et al.* (2022) 'A systematic review of emerging contaminants in the Greater Bay Area (GBA), China: Current baselines, knowledge gaps, and research and management priorities', *Environmental Science and Policy*. Elsevier Ltd, pp. 196–208. doi:10.1016/j.envsci.2022.02.002.

Cundy, A.B. and Croudace, I.W. (2017) 'The Fate of Contaminants and Stable Pb Isotopes in a Changing Estuarine Environment: 20 Years on', *Environmental Science and Technology*, 51(17), pp. 9488–9497. doi:10.1021/acs.est.7b00973.

Dai, X. *et al.* (2022) 'Sorption and desorption of sex hormones in soil- and sediment-water systems: A review', *Soil Ecology Letters*. Higher Education Press Limited Company. doi:10.1007/s42832-020-0074-y.

Deich, C. *et al.* (2021) 'Occurrence and distribution of estrogenic substances in the northern South China Sea', *Science of the Total Environment*, 770. doi:10.1016/j.scitotenv.2021.145239.

Deng, W.J., Li, N. and Ying, G.G. (2018) 'Antibiotic distribution, risk assessment, and microbial diversity in river water and sediment in Hong Kong', *Environmental Geochemistry and Health*, 40(5), pp. 2191–2203. doi:10.1007/s10653-018-0092-1.

Department for Environment Food & Rural Affairs (2023) *Main River Hamble Water Body*. Available at: https://environment.data.gov.uk/catchment-planning/v/c3-plan/WaterBody/GB107042016250 (Accessed: 17 February 2025).

Desbrow, C. *et al.* (1998) 'Identification of Estrogenic Chemicals in STW Effluent. 1. Chemical Fractionation and in Vitro Biological Screening', *Environmental Science and Technology*, 32(11), pp. 1549–1558. Available at: https://pubs.acs.org/sharingguidelines.

Downham, R.P. *et al.* (2024) 'Tracking the history of polycyclic aromatic compounds in London through a River Thames sediment core and ultrahigh resolution mass spectrometry', *Journal of Hazardous Materials*, 473. doi:10.1016/j.jhazmat.2024.134605.

Du, B. *et al.* (2022) 'Migration and abiotic transformation of estrone (E1) and estrone-3-sulfate (E1-3S) during soil column transport', *Environmental Geochemistry and Health*, 44, pp. 911–924. doi:10.1007/s10653-021-00968-1.

Duan, P. *et al.* (2022) 'Effect of dissolved organic matter and heavy metals ions on sorption of phenanthrene at sedimentary particle scale', *Journal of Hazardous Materials*, 436. doi:10.1016/j.jhazmat.2022.129175.

Elliott, M. and McLusky, D.S. (2002) 'The need for definitions in understanding estuaries', *Estuarine, Coastal and Shelf Science*. Academic Press, pp. 815–827. doi:10.1006/ecss.2002.1031.

Emerson, S. *et al.* (1987) 'Estimates of degradable organic carbon in deep-sea surface sediments from 14C concentrations', *Letters to Nature*, 329(3), pp. 51–53.

European Environment Agency (2024) *Heavy metal emissions in Europe*. Available at: https://www.eea.europa.eu/en/analysis/indicators/heavy-metal-emissions-in-europe#ref-ip34W (Accessed: 3 July 2025).

European Parliament and Council (2008) *DIRECTIVE 2008/105/EC OF THE EUROPEAN PARLIAMENT AND OF THE COUNCIL of 16 December 2008 on environmental quality standards in the field of water policy*.

European Parliament and Council (2010) *DIRECTIVE 2010/75/EU OF THE EUROPEAN PARLIAMENT AND OF THE COUNCIL of 24 November 2010 on industrial emissions (integrated pollution prevention and control) (Recast)*.

Famera, M. *et al.* (2013) 'Distribution of heavy-metal contamination in regulated river-channel deposits: A magnetic susceptibility and grain-size approach; River morava, Czech republic', *Water, Air, and Soil Pollution*, 224(5). doi:10.1007/s11270-013-1525-1.

Fang, X. *et al.* (2023) 'Exploring potential dual-stage attention based recurrent neural network machine learning application for dosage prediction in intelligent municipal management', *Environmental Science: Water Research and Technology*, 9(3), pp. 890–899. doi:10.1039/d2ew00560c.

Fang, Z. and Wang, W.X. (2022) 'Dynamics of trace metals with different size species in the Pearl River Estuary, Southern China', *Science of the Total Environment*, 807. doi:10.1016/j.scitotenv.2021.150712.

Fawell, J. and Ong, C.N. (2012) 'Emerging Contaminants and the Implications for Drinking Water', *International Journal of Water Resources Development*, 28(2), pp. 247–263. doi:10.1080/07900627.2012.672394.

Fei, Y. heng, Leung, K.M.Y. and Li, X. yan (2017) 'Adsorption of 17 A-ethyl estradiol with the competition of bisphenol A on the marine sediment of Hong Kong', *Marine Pollution Bulletin*, 124(2), pp. 753–759. doi:10.1016/j.marpolbul.2017.06.068.

Fernandes, A.M. *et al.* (2016) 'Combined analysis of trace elements and isotopic composition of particulate organic matter in suspended sediment to assess their origin and flux in a tropical disturbed watershed', *Environmental Pollution*, 218, pp. 844–854. doi:10.1016/j.envpol.2016.08.008.

Förstner, U. and Wittmann, G.T.W. (1981) *Metal Pollution in the Aquatic Environment*, *Metal Pollution in the Aquatic Environment*. Springer Berlin Heidelberg. doi:10.1007/978-3-642-69385-4.

Freeman, L.A. *et al.* (2019) 'Impacts of Urbanization and Development on Estuarine Ecosystems and Water Quality', *Estuaries and Coasts*. Springer New York LLC, pp. 1821–1838. doi:10.1007/s12237-019-00597-z.

Galarneau, E. (2008) ‘Source specificity and atmospheric processing of airborne PAHs: Implications for source apportionment’, *Atmospheric Environment*, 42(35), pp. 8139–8149. doi:10.1016/j.atmosenv.2008.07.025.

Gao, L. *et al.* (2016) ‘Distribution characteristics and sources of trace metals in sediment cores from a trans-boundary watercourse: An example from the Shima River, Pearl River Delta’, *Ecotoxicology and Environmental Safety*, 134, pp. 186–195. doi:10.1016/j.ecoenv.2016.08.020.

Gao, L. *et al.* (2023) ‘Remobilization characteristics and diffusion kinetic processes of sediment zinc (Zn) in a tidal reach of the Pearl River Estuary, South China’, *Journal of Hazardous Materials*, 457. doi:10.1016/j.jhazmat.2023.131692.

Goldberg, E.D. *et al.* (1977) ‘Pollution History of Narragansett Bay as Recorded in its Sediments’, *Estuarine and Coastal Marine Science*, 5, pp. 549–561.

Gong, J. *et al.* (2011) ‘Occurrence of endocrine-disrupting chemicals in riverine sediments from the Pearl River Delta, China’, *Marine Pollution Bulletin*, 63(5–12), pp. 556–563. doi:10.1016/j.marpolbul.2011.01.026.

Gong, J. *et al.* (2019) ‘Vertical profiles and distributions of aqueous endocrine-disrupting chemicals in different matrices from the Pearl River Delta and the influence of environmental factors’, *Environmental Pollution*, 246, pp. 328–335. doi:10.1016/j.envpol.2018.12.015.

Grobin, A., Roškar, R. and Trontelj, J. (2022) ‘Multi-parameter risk assessment of forty-one selected substances with endocrine disruptive properties in surface waters worldwide’, *Chemosphere*, 287. doi:10.1016/j.chemosphere.2021.132195.

Hanfi, M.Y., Mostafa, M.Y.A. and Zhukovsky, M. V. (2020) ‘Heavy metal contamination in urban surface sediments: sources, distribution, contamination control, and remediation’, *Environmental Monitoring and Assessment*, 192(1). doi:10.1007/s10661-019-7947-5.

Harries, J.E. *et al.* (1997) ‘Estrogenic activity in five United Kingdom rivers detected by measurement of vitellogenesis in caged male trout’, *Environmental Toxicology and Chemistry*, 16(3), pp. 534–542. doi:10.1002/etc.5620160320.

He, X. *et al.* (2016) ‘Eddy-entrained Pearl River plume into the oligotrophic basin of the South China Sea’, *Continental Shelf Research*, 124, pp. 117–124. doi:10.1016/j.csr.2016.06.003.

Hellawell, E.E. *et al.* (2022) ‘An analysis of PAH soil contamination in south east England: A case study leading to an evidence-based portfolio and process route map’, *Geoderma Regional*, 30. doi:10.1016/j.geodrs.2022.e00533.

Hillyer, K.E. *et al.* (2022) 'Metabolomics as a tool for in situ study of chronic metal exposure in estuarine invertebrates', *Environmental Pollution*, 292. doi:10.1016/j.envpol.2021.118408.

Himson, S. *et al.* (2023) 'The San Francisco Estuary, USA as a reference section for an Anthropocene series', *Anthropocene Review* [Preprint]. doi:10.1177/20530196221147607.

Hissler, C. and Probst, J.L. (2006) 'Impact of mercury atmospheric deposition on soils and streams in a mountainous catchment (Vosges, France) polluted by chlor-alkali industrial activity: The important trapping role of the organic matter', *Science of the Total Environment*, 361(1–3), pp. 163–178. doi:10.1016/j.scitotenv.2005.05.023.

Holme, J.A. *et al.* (2019) 'Potential role of polycyclic aromatic hydrocarbons as mediators of cardiovascular effects from combustion particles', *Environmental Health 2019 18:1*, 18(1), pp. 1–18. doi:10.1186/S12940-019-0514-2.

Holthaus, K.I.E. *et al.* (2002) 'The potential for estradiol and ethinylestradiol to sorb to suspended and bed sediments in some English rivers', *Environmental Toxicology and Chemistry*, 21(12), pp. 2526–2535. doi:10.1002/etc.5620211202.

Iftikhar, F. *et al.* (2022) 'Spatial distribution of trace elements associated with organic carbon along the Beiyun River basin, Beijing, China', *International Journal of Sediment Research*, 37(3), pp. 335–345. doi:10.1016/j.ijsrc.2021.10.005.

Incardona, J.P. and Scholz, N.L. (2016) 'The influence of heart developmental anatomy on cardiotoxicity-based adverse outcome pathways in fish', *Aquatic Toxicology*, 177, pp. 515–525. doi:10.1016/J.AQUATOX.2016.06.016.

International Copper Study Group (2024) *The World Copper Factbook 2024*. Available at: www.icsg.org.

International Lead and Zinc Study Group (ILZSG) (2025) *Lead and Zinc Statistics*. Available at: https://www.ilzsg.org/free-access-data/ (Accessed: 4 July 2025).

Ip, C.C.M. *et al.* (2004) 'Over one hundred years of trace metal fluxes in the sediments of the Pearl River Estuary, South China', *Environmental Pollution*, 132(1), pp. 157–172. doi:10.1016/j.envpol.2004.03.028.

Ip, C.C.M. *et al.* (2007) 'Trace metal distribution in sediments of the Pearl River Estuary and the surrounding coastal area, South China', *Environmental Pollution*, 147(2), pp. 311–323. doi:10.1016/j.envpol.2006.06.028.

Jahromi, F.A. *et al.* (2021) 'Source and risk assessment of heavy metals and microplastics in bivalves and coastal sediments of the Northern Persian Gulf, Hormogzan Province', *Environmental Research*, 196. doi:10.1016/j.envres.2021.110963.

Järup, L. (2003) 'Hazards of heavy metal contamination', *British Medical Bulletin*, pp. 167–182. doi:10.1093/bmb/ldg032.

Jia, Y.W. *et al.* (2024) 'Time evolution of estrogen contamination in the Scheldt estuary', *Science of the Total Environment*, 957. doi:10.1016/j.scitotenv.2024.177432.

Karp, A.T. *et al.* (2020) 'Fire distinguishers: Refined interpretations of polycyclic aromatic hydrocarbons for paleo-applications', *Geochimica et Cosmochimica Acta*, 289, pp. 93–113. doi:10.1016/j.gca.2020.08.024.

Katsoyiannis, A., Sweetman, A.J. and Jones, K.C. (2011) 'PAH molecular diagnostic ratios applied to atmospheric sources: A critical evaluation using two decades of source inventory and air concentration data from the UK', *Environmental Science and Technology*, 45(20), pp. 8897–8906. doi:10.1021/es202277u.

Kidd, K.A. *et al.* (2007) 'Collapse of a fish population after exposure to a synthetic estrogen', *PNAS*, 104(21), pp. 8897–8901. Available at: www.pnas.orgcgidoi10.1073pnas.0609568104.

Kidd, K.A. *et al.* (2014) 'Direct and indirect responses of a freshwater food web to a potent synthetic oestrogen', *Philosophical Transactions of the Royal Society B: Biological Sciences*, 369(1656). doi:10.1098/rstb.2013.0578.

King, C.K., Gale, S.A. and Stauber, J.L. (2006) 'Acute toxicity and bioaccumulation of aqueous and sediment-bound metals in the estuarine amphipod Melita plumulosa', *Environmental Toxicology*, 21(5), pp. 489–504. doi:10.1002/tox.20211.

Koukina, S.E. and Lobus, N. V. (2020) 'Relationship between enrichment, toxicity, and chemical bioavailability of heavy metals in sediments of the Cai River estuary', *Environmental Monitoring and Assessment*, 192(5). doi:10.1007/s10661-020-08282-6.

Kranck, K. (1973) 'Flocculation of Suspended Sediment in the Sea', *Nature*, 246.

Kumirska, J. *et al.* (2013) 'Chemometric optimization of derivatization reactions prior to gas chromatography-mass spectrometry analysis', *Journal of Chromatography A*, 1296, pp. 164–178. doi:10.1016/j.chroma.2013.04.079.

Kümmerer, K. (2011) 'Emerging Contaminants versus Micro-pollutants', *Clean - Soil, Air, Water*, pp. 889–890. doi:10.1002/clen.201110002.

Labadie, P. *et al.* (2007) 'Evidence for the migration of steroidal estrogens through river bed sediments', *Environmental Science and Technology*, 41(12), pp. 4299–4304. doi:10.1021/es063062j.

Lai, K.M. *et al.* (2000) 'Binding of waterborne steroid estrogens to solid phases in river and estuarine systems', *Environmental Science and Technology*, 34(18), pp. 3890–3894. doi:10.1021/es9912729.

Lake, J.L. *et al.* (1979) 'Origins of polycyclic aromatic hydrocarbons in estuarine sediments', *Geochimica et Cosmochimica Acta*, 43, pp. 1847–1854.

Lamb, A.L., Wilson, G.P. and Leng, M.J. (2006) 'A review of coastal palaeoclimate and relative sea-level reconstructions using δ13C and C/N ratios in organic material', *Earth-Science Reviews*, 75(1–4), pp. 29–57. doi:10.1016/j.earscirev.2005.10.003.

Lange, I.G. *et al.* (2002) 'Sex hormones originating from different livestock production systems: fate and potential disrupting activity in the environment', *Analytica Chimica Acta*, 473, pp. 27–37.

Langston, W.J. (1982) 'The Distribution of Mercury in British Estuarine Sediments and its Availability to Deposit-Feeding Bivalves', *Journal of the Marine Biological Association of the United Kingdom*, 62(3), pp. 667–684. doi:10.1017/S0025315400019822.

Laxen, D.P.H. and Harrison, R.M. (1977) 'The Highway as a Source of Water Pollution: An Appraisal with the Heavy Metal Lead', *Water Research*, 11, pp. 1–11.

Lee, H.B. and Liu, D. (2002) 'Degradation of 17β-Estradiol and its metabolites by sewage bacteria', *Water, Air, and Soil Pollution*, 134, pp. 353–368.

Lee, L.S. *et al.* (2003) 'Sorption and dissipation of testosterone, estrogens, and their primary transformation products in soils and sediment', *Environmental Science and Technology*, 37(18), pp. 4098–4105. doi:10.1021/es020998t.

Levasseur, A. (2008) *Observations and modelling of the variability of the Solent-Southampton Water estuarine system*. University of Southampton.

Li, C. *et al.* (2022) 'From a "World Factory" to China's Bay Area: A Review of the Outline of the Development Plan for the Guangdong-Hong Kong-Macao Greater Bay Area', *Planning Theory & Practice*, 23(2), pp. 310–314. doi:10.1080/14649357.2021.1958539.

Li, H. *et al.* (2021) 'Occurrence, source identification, and ecological risk assessment of polycyclic aromatic hydrocarbons in sediments of the Pearl River Delta, China', *Marine Pollution Bulletin*, 170. doi:10.1016/j.marpolbul.2021.112666.

Li, J., Carter, L.J. and Boxall, A.B.A. (2020) 'Evaluation and development of models for estimating the sorption behaviour of pharmaceuticals in soils', *Journal of Hazardous Materials*, 392. doi:10.1016/j.jhazmat.2020.122469.

Li, X. *et al.* (2023) 'Impacts of river discharge, coastal geomorphology, and regional sea level rise on tidal dynamics in Pearl River Estuary', *Frontiers in Marine Science*, 10, p. 1065100. doi:10.3389/FMARS.2023.1065100/BIBTEX.

Li, Y. *et al.* (2014) 'Adsorption interference mechanism for endocrine disrupting compounds in sediment-water system by quantitative structure-property relationship models', *Clean - Soil, Air, Water*, 42(6), pp. 738–744. doi:10.1002/clen.201300033.

Li, Y. *et al.* (2024) 'Quantitative effects of anthropogenic and natural factors on the spatial distribution of heavy metals and bacterial communities in sediments of the Pearl River Delta', *Environmental Technology and Innovation*, 35. doi:10.1016/j.eti.2024.103648.

Lima, D.L.D., Schneider, R.J. and Esteves, V.I. (2012) 'Sorption behavior of EE2 on soils subjected to different long-term organic amendments', *Science of the Total Environment*, 423, pp. 120–124. doi:10.1016/j.scitotenv.2012.02.014.

Lin, P. *et al.* (2024) 'Uranium and Nickel Partitioning in a Contaminated Riparian Wetland', *Water (Switzerland)*, 16(7). doi:10.3390/w16070966.

Lindberg, S.E. and Harriss, R.C. (1974) 'Mercury-Organic Matter Associations in Estuarine Sediments and Interstitial Water', *Environmental Science and Technology*, 8(5), pp. 459–462. Available at: https://pubs.acs.org/sharingguidelines.

Lion, L.W., Altmann, R.S. and Leckie, J.O. (1982) 'Trace-Metal Adsorption Characteristics of Estuarine Particulate Matter: Evaluation of Contributions of Fe/Mn Oxide and Organic Surface Coatings', *Environmental Science and Technology*, 16(10), pp. 660–666. doi:10.1021/es00104a007.

Liu, H. *et al.* (2014) 'Occurrence and distribution of phthalate esters in riverine sediments from the Pearl River Delta region, South China', *Marine Pollution Bulletin*, 83(1), pp. 358–365. doi:10.1016/j.marpolbul.2014.03.038.

Liu, X. *et al.* (2020) 'Characteristics, distribution, source and ecological risk of polycyclic aromatic hydrocarbons (PAHs) in sediments along the Yangtze River Estuary Deepwater Channel', *Marine Pollution Bulletin*, 150. doi:10.1016/j.marpolbul.2019.110765.

López de Alda, M.J. *et al.* (2002) 'Occurrence and analysis of estrogens and progestogens in river sediments by liquid chromatography-electrospray-mass spectrometry', *Analyst*, 127(10), pp. 1299–1304. doi:10.1039/b207658f.

Loring, D.H. (1991) 'Normalization of heavy-metal data from estuarine and coastal sediments', *ICES J. mar. Sci*, 48, pp. 101–115. Available at: https://academic.oup.com/icesjms/article/48/1/101/696084.

Luan, F. *et al.* (2022) 'Molecular size-fraction and seasonal characteristics of dissolved trace metals in river and estuarine waters of the Yellow River, China', *Frontiers in Marine Science*, 9. doi:10.3389/fmars.2022.1074829.

Lv, Y.Z. *et al.* (2019) 'Bioaccumulation, metabolism, and risk assessment of phenolic endocrine disrupting chemicals in specific tissues of wild fish', *Chemosphere*, 226, pp. 607–615. doi:10.1016/j.chemosphere.2019.03.187.

Ma, L. and Yates, S.R. (2018) 'Dissolved organic matter and estrogen interactions regulate estrogen removal in the aqueous environment: A review', *Science of the Total Environment*. Elsevier B.V., pp. 529–542. doi:10.1016/j.scitotenv.2018.05.301.

Magnuson, J.T. *et al.* (2018) 'Effects of Deepwater Horizon crude oil on ocular development in two estuarine fish species, red drum (Sciaenops ocellatus) and sheepshead minnow (Cyprinodon variegatus)', *Ecotoxicology and Environmental Safety*, 166, pp. 186–191. doi:10.1016/j.ecoenv.2018.09.087.

Mai, B. *et al.* (2005) 'Distribution of polybrominated diphenyl ethers in sediments of the Pearl River Delta and adjacent South China Sea', *Environmental Science and Technology*, 39(10), pp. 3521–3527. doi:10.1021/es048083x.

Mallah, Manthar Ali *et al.* (2022) 'Polycyclic aromatic hydrocarbon and its effects on human health: An overeview', *Chemosphere*. Elsevier Ltd. doi:10.1016/j.chemosphere.2022.133948.

McLusky, D.S. and Elliott, M. (2004) 'The Estuarine Ecosystem: Ecology, Threats and Management', *The Estuarine Ecosystem* [Preprint]. doi:10.1093/ACPROF:OSO/9780198525080.001.0001.

Menzie, C.A. and Santodonato, J. (1992) 'Exposure to Carcinogenic PAHs in the Environment', *Environ. Sci. Technol.*, 26(7).

Metcalfe, C.D. *et al.* (2001) 'Estrogenic potency of chemicals detected in sewage treatment plant effluents as determined by in vivo assays with Japanese medaka (Oryzias latipes)', *Environmental Toxicology and Chemistry*, 20(2), pp. 297–308. doi:10.1002/etc.5620200210.

Meyer, M.F., Powers, S.M. and Hampton, S.E. (2019) 'An Evidence Synthesis of Pharmaceuticals and Personal Care Products (PPCPs) in the Environment: Imbalances among Compounds, Sewage Treatment Techniques, and Ecosystem Types', *Environmental Science and Technology*. American Chemical Society, pp. 12961–12973. doi:10.1021/acs.est.9b02966.

Middelburg, J.J. (1989) 'A simple rate model for organic matter decomposition in marine sediments', *Geochimica et Cosmochimica Acta*, 53, pp. 1577–1581.

Mil-Homens, M. *et al.* (2025) 'Sources and distribution of organic matter and polycyclic aromatic hydrocarbons in sediments of the southwestern Portuguese shelf', *Marine Pollution Bulletin*, 210. doi:10.1016/j.marpolbul.2024.117303.

Miranda, L.S. *et al.* (2021) 'Water-sediment interactions and mobility of heavy metals in aquatic environments', *Water Research*, 202. doi:10.1016/j.watres.2021.117386.

Mohammed, R. *et al.* (2021) 'Fate and occurrence of polycyclic aromatic hydrocarbons and their derivatives in water and sediment from Songhua river, northeast China', *Water (Switzerland)*, 13(9). doi:10.3390/w13091196.

Morais, H. *et al.* (2023) 'Baseline progestins characterization in surface waters of three main Portuguese estuaries', *Marine Pollution Bulletin*, 194. doi:10.1016/j.marpolbul.2023.115352.

Müller, A.K. *et al.* (2019) 'Bioavailability of estrogenic compounds from sediment in the context of flood events evaluated by passive sampling', *Water Research*, 161, pp. 540–548. doi:10.1016/j.watres.2019.06.020.

Nayak, Y. *et al.* (2023) 'Distribution, Variations, Fate and Sources of Polycyclic Aromatic Hydrocarbons and Carbon in Particulate Matter, Road Dust, and Sediments in Central India', *Polycyclic Aromatic Compounds*, 43(2), pp. 1309–1331. doi:10.1080/10406638.2022.2026991.

Neale, P.A. *et al.* (2010) 'Sorption of micropollutant estrone to a water treatment ion exchange resin', *Journal of Environmental Monitoring*, 12(1), pp. 311–317. doi:10.1039/B913338K.

Neale, P.A., Escher, B.I. and Schäfer, A.I. (2009) 'pH dependence of steroid hormone-organic matter interactions at environmental concentrations', *Science of the Total Environment*, 407(3), pp. 1164–1173. doi:10.1016/j.scitotenv.2008.09.035.

Nimrod, A.C. and Benson, W.H. (1998) 'Reproduction and development of Japanese medaka following an early life stage exposure to xenoestrogens', *Aquatic Toxicology*, 44, pp. 141–156.

Niu, L. *et al.* (2018) 'Dynamics of polycyclic aromatic hydrocarbons (PAHs) in water column of Pearl River estuary (China): Seasonal pattern, environmental fate and source implication', *Applied Geochemistry*, 90, pp. 39–49. doi:10.1016/j.apgeochem.2017.12.014.

Nriagu, J.O. (1996) 'A history of global metal pollution', *Science*, pp. 223–224. doi:10.1126/science.272.5259.223.

Nybom, I. *et al.* (2024) 'Water column organic carbon composition as driver for water-sediment fluxes of hazardous pollutants in a coastal environment', *Journal of Hazardous Materials*, 465. doi:10.1016/j.jhazmat.2023.133393.

Olatunji, O.S. *et al.* (2017) 'Determination of selected steroid hormones in some surface water around animal farms in Cape Town using HPLC-DAD', *Environmental Monitoring and Assessment*, 189(7), pp. 1–10. doi:10.1007/S10661-017-6070-8/TABLES/4.

de Oliveira Santos, A.D. *et al.* (2022) 'Pharmaceuticals, natural and synthetic hormones and phenols in sediments from an eutrophic estuary, Jurujuba Sound, Guanabara Bay, Brazil', *Marine Pollution Bulletin*, 184. doi:10.1016/j.marpolbul.2022.114176.

Oyo-Ita, I. *et al.* (2022) 'Seasonal Changes of PAHs in Water and Suspended Particulate Matter from Cross River Estuary, SE Nigeria in Response to Human-Induced Activity and Hydrological Cycle', *Polycyclic Aromatic Compounds*, 42(8), pp. 5456–5473. doi:10.1080/10406638.2021.1939070.

Passos, T. *et al.* (2022) 'Assessment of the temporal retention of mercury and nutrient records within the mangrove sediments of a highly impacted estuary', *Environmental Research*, 206. doi:10.1016/j.envres.2021.112569.

Peck, M. *et al.* (2004) 'Sediments are major sinks of steroidal estrogens in two United Kingdom rivers', *Environmental Toxicology and Chemistry*, 23(4), pp. 945–952. doi:10.1897/03-41.

Peng, X. *et al.* (2007) 'Temporal trends of nonylphenol and bisphenol A contamination in the Pearl River Estuary and the adjacent South China Sea recorded by dated sedimentary cores', *Science of the Total Environment*, 384(1–3), pp. 393–400. doi:10.1016/j.scitotenv.2007.05.043.

Peng, X. *et al.* (2008) 'Temporal trends of hydrocarbons in sediment cores from the Pearl River Estuary and the northern South China Sea', *Environmental Pollution*, 156(2), pp. 442–448. doi:10.1016/j.envpol.2008.01.037.

Petrie, B., Barden, R. and Kasprzyk-Hordern, B. (2015) 'A review on emerging contaminants in wastewaters and the environment: Current knowledge, understudied areas and recommendations for future monitoring', *Water Research*, 72, pp. 3–27. doi:10.1016/j.watres.2014.08.053.

Potapowicz, J. *et al.* (2022) 'Sources and composition of chemical pollution in Maritime Antarctica (King George Island), part 1: Sediment and water analysis for PAH sources evaluation in the vicinity of Arctowski station', *Chemosphere*, 288. doi:10.1016/j.chemosphere.2021.132637.

Potter, I.C. *et al.* (2010) 'The concept of an estuary: A definition that incorporates systems which can become closed to the ocean and hypersaline', *Estuarine, Coastal and Shelf Science*, 87(3), pp. 497–500. doi:10.1016/j.ecss.2010.01.021.

Pratush, A. *et al.* (2020) 'Biotransformation strategies for steroid estrogen and androgen pollution', *Applied Microbiology and Biotechnology*. Springer, pp. 2385–2409. doi:10.1007/s00253-020-10374-9.

Purdom, C.E. *et al.* (1994) 'Estrogenic Effects of Effluents from Sewage Treatment Works', *Chemistry and Ecology*, 8(4), pp. 275–285. doi:10.1080/02757549408038554.

Qi, Y., Zhang, T.C. and Ren, Y. (2014) 'Testosterone sorption and desorption: Effects of soil particle size', *Journal of Hazardous Materials*, 279, pp. 493–501. doi:10.1016/j.jhazmat.2014.06.077.

Ravindra, K., Sokhi, R. and Van Grieken, R. (2008) 'Atmospheric polycyclic aromatic hydrocarbons: Source attribution, emission factors and regulation', *Atmospheric Environment*, pp. 2895–2921. doi:10.1016/j.atmosenv.2007.12.010.

Rodríguez-Hernández, J.A. *et al.* (2022) 'Environmental persistence, detection, and mitigation of endocrine disrupting contaminants in wastewater treatment plants – a review with a focus on tertiary treatment technologies', *Environmental Science: Advances*, 1(5), pp. 680–704. doi:10.1039/D2VA00179A.

Runnalls, T.J. *et al.* (2013) 'Several synthetic progestins with different potencies adversely affect reproduction of fish', *Environmental Science and Technology*, 47(4), pp. 2077–2084. doi:10.1021/es3048834.

Sahu, S.K. and Pandit, G.G. (2003) 'Estimation of Octanol-Water Partition Coefficients for Polycylic Aromatic Hydrocarbons Using Reverse-Phase HPLC', *Journal of Liquid Chromatography and Related Technologies*, 26(1), pp. 135–146. doi:10.1081=JLC-120017158.

Salomons, W. and Mook, W.G. (1977) 'Trace Metal Concentrations in Estuarine Sediments: Mobilization, Mixing or Precipitation', *Netherlands Journal of Sea Research*, 11(2), pp. 119–129.

Sangster, J.L. *et al.* (2015) 'The effect of particle size on sorption of estrogens, androgens and progestagens in aquatic sediment', *Journal of Hazardous Materials*, 299, pp. 112–121. doi:10.1016/j.jhazmat.2015.05.046.

Sangster, J.L. *et al.* (2016) 'Bioavailability and Fate of Sediment-Associated Progesterone in Aquatic Systems', *Environmental Science and Technology*, 50(7), pp. 4027–4036. doi:10.1021/acs.est.5b06082.

Santos, A.D. de O. *et al.* (2024) 'Estrogenic activity and acute toxicity assessments of sediments from a chronically polluted estuarine area in southeastern Brazil', *Environmental Quality Management*, 33(3), pp. 183–194. doi:10.1002/tqem.22104.

Sharples, J. (2000) 'Water Circulation in Southampton Water and the Solent', in Collins, M. and Ansell, K. (eds) *Solent Science - A Review*. 2000 Elsevier Science B.V., pp. 45–53. Available at: https://www.researchgate.net/publication/313210909_Water_circulation_in_Southampton_Water_and_the_Solent (Accessed: 8 July 2025).

Shi, C. *et al.* (2022) 'Heavy metals and Pb isotopes in a marine sediment core record environmental changes and anthropogenic activities in the Pearl River Delta over a century', *Science of the Total Environment*, 814. doi:10.1016/j.scitotenv.2021.151934.

Shi, J. *et al.* (2013) 'Sludge/water partition and biochemical transformation of estrone and 17β-estradiol in a pilot-scale step-feed anoxic/oxic wastewater treatment system', *Biochemical Engineering Journal*, 74, pp. 107–114. doi:10.1016/j.bej.2013.03.001.

Sholkovitz, E.R. and Copland, D. (1981) 'The coagulation, solubility and adsorption properties of Fe, Mu, Cu, Ni, Cd, Co and humic acids in a river water', *Geochimica et Cosmochimica Acta*, 45, pp. 181–189.

Song, X. *et al.* (2024) 'Natural mineral colloids facilitated transport of EE2 in saturated porous media: Effects of humic acid and conjugate form', *Journal of Contaminant Hydrology*, 265. doi:10.1016/j.jconhyd.2024.104387.

de Sousa, D.N.R. *et al.* (2018) 'Spatio-temporal evaluation of emerging contaminants and their partitioning along a Brazilian watershed', *Environmental Science and Pollution Research*, 25(5), pp. 4607–4620. doi:10.1007/s11356-017-0767-7.

Southampton City Council; and Southampton Data Observatory (2024) *Southampton Strategic Assessment: Population size and structure*. Available at:

https://data.southampton.gov.uk/population/population-size-and-structure/ (Accessed: 28 February 2025).

Southern Water (2025) *Rivers and Sea Watch*. Available at: https://www.southernwater.co.uk/our-region/clean-rivers-and-seas-task-force/rivers-and-seas-watch/ (Accessed: 18 March 2025).

de Souza Machado, A.A. *et al.* (2016) 'Metal fate and effects in estuaries: A review and conceptual model for better understanding of toxicity', *Science of the Total Environment*. Elsevier, pp. 268–281. doi:10.1016/j.scitotenv.2015.09.045.

Souza, T. *et al.* (2016) 'New insights into BaP-induced toxicity: role of major metabolites in transcriptomics and contribution to hepatocarcinogenesis', *Archives of Toxicology*, 90(6), pp. 1449–1458. doi:10.1007/S00204-015-1572-Z/TABLES/1.

Spencer, K.L., Cundy, A.B. and Croudace, I.W. (2003) 'Heavy metal distribution and early-diagenesis in salt marsh sediments from the Medway Estuary, Kent, UK', *Estuarine, Coastal and Shelf Science*, 57(1–2), pp. 43–54. doi:10.1016/S0272-7714(02)00324-4.

Stemberger, R.S. and Chen, C.Y. (1998) 'Fish tissue metals and zooplankton assemblages of northeastern U.S. lakes', *Canadian Journal of Fisheries and Aquatic Sciences*, 55(2), pp. 339–352. doi:10.1139/F97-223;PAGE:STRING:ARTICLE/CHAPTER.

Sun, K. *et al.* (2008) 'Sorption of phenanthrene by nonhydrolyzable organic matter from different size sediments', *Environmental Science and Technology*, 42(6), pp. 1961–1966. doi:10.1021/es7024627.

Sun, K. *et al.* (2012) 'Sorption of 17α-ethinyl estradiol, bisphenol A and phenanthrene to different size fractions of soil and sediment', *Chemosphere*, 88(5), pp. 577–583. doi:10.1016/j.chemosphere.2012.03.034.

Sunda, W.G., Tester, P.A. and Huntsman, S.A. (1990) 'Toxicity of Trace Metals to Acartiu tonsa in the Elizabeth River and Southern Chesapeake Bay', *Estuarine, Coastal and Shelf Science*, 30, pp. 207–221.

Suri, R.P.S., Singh, T.S. and Abburi, S. (2010) 'Influence of alkalinity and salinity on the sonochemical degradation of estrogen hormones in aqueous solution', *Environmental Science and Technology*, 44(4), pp. 1373–1379. doi:10.1021/es9024595.

Tamtam, F. *et al.* (2011) 'A 50-year record of quinolone and sulphonamide antimicrobial agents in Seine River sediments', *Journal of Soils and Sediments*, 11(5), pp. 852–859. doi:10.1007/s11368-011-0364-1.

Tao, D. *et al.* (2022) 'Widespread occurrence of emerging E-waste contaminants – Liquid crystal monomers in sediments of the Pearl River Estuary, China', *Journal of Hazardous Materials*, 437. doi:10.1016/j.jhazmat.2022.129377.

Teixeira, M. *et al.* (2023) 'Ecological risk assessment of metal and hydrocarbon pollution in sediments from an urban tropical estuary: Tijuca lagoon (Rio de Janeiro, Brazil)', *Environmental Science and Pollution Research*, 30(1), pp. 184–200. doi:10.1007/s11356-022-22214-6.

Thiebault, T. *et al.* (2017) 'Record of pharmaceutical products in river sediments: A powerful tool to assess the environmental impact of urban management?', *Anthropocene*, 18, pp. 47–56. doi:10.1016/j.ancene.2017.05.006.

Tobiszewski, M. and Namieśnik, J. (2012) 'PAH diagnostic ratios for the identification of pollution emission sources', *Environmental Pollution*, pp. 110–119. doi:10.1016/j.envpol.2011.10.025.

Torres-Moreno, C. *et al.* (2022) 'Polycyclic aromatic hydrocarbons (PAHs) in human breast milk from Colombia: Spatial occurrence, sources and probabilistic risk assessment', *Environmental Research*, 204. doi:10.1016/j.envres.2021.111981.

Tubbs, C.R. *et al.* (1980) 'The Solent Estuarine System: An Assessment of Present Knowledge', *The Natural Environment Research Council Publication Series* , C(22).

Turekian, K.K. and Wedepohl, K.H. (1961) 'Distribution of the Elements in Some Major Units of the Earth's Crust', *Geological Society of America Bulletin*, 72, pp. 175–192.

United Nations (1998) 'Aarhus Protocol 1979 - Protocol to the 1979 Convention on long-Range Transboundary Air Pollution on Heavy Metals'.

United Nations Environment Programme (UNEP) (2019a) *Global Mercury Assessment 2018*.

United Nations Environment Programme (UNEP) (2019b) *Stockholm Convention on Persistent Organic Pollutants (POPs): text and annexes revised in 2019*. Stockholm: United Nations Environment Programme.

United Nations Environment Programme (UNEP) (2021) *Inside the 20-year campaign to rid the world of leaded fuel*. Available at: https://www.unep.org/news-and-stories/story/inside-20-year-campaign-rid-world-leaded-fuel (Accessed: 3 July 2025).

United Nations Environment Programme (UNEP) (2024) *Minamata Convention on Mercury: text and annexes*. Available at: www.minamataconvention.org (Accessed: 3 July 2025).

United Nations Environment Programme (UNEP) and World Health Organisation (WHO) (2013) *State of the science of endocrine disrupting chemicals - 2012 : an assessment of the state of the*

science of endocrine disruptors United Nations Environment Programme (UNEP) and WHO. United National Environment Programme : World Health Organization.

Valette-Silver, N.J. (1993) 'The Use of Sediment Cores to Reconstruct Historical Trends in Contamination of Estuarine and Coastal Sediments', *Estuaries*, 16(3B), pp. 577–588.

Valizadeh, F. *et al.* (2014) 'Polycyclic Aromatic Hydrocarbons Identification and Source Discrimination in Rural Soil of the Northern Persian Gulf Coast', *EnvironmentAsia*, 1, pp. 104–11. doi:10.14456/ea.2014.14.

Valle-Levinson, A. (2010) 'Definition and classification of estuaries', in *Contemporary Issues in Estuarine Physics*. Cambridge University Press, pp. 1–11. doi:10.1017/CBO9780511676567.002.

Vane, C.H. *et al.* (2022) 'Contrasting sewage, emerging and persistent organic pollutants in sediment cores from the river Thames estuary, London, England, UK', *Marine Pollution Bulletin*, 175. doi:10.1016/j.marpolbul.2022.113340.

Vieira, L.R. *et al.* (2009) 'Acute effects of copper and mercury on the estuarine fish Pomatoschistus microps: Linking biomarkers to behaviour', *Chemosphere*, 76(10), pp. 1416–1427. doi:10.1016/j.chemosphere.2009.06.005.

Virtasalo, J.J., Österholm, P. and Asmala, E. (2023) 'Estuarine flocculation dynamics of organic carbon and metals from boreal acid sulfate soils', *Biogeosciences*, 20(14), pp. 2883–2901. doi:10.5194/BG-20-2883-2023,.

Vulliet, E. *et al.* (2014) 'A national reconnaissance for selected organic micropollutants in sediments on French territory', *Environmental Science and Pollution Research*, 21(19), pp. 11370–11379. doi:10.1007/s11356-014-3089-z.

Wai, O.W.H. *et al.* (2004) 'The formation mechanisms of turbidity maximum in the Pearl River estuary, China', *Marine Pollution Bulletin*, 48(5–6), pp. 441–448. doi:10.1016/J.MARPOLBUL.2003.08.019.

Wang, W.-X. and Rainbow, P.S. (2020) *Estuaries of the World: Environmental Pollution of the Pearl River Estuary, China - Status and Impact of Contaminants in a Rapidly Developing Region*. Edited by J.-P. Ducrotoy. Hull: Springer-Verlag GmbH Germany. Available at: http://www.springer.com/series/11705.

Wang, Z. *et al.* (2020) 'Toward a Global Understanding of Chemical Pollution: A First Comprehensive Analysis of National and Regional Chemical Inventories', *Environmental Science and Technology*, 54(5), pp. 2575–2584. doi:10.1021/acs.est.9b06379.

Wilkinson, J.L. *et al.* (2017) 'Spatial distribution of organic contaminants in three rivers of Southern England bound to suspended particulate material and dissolved in water', *Science of the Total Environment*, 593–594, pp. 487–497. doi:10.1016/j.scitotenv.2017.03.167.

Wilkinson, J.L. *et al.* (2018) 'Spatial (bio)accumulation of pharmaceuticals, illicit drugs, plasticisers, perfluorinated compounds and metabolites in river sediment, aquatic plants and benthic organisms', *Environmental Pollution*, 234, pp. 864–875. doi:10.1016/j.envpol.2017.11.090.

Wilson, J.G. (2002) 'Productivity, Fisheries and Aquaculture in Temperate Estuaries', *Estuarine, Coastal and Shelf Science*, 55(6), pp. 953–967. doi:10.1006/ECSS.2002.1038.

Windom, H.L. *et al.* (1989) 'Natural Trace Metal Concentrations in Estuarine and Coastal Marine Sediments of the Southeastern United States', *Environmental Science and Technology*, 23(3), pp. 314–320.

Wong, F.K.K. and Fung, T. (2016) 'Ecotourism planning in Lantau Island using multiple criteria decision analysis with geographic information system', *Environment and Planning B: Planning and Design*, 43(4), pp. 640–662. doi:10.1177/0265813515618583/FORMAT/EPUB.

Xu, W. *et al.* (2014) 'Endocrine-disrupting chemicals in the Pearl River Delta and coastal environment: sources, transfer, and implications', *Environmental Geochemistry and Health*, 36(6), pp. 1095–1104. doi:10.1007/s10653-014-9618-3.

Yamamoto, H. *et al.* (2003) 'Effects of physical-chemical characteristics on the sorption of selected endocrine disruptors by dissolved organic matter surrogates', *Environmental Science and Technology*, 37(12), pp. 2646–2657. doi:10.1021/es026405w.

Yamamoto, H. and Liljestrand, H.M. (2003) 'The fate of estrogenic compounds in the aquatic environment: sorption onto organic colloids', *Water Science and Technology*, 47(9), pp. 77–84. Available at: http://iwaponline.com/wst/article-pdf/47/9/77/422875/77.pdf.

Yang, B. *et al.* (2025) 'Polycyclic aromatic hydrocarbons are associated with sleep-related disorders in adults: the potential mediating role of inflammation', *BMC Public Health*, 25(1). doi:10.1186/s12889-025-23058-8.

Yang, X. *et al.* (2019) 'Sorption and transport of trenbolone and altrenogest photoproducts in soil-water systems', *Environmental Science: Processes and Impacts*, 21(10), pp. 1650–1663. doi:10.1039/c9em00305c.

Yang, X., Lin, H., Zhang, Y., *et al.* (2020) 'Sorption and desorption of seven steroidal synthetic progestins in five agricultural soil-water systems', *Ecotoxicology and Environmental Safety*, 196. doi:10.1016/j.ecoenv.2020.110586.

Yang, X., Lin, H., Dai, X., *et al.* (2020) 'Sorption, transport, and transformation of natural and synthetic progestins in soil-water systems', *Journal of Hazardous Materials*, 384. doi:10.1016/j.jhazmat.2019.121482.

Yang, Y. *et al.* (2011) 'Sorption behavior of phenanthrene in Yangtze estuarine sediments: Sequential separation', *Marine Pollution Bulletin*, 62(5), pp. 1025–1031. doi:10.1016/j.marpolbul.2011.02.033.

Yang, Z., Wang, L. and Niu, J. (2011) 'Sorption mechanisms of coexisting PAHs on sediment organic fractions', *Environmental Toxicology and Chemistry*, 30(3), pp. 576–581. doi:10.1002/ETC.426.

Yarahmadi, H. *et al.* (2018) 'Seasonal variations of steroid hormones released by wastewater treatment plants to river water and sediments: Distribution between particulate and dissolved phases', *Science of the Total Environment*, 635, pp. 144–155. doi:10.1016/j.scitotenv.2018.03.370.

Ye, X. *et al.* (2021) 'Effects of methylmercury on the early life stages of an estuarine forage fish using two different dietary sources', *Marine Environmental Research*, 164. doi:10.1016/j.marenvres.2020.105240.

Yu, D. *et al.* (2024) 'Simulation and parameter determination of the net sorption of phenanthrene by sediment particles', *Ecotoxicology and Environmental Safety*, 278. doi:10.1016/j.ecoenv.2024.116440.

Yu, W. *et al.* (2019) 'Occurrence, sorption, and transformation of free and conjugated natural steroid estrogens in the environment', *Environmental Science and Pollution Research*. Springer Verlag, pp. 9443–9468. doi:10.1007/s11356-019-04402-z.

Yu, Y. *et al.* (2011) 'Polycyclic aromatic hydrocarbon residues in human milk, placenta, and umbilical cord blood in Beijing, China', *Environmental Science and Technology*, 45(23), pp. 10235–10242. doi:10.1021/es202827g.

Yuan, K. *et al.* (2015) 'Determination of 13 endocrine disrupting chemicals in sediments by gas chromatography-mass spectrometry using subcritical water extraction coupled with dispersed liquid-liquid microextraction and derivatization', *Analytica Chimica Acta*, 866, pp. 41–47. doi:10.1016/j.aca.2015.02.011.

Zelinkova, Z. and Wenzl, T. (2015) 'The Occurrence of 16 EPA PAHs in Food – A Review', *Polycyclic Aromatic Compounds*, 35(2–4), pp. 248–284. doi:10.1080/10406638.2014.918550.

Zhang, D. *et al.* (2013) 'Seasonal and spatial dynamics of trace elements in water and sediment from Pearl River Estuary, South China', *Environmental Earth Sciences*, 68(4), pp. 1053–1063. doi:10.1007/s12665-012-1807-8.

Zhang, G. *et al.* (2002) 'Sedimentary records of DDT and HCH in the Pearl River Delta, South China', *Environmental Science and Technology*, 36(17), pp. 3671–3677. doi:10.1021/es0102888.

Zhang, J. *et al.* (2013) 'Study on the sorption behaviour of estrone on marine sediments', *Marine Pollution Bulletin*, 76(1–2), pp. 220–226. doi:10.1016/j.marpolbul.2013.08.038.

Zhang, J. *et al.* (2019) 'Historical Pollution and Source Contributions of PAHs in Sediment Cores from the Middle Reach of Huai River, China', *Bulletin of Environmental Contamination and Toxicology*, 102(4), pp. 531–537. doi:10.1007/s00128-019-02576-3.

Zhang, J. *et al.* (2024) 'Enhanced human activities since 20th century in pearl river delta, southern China: Evidence from high-resolution sedimentary records of polycyclic aromatic hydrocarbons and synthetic musks', *Marine Pollution Bulletin*, 207. doi:10.1016/j.marpolbul.2024.116890.

Zhang, S. *et al.* (2024) 'Novel insights into aerobic 17β-estradiol degradation by enriched microbial communities from mangrove sediments', *Journal of Hazardous Materials*, 465. doi:10.1016/j.jhazmat.2023.133045.

Zhang, Y., Gan, J. and Yang, Q. (2024) 'Spatiotemporal variability of streamflow in the Pearl River Basin: Controls of land surface processes and atmospheric impacts', *Hydrological Processes*, 38(4). doi:10.1002/hyp.15151.

Zhang, Z. *et al.* (2014) 'Occurrence of endocrine-disrupting phenols and estrogens in water and sediment of the Songhua River, Northeastern China', *Archives of Environmental Contamination and Toxicology*, 66(3), pp. 361–369. doi:10.1007/s00244-014-9998-5.

Zhao, X. *et al.* (2025) 'Spatiotemporal occurrence, distribution, and risk of steroid hormones along the coast of Guangdong, China', *Frontiers in Marine Science*, 12. doi:10.3389/fmars.2025.1546186.

Zhou, G. *et al.* (2014) 'Vertical distribution of trace elements in the sediment cores from major rivers in east China and its implication on geochemical background and anthropogenic effects', *Journal of Geochemical Exploration*, 139, pp. 53–67. doi:10.1016/j.gexplo.2013.03.007.

Zhu, D. *et al.* (2004) 'Evidence for π-π electron donor-acceptor interactions between π-donor aromatic compounds and π-acceptor sites in soil organic matter through pH effects on sorption', *Environmental Science and Technology*, 38(16), pp. 4361–4368. doi:10.1021/es035379e.

Zhu, X. *et al.* (2024) 'Typical emerging contaminants in sewage treatment plant effluent, and related watersheds in the Pearl River Basin: Ecological risks and source identification', *Journal of Hazardous Materials*, 476. doi:10.1016/j.jhazmat.2024.135046.